UCSF
UC San Francisco Electronic Theses and Dissertations

Title

Understanding the Role of Ras Signaling in Craniofacial and Dental Development Utilizing the RASopathies

Permalink

https://escholarship.org/uc/item/1x99h14x

Author

Goodwin, Alice

Publication Date

2013

Peer reviewed|Thesis/dissertation

Understanding the Role of RAS Signaling in Craniofacial and Dental
Development Utilizing the RASopathies

by

Alice Fitzgerald Goodwin

DISSERTATION

Submitted in partial satisfaction of the requirements for the degree of

DOCTOR OF PHILOSOPHY

in

Oral and Craniofacial Sciences

in the

GRADUATE DIVISION

of the

UNIVERSITY OF CALIFORNIA, SAN FRANCISCO

ACKNOWLEDGEMENTS

I would like to thank, first and foremost, my mentor Dr. Ophir Klein for his unwavering support during my thesis. Dr. Klein has taught me to think, read, and write as a scientist, and for that, I am tremendously grateful, and I look forward to maintaining a relationship for many years to come.

I would also like to thank the members of my thesis committee, Drs. Jeroen Roose, Diane Barber, and Katherine Rauen for their constructive criticism and guidance in the development and execution of this thesis project. Thank you in particular to Dr. Barber for her mentorship and career guidance as my graduate advisor. Also, a special thanks to Dr. Rauen for introducing me to the RASopathies and interacting compassionately with patients and families in the clinical research setting, and for all of the time and energy she dedicated to my thesis project. I am truly grateful.

I have been lucky to meet and work with some wonderful people in the Klein lab and UCSF community. A special thanks to Dr. Andrew Jheon, a lovely friend and colleague, for all of the productive scientific conversations and back and forth manuscript revisions. Also, thanks to Dr. Saunders Ching for his advice and help inside and outside of lab, and Drs. Kerstin Seidel, Miquella Chavez, and Gemma Rooney for their support as strong, independent women in science.

A very special thanks and love for my family and friends. Thank you Katie for being a friend and constant source of support and love, always there and willing to listen and give your professional advice, and Julie for your support, love, and ability to make me laugh. Thank you Lou for being a generous and loving father. And to my Mom, you have been a constant source of love, strength, and support throughout my life, and it is because of you that I believe I can pursue this career as a woman in science, and so this thesis work is dedicated to you.

Understanding the Role of Ras Signaling in Craniofacial and Dental Development Utilizing the RASopathies

by

Alice Fitzgerald Goodwin

ABSTRACT

Very little is known about the role of Ras signaling in tooth development although upstream receptor tyrosine (RTK) signaling that activates Ras and regulators of Ras signaling, like proteins encoded by the Sprouty genes, are known to be important in tooth development. The RASopathies, including Costello syndrome (CS) and Cardio-facio-cutaneous syndrome (CFC), are syndromes caused by gain-of-function mutations in the Ras pathway and are characterized by a wide range of cardiac, musculoskeletal, dermatological, and developmental abnormalities. These syndromes provide an excellent model to study the role of Ras signaling in tooth development, and thus, we analyzed the craniofacial and dental phenotypes of CS and CFC at family conferences in 2009 and 2011. CS and CFC have in common craniofacial characteristics including macrocephaly, bitemporal narrowing, and convex facial profile. Additionally, individuals with CFC have hypoplastic supraorbital ridges, and CS individuals have characteristic micrognathia, full cheeks, large appearing mouth, and thick appearing lips. There were some overlapping dental characteristics between CS and CFC, including malocclusion, but overall, CS had more dysmorphic dental characteristics compared to CFC. CS individuals had class III molar relationship, delayed tooth development and eruption, gingival hyperplasia, thickening of the alveolar ridge, and high-arched palate more often compared

to CFC. Moreover, CS individuals had a hypoplastic enamel defect that was not present in CFC. To further understand the role Ras in enamel formation, we obtained a CS mouse model and found that the CS mouse model had a similar hypoplastic enamel phenotype. Further analysis revealed that the progenitor cells were hyperproliferative, and the enamel producing ameloblasts lacked cell polarity and had delayed enamel protein expression, resulting in the enamel defect. Next, I utilized MEK1/2 (PD0325901) and PI3'K (GDC-0941) inhibitors to dissect the roles of the Ras effector pathways in amelogenesis. MEK inhibition rescued the ameloblast loss of polarity and delayed differentiation while MEK or PI3'K inhibition rescued the hyperproliferation phenotype. Thus, this dissertation work reveals a role for Ras signaling in amelogenesis, and knowledge gained about Ras signaling in the tooth may be applied to efforts to bioengineer teeth and further understand Ras in development and cancer.

TABLE OF CONTENTS

LIST OF TABLES

LIST OF FIGURES

LIST OF SUPPLEMENTAL FIGURES

CHAPTER 1:

Introduction to Tooth Development, Ras Signaling, and the RASopathies

The work reported in this thesis dissertation answers the question: what is the role of Ras signaling in tooth development? To address this, I have used the RASopathies as a model. First, the craniofacial and dental phenotype was analyzed in individuals with Costello syndrome (CS) and Cardio-facio-cutaneous syndrome (CFC), and then an enamel defect observed in CS patients was further analyzed in a CS mouse model, revealing the role of Ras signaling in the mouse incisor. By way of introduction, tooth development, Ras signaling, and the RASopathies are reviewed in this chapter.

1.1 Tooth Development

1.1.1 *Tooth Structure*

The mammalian tooth is comprised of enamel, dentin, and cementum. The crown of the tooth is the portion covered by enamel that erupts into the oral cavity, while the root is the subgingival part that anchors the tooth into the bone (Figure 1.1). Enamel is about 95% mineral by weight (Deakins and Volker, 1941), which makes it the hardest structure in the body. Only 1% of the non-mineral content is protein, while the rest is water. The main mineral component of enamel is hydroxyapatite, a crystalline calcium phosphate. Dentin, cementum, and bone are about 50% hydroxyapatite by weight. The high mineral density of enamel makes it very hard but also quite brittle. The underlying dentin provides some flexibility and resistance for the tooth. The tooth is anchored into the alveolar bone by the periodontal ligament (PDL), which consists of individual collagen fibrils that originate from the cementum and attach to the bone (Ho et al., 2007). The center of the tooth, enclosed by the dentin, is filled by the dental pulp, which is a mass of connective tissue that contains blood vessels and nerves.
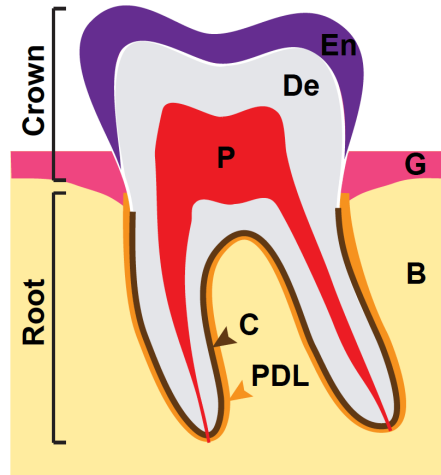
Figure 1.1 The human tooth. Illustration of the human molar. Components and structure of the tooth are described in the text. (enamel, En; dentin, De; pulp, P; cementum, C; periodontal ligament, PDL; gingiva, G; bone, B)

1.1.2 *Epithelial-Mesenchymal Interactions*

The tooth is an organ that develops via reciprocal signaling between the oral ectoderm-derived epithelium and underlying neural crest-derived mesenchyme. The reciprocal interactions between epithelium and mesenchyme are temporally and spatially controlled during tooth development, as shown by a series of tissue recombination experiments. At the beginning of tooth morphogenesis, the tooth forming potential lies in the epithelium; oral epithelium from murine embryos between E9 and E11.5 induced tooth formation in non-dental neural crest derived mesenchyme (Mina and Kollar, 1987; Lumsden, 1988). After E11.5, the mesenchyme is able to instruct non-dental epithelium to undergo tooth morphogenesis (Kollar and Baird, 1970); however, the dental epithelium loses its ability to induce tooth formation. Furthermore, after E11, the mesenchyme has the ability to

3

determine tooth shape, since combination of mesenchyme from a molar with epithelium from an incisor resulted in the formation of a molar tooth and *vice versa* (Kollar and Baird, 1969). Thus, epithelial-mesenchymal interactions are critical in tooth formation, and tooth forming potential shifts from the epithelium to mesenchyme during tooth development. The tooth develops via reciprocal epithelial and mesenchyme interactions, much like other organs including lungs, mammary glands, and hair follicles, making the tooth an excellent model to study organ development.

1.1.3 *Stages of Tooth Development*

Tooth formation is initiated by a signal from the oral ectoderm to the underlying neural crest-derived mesenchyme (E9.5 in mouse) (Mina and Kollar, 1987; Lumsden, 1988). The reciprocal signal from the mesenchyme induces the oral epithelium to thicken, forming the dental lamina at E11 in mouse and 7 weeks in human, which demarcates the future tooth field (Figure 1.2). The dental lamina then invaginates into the underlying mesenchyme, which condenses around the epithelium to form the bud between E12.5 and E13.5. The epithelium further invaginates to form the cap at E14, and the mesenchyme surrounded by the epithelium gives rise to dental papilla. The mesenchyme adjacent to the dental papilla or outside of the enamel epithelium forms the dental follicle. During the cap stage, a transient signaling center in the epithelium called the primary enamel knot forms. The enamel knot expresses several signaling molecules that control cell proliferation and

apoptosis to regulate cusp morphogenesis. The enamel epithelium continues to dive downward into the mesenchyme to form the bell at E16, which begins to resemble the complete tooth crown. The secondary enamel knots form during the bell stage in molar development to determine the multi-cuspid pattern of molar crowns (Jernvall et al., 1994).
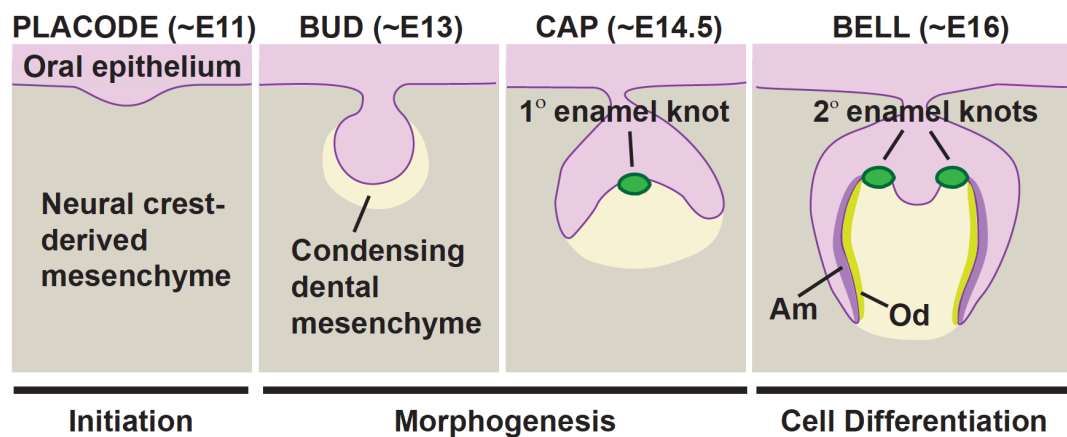
Figure 1.2 Stages of tooth development. Illustration of the stages of tooth development, which are described fully in the text. (ameloblast, Am; odontoblast, Od)

The epithelium at the cap and bell stages is termed the enamel organ and is composed of multiple cell types: the inner enamel epithelium closest to the dental papilla that later differentiates into ameloblasts, the outer enamel epithelium, and the stellate reticulum and stratum intermedium in between. At the later bell stage, dental papilla cells differentiate into odontoblasts that produce a dentin matrix which induces the epithelium to differentiate into

ameloblasts that deposit enamel matrix, forming the hard tissues of the tooth crown (Thesleff and Hurmerinta, 1981).

Once crown development is complete, root formation begins when the inner epithelium forms Hertwig's epithelial root sheath (HERS) at the crown-root boundary. HERS then proliferates and migrates downward, guiding root formation and inducing the differentiation of odontoblasts from the dental papillae to form the root dentin. Once the root reaches the appropriate length, the HERS disintegrates, resulting in the formation of an epithelial network called the epithelial rests of Malassez (ERM). Formation of the ERM allows the cells of the dental follicle to come into contact with the root dentin, which induces their differentiation into cementoblasts that deposit cementum on the root surface. Dental follicle cells also differentiate into fibroblasts that form the periodontal ligament that connects the root to the bone. Once tooth development is complete, the tooth erupts into the oral cavity. Osteogenic activity at the root of the tooth provides force to push the tooth while osteoclastic activity at the crown creates a path through the alveolar bone (Wise, 2009).

1.1.4 *Amelogenesis*

Amelogenesis is the process by which odontoblasts and ameloblasts form dentin and enamel, respectively, during tooth development. During amelogenesis, the ameloblasts undergo multiple differentiation steps: the pre-

secretory, secretory, transition, and maturation stages (Figure 1.3). The presumptive ameloblasts begin as low, columnar, proliferative cells separated from the underlying mesenchyme by a basement membrane. During the pre-secretory stage, after receiving inductive signals from the epithelium, the underlying mesenchyme layer begins to differentiate into odontoblasts that induce the inner epithelial cells to stop proliferating and elongate to form pre-ameloblasts. In the secretory stage, the pre-ameloblasts lengthen into a columnar shape, polarize, and form conical projections or Tomes' processes that begin secreting enamel matrix proteins including amelogenin, ameloblastin, enamelin, and enamelysin or matrix metalloproteinase-20 (MMP20). During the secretory stage, very thin (10nm thick) hydroxyapatite ribbons begin to form and extend from the dentin-enamel junction (DEJ) to the surface of the enamel to determine enamel thickness (Cuisinier et al., 1992). Ameloblasts move away from the DEJ as they deposit matrix, and they move in rows in an intersecting pattern that forms the decussating enamel lattice. If ameloblasts do not secrete sufficient matrix protein during the secretory stage, the resulting enamel is thin or hypoplastic.
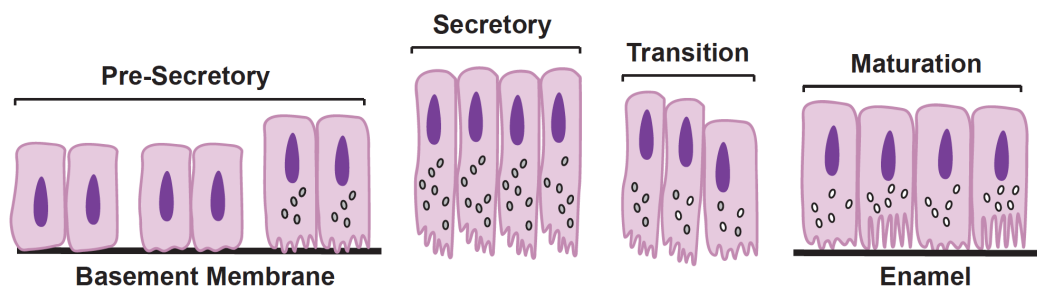
Figure 1.3 Stages of ameloblast differentiation. Ameloblasts transition from the pre-secretory to secretory, and then transition to maturation stages during amelogenesis. Stages of amelogenesis are described in the text.

Ameloblasts shorten into a cuboidal shape and lose Tomes' processes during the transition stage, and during the maturation stage, ameloblasts secrete proteins like odontogenic ameloblast associated protein (ODAM/APIN), amelotin, and kallikrein-related peptidase 4 (KLK4). Maturation stage ameloblasts absorb water and organic matrix proteins as enamel crystals replace the matrix to form mature enamel. The process by which the enamel matrix mineralizes is not clear; however, it is thought that during maturation stage, mineral is added to the hydroxyapatite ribbons formed during the secretory stage, and these ribbons do not lengthen but thicken to form the mature enamel rods. Failure of ameloblasts to remove organic matrix results in hypomaturation or soft, mottled, brownish-yellow enamel, and extreme failure to mineralize results in hypocalcification or rough, soft enamel of normal thickness (Hu et al., 2007).

1.1.5 *Amelogenesis Imperfecta and Enamel Proteins in Human and Mouse*

Amelogenesis imperfecta (AI) is a group of inherited disorders characterized by abnormal enamel formation and not associated with other systemic abnormalities. AI enamel defects are highly variable and classified as hypoplasia (defect in amount of enamel due to secretory defect), hypomaturation (defect in maturation of enamel due to improper removal of organic material), and hypocalcification (defect in initial formation and growth of crystallites). AI can be inherited in an X-linked, autosomal recessive (AR), or autosomal dominant (AD) manner. Mutations in multiple genes encoding

8

enamel proteins have been implicated in the etiology of AI, although there are many AI cases for which the molecular basis is not known. Mutations in amelogenin (*AMELX*), enamelin (*ENAM*), *KLK4*, and *MMP20* are all associated with AI (Lagerström et al., 1990; Rajpar et al., 2001; Hart et al., 2004; Kim et al., 2005). More than 14 mutations have been identified in the *AMELX* gene on the X-chromosome, and those resulting in a loss of the C-terminus or total loss of the protein result in hypoplastic enamel while mutations resulting in single amino acid changes cause hypomaturation defects (Wright et al., 2003). *ENAM* mutations are inherited in an AD manner and cause a hypoplastic phenotype, while mutations in both *KLK4* and *MMP20* cause pigmented, hypomaturation, autosomal recessive AI. There are also mutations in the *FAM83H* gene that cause hypocalcified, autosomal dominant AI (Kim et al., 2008). The function of the protein encoded by *FAM83H* is not known in amelogenesis, and over-expression in a mouse model had no effect on enamel or dentin formation (Kweon et al., 2013).

Although mutations in genes encoding enamel proteins have been associated with AI, there are many cases of enamel hypoplasia, hypomaturation, and hypocalcification in which the genetic etiology is unknown. Identifying novel genes associated with enamel defects in patients or diagnosing enamel defects in patients with a known genetic disorder will greatly expand our understanding of the signal transduction pathways that control amelogenesis and may elucidate new pathways regulating enamel formation. In this dissertation, I define novel roles for Ras in amelogenesis by

examining CS and CFC patients with activating mutation in the Ras pathway.

Much has been learned about the functions of enamel proteins secreted at the secretory stage, including amelogenin, ameloblastin, enamelin, and MMP20 by studying mouse models. Amelogenin is the predominate secretory product of ameloblasts and composes 90% of the enamel matrix. Amelogenin assembles into spheres in between the forming crystal ribbons and separates and supports them (Oldak et al., 1994; Fincham et al., 1995). There are at least 15 different splicing variants of the amelogenin protein from the single murine X-chromosomal gene (Simmer et al., 1994), and deletion of a portion of the amelogenin gene that resulted in a loss of amelogenin protein caused enamel hypoplasia and disorganized enamel crystal pattern (Gibson et al., 2001). Ameloblastin is a critical adhesion protein that attaches the ameloblast to the enamel matrix and maintains its differentiated state. In the ameloblastin-null mouse, the ameloblasts detach from the matrix, lose cell polarity, and begin to proliferate, forming multiple layers, resulting in hypoplastic enamel (Fukumoto, 2004). These mice also form odontogenic tumors of dental epithelial origin (Fukumoto et al., 2006). Enamelin is important in mineralization of the enamel, since enamelin-null mice form an enamel matrix, but the matrix lacks mineral content (Hu et al., 2008). MMP-20 is a proteinase that degrades the enamel matrix to allow mineral deposition, and deletion of MMP-20 in mice resulted in less mineralized enamel with an altered enamel rod pattern that flaked off at the DEJ (Caterina et al., 2002). Additionally, although MMP-20 is no longer expressed during the maturation

stage, MMP-20 deficient mice form ectopic, calcified nodules on the enamel surface (Chen et al., 1996; Bartlett et al., 2011).

Ameloblasts secrete maturation stage proteins such as amelotin, APIN/ODAM, and kallikrein-related peptidase 4 (KLK4). Amelotin is expressed during maturation stage; however, the function of amelotin is not yet clear (Iwasaki et al., 2005; Somogyi-Ganss et al., 2012). Over-expression of the amelotin gene during secretory stage under the control of the amelogenin promoter resulted in thin, disorganized enamel with a rough surface and loss of Tomes' processes, however, the role of endogenous amelotin is uncertain. APIN/ODAM is also secreted by maturation stage ameloblasts and is thought to regulate MMP-20 *in vitro* (Moffatt et al., 2008; Lee et al., 2010). KLK4 is a better-understood proteinase that degrades the enamel matrix to allow proper mineralization. Ablating KLK4 resulted in enamel with normal thickness and enamel rod organization but decreased mineral content so that the enamel abraded easily and fractured above the DEJ (Simmer et al., 2009; Smith et al., 2011).

Although much is known about the functions of the enamel proteins in amelogenesis, there are many questions remaining about the regulation of their expression at the appropriate time and place during tooth formation. By further studying the role of signal transduction pathways like Ras in enamel formation, we will gain a greater understanding of amelogenesis and determine targets for treatment of enamel defects.

11

1.1.6 *Human vs Mouse Dentition*

Humans have 8 teeth in each quadrant of the mouth: 2 incisors, 1 canine, 2 premolars, and 3 molars. Mice have a reduced dentition with 4 teeth in each quadrant: 1 incisor separated from the 3 molars by a toothless diastema. While humans have a primary and permanent set of dentition, mice have only one set of permanent teeth that are never replaced.

In contrast to the mouse molars, that are similar to human molars, the mouse incisor is a remarkable tooth in that it grows continuously throughout the lifetime of the mouse, which makes the mouse incisor an excellent model to examine the stages of tooth development (Figure 1.4). Enamel is present only on the labial and not lingual aspect of the mouse incisor, which enables the mouse to abrade the lingual side of the enamel into a sharp point and thus maintain the incisor tip through self-sharpening. The rodent incisor is fueled by a presumptive stem cell population in the inner enamel epithelium in the cervical loop (CL) at the most proximal portion of the incisor, which has been identified through many lineage tracing experiments (Smith and Warshawsky, 1975; 1977; Harada et al., 1999; Seidel et al., 2010; Juuri et al., 2012; Biehs et al.). Progenitor cells exit the CL, proliferate as they move into the transit-amplifying (TA) region, and differentiate into ameloblasts. As the ameloblasts move along the incisor, they transition from the secretory stage, during which they secrete enamel proteins including amelogenin and ameloblastin to form the enamel matrix, to the maturation stage, when ameloblasts secrete proteins such as ODAM/APIN, amelotin, and KLK4 that

enable the mineralization of the enamel matrix. Thus, the distinct steps of amelogenesis can be observed in a "conveyor belt-like" fashion along the length of the mouse incisor, and the mouse incisor, which I utilize in this thesis dissertation, serves as an excellent model to study the multiple stages of tooth development.
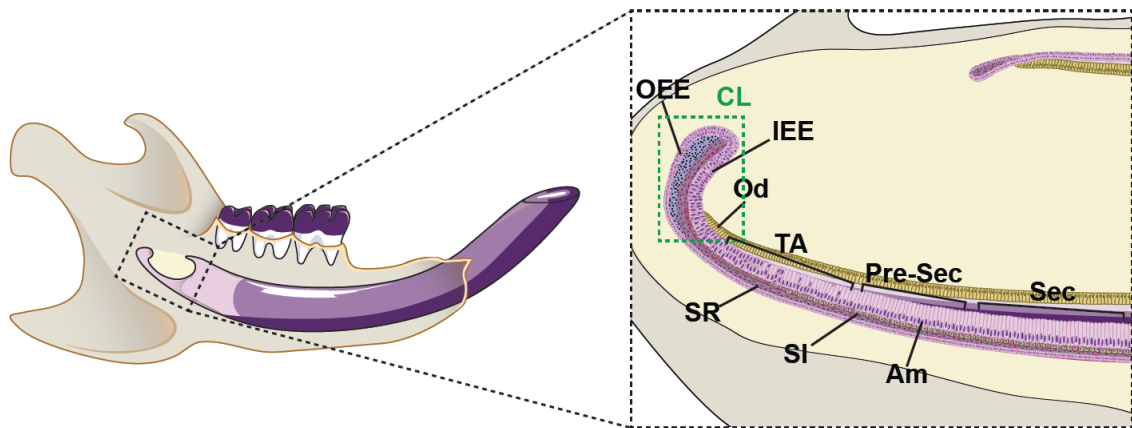
Figure 1.4 The continuously growing mouse incisor. Image of the mouse hemi-mandible with 1 incisor and 3 molars, and magnified view of the cervical loop (CL) outlined by the dashed line. Ameloblast progenitor cells move out of the CL, proliferate in the transit-amplifying (TA) region and transition from pre-secretory (Pre-Sec) to secretory (Sec) stage as they move along the incisor (transition and maturation stage ameloblasts would be further along the incisor in the more distal region not pictured). Thus, the mouse incisor serves as an excellent model to study amelogenesis. (Enamel is dark purple and dentin is light purple; stellate reticulum, SR; stratum intermedium, SI; outer enamel epithelium, OEE; inner enamel epithelium, IEE; ameloblast, Am; odontoblast, Od)

1.1.7 *RTK Signaling in Tooth Development*

As discussed above, tooth morphogenesis is regulated by reciprocal epithelial-mesenchymal interactions, which are mediated by conserved signaling pathways including Hedgehog (Hh), Wnt, Fibroblast growth factor (FGF), Transforming growth factor β (TGFβ), Bone morphogenic protein

13

(Bmp), and Ectodysplasin (Eda) (Figure 1.5). The primary focus of this section is FGF and downstream signaling in tooth development.

The role of RTK signaling has been studied extensively in tooth morphogenesis, and FGFs play a critical role in determining tooth number, size, and morphology. At early stages of tooth patterning, *Fgf8* and *Fgf9* are expressed in the proximal portion of the mouse mandible, overlying the presumptive molar field, while BMP4 is expressed distally, near the presumptive incisor field (Neubüser et al., 1997). Wnt/β-catenin signaling is thought to regulate *Fgf8* expression in the early epithelium (Wang et al., 2009), and dental placodes do not form in mice overexpressing the Wnt inhibitor Dkk1 (Andl et al., 2002). These signaling molecules control the expression of homeobox genes in the underlying neural crest derived mesenchyme. FGF8, and to a lesser extent FGF9, induce expression of *Barx1* (BarH-like homeobox 1) and *Dlx2* (distal-less homeobox 2) while BMP4 positively regulates expression of *Msx1* and *Msx2* (homeobox, msh-like 1 and 2) and negatively regulates *Barx1*. FGF8 positively regulates and BMP4 represses expression of the paired related homeobox gene *Pitx2*, which is expressed early in the dental epithelium (Mucchielli et al., 1997; St Amand et al., 2000). Later, FGF8 stimulates and BMP2/4 inhibit *Pax9* expression in the mesenchyme, a paired box transcription factor. Loss of *Fgf8*, *Msx1/Msx2*, *Dlx1/Dlx2*, or *Pitx2* results in initiation stage arrest while deletion of *Pax9* or *Barx1* causes bud stage arrest (Trumpp et al., 1999; Bei and Maas, 1998; Thomas et al., 1997; Liu et al., 2003; Peters et al., 1998; Tucker, 1998). In

14

addition, over-expression of a dominant negative form of *Fgfr2b* resulted in bud stage arrest (De Moerlooze et al., 2000). Thus, FGFs are critical in determining the location and number of teeth.
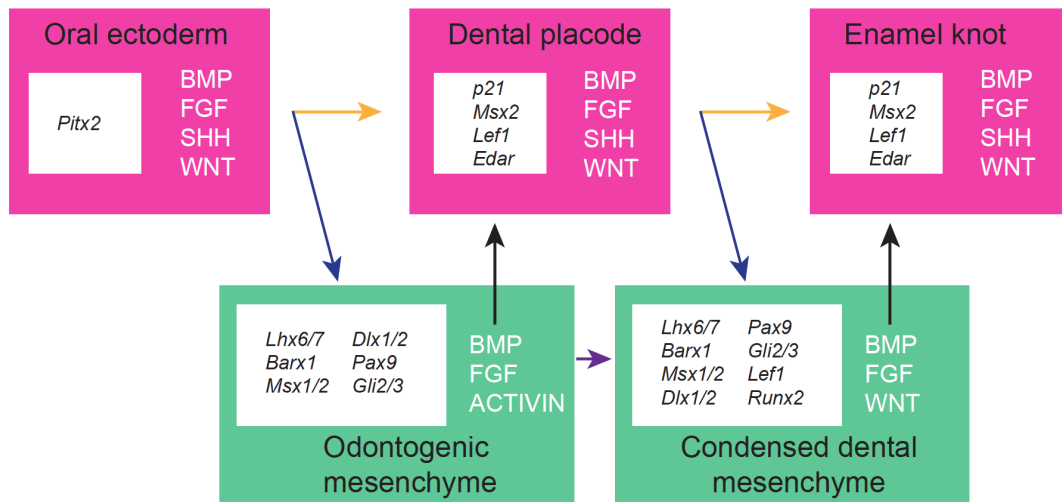
Figure 1.5 Signaling in the developing tooth. Diagram of multiple signaling pathways involved in tooth development. Specific factors discussed in text. Adapted from Thesleff and Tummers.

Later, FGFs regulate tooth morphogenesis. During the transition from cap to bud stage, *Fgf4* and *Fgf9* are expressed in the enamel knot and are thought to stimulate proliferation in adjacent epithelial and mesenchymal tissues (Jernvall et al., 1994; Kettunen et al., 1998), while the enamel knot itself remains non-proliferative since it expresses the cyclin-dependent kinase inhibitor p21 and lacks Fgf receptors (Roose et al., 2007; Jernvall et al., 1998). The localized proliferation induces epithelial folding which determines cusp morphology. Additionally, FGF4/9 induce expression of FGF3 and FGF10 in the dental mesenchyme, which signal back to the epithelium to regulate

15

subsequent epithelial morphogenesis and enamel knot formation (Feng et al., 2004; Kettunen et al., 2000). Deletion of *Fgf3* and *Fgf10* in mice results in smaller teeth with aberrant cusp morphology (Wang et al., 2007). Antagonists of the RTK signaling pathway also affect tooth development. The inactivation of *Sprouty* genes, which are inhibitors of FGF signaling, results in the formation of supernumerary teeth (Klein et al., 2006) and the generation of ectopic enamel on the lingual surface of the incisor (Klein et al., 2007). Little is known about the downstream targets of RTK signaling in tooth morphogenesis. p-ERK is expressed in the epithelium during the cap, bud, and bell stage and later in the ameloblasts, and inhibiting MEK in tooth organ culture results in small, dysmorphic teeth (Cho et al., 2009). Interestingly, normal tooth size and morphology was restored *in vitro* with addition of FGF10 (Hanafusa et al., 2002; Cho et al., 2009).

Little is known about the role of RTK or downstream Ras signaling in enamel formation. Thus, it is an open area of research, and this thesis dissertation begins to explore the role of Ras in amelogenesis. Inactivation of *Fgfr1* in the epithelium resulted in dysfunctional ameloblasts that produced disorganized enamel (Takamori et al., 2008). Overexpression of *Fgf2* in cultured embryonic molars resulted in decreased expression of amelogenin, while inhibition of FGF2 increased amelogenin expression and enamel formation (Tsuboi et al., 2003). Interestingly, Ras superfamily members have been shown to play a role in amelogenesis, including Rac, a GTPase involved in cytoskeletal remodeling. Conditional inactivation of *Rac1* in the epithelium

16

resulted in ameloblasts that expressed decreased levels of amelogenin and lost attachment to the secreted enamel matrix, resulting in hypo-mineralized enamel (Huang et al., 2011). Thus, although studies have examined the role of RTK in tooth morphogenesis, little is known about the role of downstream effectors, including Ras, especially in later stages of tooth development, and this thesis dissertation is the first to define a role for Ras in amelogenesis.

1.2 The Ras Pathway

1.2.1 *The RAS Genes*

RAS genes have been a focus of study for the last 30 years as researchers work to understand the role of these genes in development and cancer pathogenesis (Malumbres and Barbacid, 2003). The Ras field began during the late 1970s, when it was discovered that rat-derived Harvey and Kirsten murine sarcoma retroviruses contribute to cancer pathogenesis through a common set of *RAS* (rat sarcoma virus) genes (Scolnick et al., 1973; Scolnick and Parks, 1974; Karnoub and Weinberg, 2008). These *RAS* genes were identified in the rat and then mouse and human genomes (DeFeo et al., 1981; Ellis et al., 1982; Chang et al., 1982), and the Harvey sarcoma virus associated oncogene was named *HRAS* and the Kirsten sarcoma virus was termed *KRAS*. Mutant *RAS* genes encoding constitutively active Ras proteins were discovered in multiple human tumors during the early 1980s (Santos et al., 1984; Fujita et al., 1984). In 1983, a new oncogene was identified and found to be a third member of the *RAS* gene family and named *NRAS* (neuroblastoma RAS viral (v-ras) oncogene homolog) (Hall et al., 1983; Taparowsky et al., 1983).

1.2.2 *Ras Protein Biology*

The *RAS* genes encode the Ras proteins, HRAS, NRAS, and KRAS4A and KRAS4B, which are alternatively spliced proteins encoded by *KRAS*. KRAS4B is the main *KRAS* protein product and will hereafter be referred to

18

as KRAS. The Ras proteins are part of a large family of small, monomeric GTPases, which are divided into 5 major subfamilies: Ras, Rho, Rab, Ran, and Arf. Ras GTPases cycle between inactive GDP bound (Ras-GDP) and active GTP bound (Ras-GTP) states (Vetter, 2001). Ras guanine nucleotide exchange factors (RasGEFs) facilitate the activation of Ras by releasing the tightly bound GDP and stabilizing Ras in a nucleotide free state, so that GTP, which is at higher concentrations in the cell than GDP, preferentially binds Ras (Bos et al., 2007). Hydrolysis of GTP to GDP is required to inactivate Ras. Ras has a very low intrinsic rate of hydrolysis, and so there are Ras GTPase activating proteins (RasGAPs) that increase GTP hydrolysis to convert Ras-GTP to Ras-GDP and inactivate it (Scheffzek et al., 1997).

The GTPase activity of Ras is critical since it allows Ras proteins to switch on or off to relay extracellular signals into the cell to control proliferation, differentiation, and apoptosis. Thus, the GDP/GTP binding region from amino acid (aa) 1 to 85 of the highly homologous G domain (aa1-165) is critical and is identical in the Ras proteins. Within the G domain, Ras proteins also contain a phosphate-binding loop (p-loop), to which the arginine fingers of GAPs bind, and switch 1 and switch 2 that bind Ras regulators and effectors, including GEFs. In the remaining aa85-165 of the G domain, the Ras proteins share 85-90% homology.

The Ras proteins differ most at the hypervariable region at the C-terminus (aa165-189), which contains residues that specify post-translational modifications. Differences in post-translational modification of the Ras

19

proteins are thought to determine the trafficking and localization of the Ras proteins, which may in turn affect their activity. All of the Ras proteins contain a CAAX motif recognized by two prenyltransferases: farnesyl transferase (FT) and geranylgeranyl transferase type 1 (GGT1). In general, FT adds farnesyl, a 15-carbon isoprene, to CAAX (Casey et al., 1989); however, in the absence of FT, GGT1 adds geranylgeranyl, a 20-carbon isoprene, to CAAX (Mor and Philips, 2006). Once prenylated, the modified CAAX motif targets Ras proteins to the endoplasmic reticulum (ER) where they encounter the protease RCE1 that cleaves the AAX sequence (Boyartchuk et al., 1997; Choy et al., 1999). Then, the new C-terminal prenylcysteine is recognized by isoprenylcysteine carboxyl methyltransferase (ICMT) that methylesterfies the carboxyl group (Dai et al., 1998). The end result of modification at the CAAX domain is the creation of a hydrophobic domain at the C-terminus that mediates membrane association. It is essential for Ras to associate with membranes to be activated, and so the CAAX modification has been a target in cancer treatment, which will be discussed later.

A second signal is then added to the Ras proteins to target them to membranes including the plasma membrane, endoplasmic reticulum, mitochondria, Golgi, and endosomes. NRAS and HRAS undergo palmitoylation on the Golgi that adds palmitic acids on cysteines upstream of CAAX. Palmitoylated NRAS and HRAS are trapped in the Golgi and transported to the plasma membrane in vesicles. They are then depalmitoylated at the membrane and diffuse back to the Golgi to undergo

another round of palmitoylation and transport to the membrane (Rocks et al., 2005; Goodwin et al., 2005; Ahearn et al., 2011). NRAS and HRAS have been found to signal from the Golgi and endosomes in addition to the plasma membrane (Chiu et al., 2002). In contrast, KRAS does not undergo palmitoylation, but instead KRAS contains a positively charged, polybasic lysine rich domain in its hypervariable region that forms an electrostatic interaction with the negatively charged inner leaflet of the plasma membrane, targeting KRAS to the plasma membrane (Hancock et al., 1990). Additionally, the prenyl binding protein PDEδ has been shown to bind Ras and is thought to facilitate the diffusion of KRAS to the plasma membrane (Zhang et al., 2004; Chandra et al., 2011). Thus, HRAS and NRAS are trafficked differently in the cell than KRAS, which results in HRAS and NRAS signaling from multiple membrane compartments while KRAS only signals from the plasma membrane, but how the differences in cellular location affect function remains to be determined. Understanding the mechanism of localization and signaling of the Ras proteins is critical since it will provide new approaches in targeting activated Ras signaling in cancer.

1.2.3 *Ras Signaling*

Ras proteins are activated by many receptor types, including receptor tyrosine kinase (RTK) receptors, G-protein-coupled receptors, and integrins. When ligand (like FGF or EGF) binds RTK receptors at the membrane, the receptors dimerize and autophosphorylate. The cytosolic domain of the

activated receptor binds GRB2 at its SH2 (Src homology 2) domain, which is bound to the RasGEF SOS 1 and 2 (encoded by *son-of-sevenless 1 and 2*) at its SH3 domain (Figure 1.6). The RTK receptor also binds SHP2, a protein encoded by *PTPN11* that contains N- and C-terminal SH2 domains and a catalytic protein tyrosine phosphatase (PTP) domain. RTK binding to GRB2 and SHP2 recruits SOS to the membrane where it converts membrane bound, inactive Ras-GDP to active Ras-GTP.

Once activated, Ras signals through multiple effector pathways, including RAF/MEK/ERK, PI3'K/AKT, TIAM1/Rac, and RALGDS/Ral. There are multiple additional Ras effector pathways, and crosstalk between many of these effector pathways creates a complicated Ras signaling network. In simplest terms, Ras activates RAF (RAF-1, ARAF, BRAF, and CRAF), which phosphorylates MEK1/2, which in turn activates ERK1/2 (Roberts and Der, 2007). Activated ERK1/2 phosphorylates transcription factors of the ETS family, such as JUN and ELK1, that promote cell cycle progression and proliferation downstream (Chambard et al., 2007). Activated Ras can also bind phosphatidylinositol 3-kinase (PI3'K) (Rodriguez-Viciana et al., 1994; Pacold et al., 2000), which phosphorylates PIP2 to produce PIP3, and PIP3 recruits and activates phosphoinositide-dependent kinase 1 (PDK1) and AKT, which promote cell cycle progression and cell survival (Castellano and Downward, 2011). PI3'K also directly binds Rac which is involved in cytoskeletal remodeling (Welch et al., 2003). Ral guanine nucleotide dissociation stimulator (RALGDS) family members bind Ras which recruits

them to the membrane where they act as Ral-GEFs that activate Ral, which is a GTPase involved in endocytosis, exocytosis, and actin skeleton organization (Ferro and Trabalzini, 2010). RALGDS has also been shown to activate AKT by acting as a scaffold for PDK1 and AKT (Hao et al., 2008). Ras binds TIAM-1 (T lymphoma invasion and metastasis) and stimulates its Rac-GEF activity, which activates Rac and leads to cytoskeletal remodeling (Habets et al., 1994; Michiels et al., 1995). It is clear that Ras regulates many cellular processes through its downstream effector pathways. The contribution of each downstream effector pathway in various biological processes is very much an active area of research; complex interactions between the pathways have yet to be fully characterized. In an attempt to further understand the role of the Ras effector pathways, in this thesis dissertation, I dissect the roles of the MAPK and PI3'K pathways in the mouse incisor.

1.2.4 _Regulation of Ras Signaling_

Since the intensity and duration of Ras signaling is critical in controlling various cell functions, the Ras signaling pathway is regulated at multiple points. The RasGEFs and RasGAPs are critical points of regulation since they control the switch between the active GTP-bound and inactive GDP-bound state of Ras proteins. There are 3 RasGEF families which catalyze the binding of GTP and activation of Ras: son of sevenless (SOS 1 and 2), Ras guanine nucleotide releasing factor (Rasgrfs 1 and 2), and Ras guanine

nucleotide releasing proteins (RasGRPs 1-4). SOS is positively regulated when Ras-GTP binds at a second allosteric binding site and increases the catalytic activity of SOS and thus increases Ras activation (Boriack-Sjodin et al., 1998; Margarit et al., 2003). The pleckstrin homology (PH) domain of SOS acts as a gate to the allosteric binding site, and only when it binds PA or PIP2 at the membrane does it allows Ras-GTP to bind and increase catalytic activity (Chen et al., 1997; Koshiba et al., 1997; Kubiseski et al., 1997; Sondermann et al., 2004; Gureasko et al., 2008). Downstream ERK can negatively influence SOS by phosphorylating SOS and causing it to dissociate from GRB2 (Chen et al., 1996). Rasgfrs are less well understood but are thought to be closely related to SOS proteins and localize to the membrane to activate Ras most likely by a lipid interaction (Cen et al., 1993; Fernández-Medarde and Santos, 2011). RasGRPs have been studied most extensively in B- and T-lymophocytes and are recruited and activated by diacyglycerol (DAG), protein kinase C (PKC), and calcium at the membrane although the mechanism is unclear (Ebinu et al., 1998; 2000; Dower et al., 2000; Aiba et al., 2004; Brodie et al., 2004; Coughlin et al., 2005; Roose et al., 2005). RasGRPs are GEFs that activate Ras by a mechanism different than SOS, and it is thought that RasGRPs may begin converting Ras-GDP to Ras-GTP in response to stimulus first, and the activated Ras-GTP then binds the allosteric site of SOS and activates it (Roose et al., 2007).

RasGAPs, including GAPp120 and neurofibromin are important inactivators of Ras signaling since they catalyze hydrolysis of Ras-GTP to

Ras-GDP. How RasGAPs are regulated themselves is not clear, but phosphorylation appears to play a role since nuerofibromin is phosphorylated at several sites in its C-terminus by protein kinase A (PKA), which promotes its interaction with 14-3-3 proteins and correlates with a reduction in RasGAP activity (Feng et al., 2004). Phospholipids have also been shown to inhibit the catalytic activity of RasGAPs by physically interacting with the catalytic domain, however, this phenomenon has only been shown *in vitro* (Tsai et al., 1989; Bollag and McCormick, 1991; Serth et al., 1991). Thus, Ras-GEFs and Ras-GAPs are critical points of regulation of Ras signaling that are carefully regulated themselves to control the intensity and duration of Ras signals. Also, GEFs and GAPs are activated by phospholipids, localizing them to the membrane, which may also control localization of Ras signaling.

Sprouty proteins negatively regulate Ras signaling although the exact mechanism is unclear. It is known that Ras signaling induces Sprouty protein expression (Sprouty proteins 1-4), and it is thought that Sprouty protein binds GRB2, preventing SOS localization and activation of Ras (Hanafusa et al., 2002), or binds RAF, interfering with its interaction with downstream MEK (Sasaki et al., 2003; Kim and Bar-Sagi, 2004). Related to Sprouty proteins are the Spred proteins (Sprouty-related protein with an EVH domain 1-3) which, like Sprouty proteins, antagonize Ras signaling, however by different mechanisms. Spred proteins have been shown to directly bind to Ras, inhibit ERK activation in collaboration with caveolin-1, or bind and recruit neurofibromin to the membrane to inactivate Ras (Wakioka et al., 2001; Kato

et al., 2003; Nonami et al., 2005; Stowe et al., 2012). Sef is a single-pass transmembrane protein that inhibits FGFR to prevent Ras activation, resulting in decreased MEK, ERK, and AKT phosphorylation (Fürthauer et al., 2002; Tsang, 2004). Further downstream, PTEN is a major tumor suppressor that antagonizes PI3'K degradation of PIP2 to PIP3 and dephosphorylates downstream effectors of AKT thus inhibiting PI3'K/AKT/mTOR signaling (Castellano and Downward, 2011). Map kinase phosphatases (MKPs) specifically bind and dephosphorylate ERK. MKP1 deactivates ERK in the nucleus (Patil and Chamberlain, 2012; Sun et al., 1993) and MKP3 dephosphorylates ERK in the cytoplasm (Ruggieri and Packer, 2001; Muda et al., 1996). Thus, the Ras signaling pathway is regulated by multiple proteins that may be potential therapeutic targets. An in depth understanding of the Ras regulators is key to understand how the pathway may react to dysregulation at multiple points in development and cancer.

1.2.5 *Function of Ras Signaling*

The function of Ras signaling has been studied extensively in animal models. *KRas* null mice die of anemia and defective liver erythropoesis at E12-E14 (Eerola et al., 2003; Johnson et al., 1997; Koera et al., 1997), while *HRas* knock out and *HRas* and *NRas* double knock out mice are viable and fertile (Gripp, 2005; Umanoff et al., 1995; Esteban and Vicario-Abejón, 2001), revealing that in mice, the Ras proteins have both redundant and unique functions in development. When *HRas* was knocked into the *KRas* locus,

26

mice were viable, suggesting that Ras proteins have the capacity to compensate for each other, but endogenous HRras does not replace KRras because it is not expressed in the same embryonic compartment (Potenza et al., 2005). Other animal models have revealed the differences in activity of the Ras proteins. When activated *KRas*^{G12D} or *HRas*^{G12D} was expressed in the colonic epithelium, KRas induced hyperplasia and activated MEK/ERK while NRas did not (Haigis et al., 2008). Further experiments showed that NRas but not KRas suppressed apoptosis. Not only the *Ras* gene itself, but the regulatory elements controlling it determine function of the protein. An *HRas*^{KI} mouse, in which *HRas* was expressed under the control of the *KRas* regulatory elements, treated with urethane developed ten-fold more lung tumors than wild-type (To et al., 2008). Thus, *HRas*, which very rarely causes lung tumors at its endogenous locus, is able to induce tumors under the control of *KRas* regulatory elements, suggesting that not only the *Ras* gene itself but its regulatory elements control function. These studies in mouse models in which Ras signaling is disrupted highlight the differences among the Ras proteins in activity and regulation and emphasize the importance of further study to understand the different Ras proteins and their function in development and cancer.

Both *in vitro* and *in vivo* studies have revealed the role of Ras signaling in many cellular functions, including proliferation, differentiation, and cell polarity. *In vitro* studies have shown that p-ERK and p-AKT regulate proliferation by decreasing p27^{kip1} and p21^{cip1} levels to allow progression from

G$_0$ to S phase (Steelman et al., 2004; Meloche and Pouysségur, 2007). Ras may also play a role in differentiation, as in the case of a neurofibromatosis 1 null (*Nf1$^{-/-}$*) mouse model that is missing neurofibromin which result in increased Ras signaling, in which increased differentiation of neuroblasts into glial cells was observed, and the increased differentiation was rescued by inhibiting ERK (Wang et al., 2012). It is also thought that Ras signaling is important in cell polarity. Activation of KRAS and BRAF in a colon cancer cell line perturbs the polarity of cyst structures, and inhibition of ERK restores cyst polarity (Magudia et al., 2012). Activation of HRAS in cultured hippocampal neurons causes loss of polarity and multiple axon formation, and inhibition of MEK or PI3'K prevents multiple axon formation (Yoshimura et al., 2006). A recent *in vivo* study showed that ERK controls spindle orientation during cell division in the developing lung to determine lung shape (Tang et al., 2011). These studies have begun to shed light on the mechanistic role of Ras in cell biology; however, further study *in vivo* is required to understand the function of Ras signaling. Thus, in this thesis dissertation, I analyze the roles of the MAPK and PI3'K pathways in the mouse incisor, *in vivo*.

1.2.6 *RAS and Cancer*

Approximately 20-30% of tumors have mutations in *RAS* (Bos, 1989; Schubert et al., 2007b). The majority (85%) of these are *KRAS* mutations, 15% are in *NRAS*, and <1% are in *HRAS* (Downward, 2003). Some cancers have a high propensity for activating mutations in *KRAS*, such as pancreatic,

biliary tract, colon, lung, and endometrial cancers. *NRAS* mutations occur in melanoma and myeloid leukemia while *HRAS* mutations are found in bladder cancer (Schubbert et al., 2007a).

The most common mutations in Ras that cause cancer are at amino acids (aa) 12, 13, and 61. Mutations at aa12 and 13 that replace the glycine with a bulkier residue prevent GAP binding and GTP hydrolysis, resulting in a constitutively active GTP-bound Ras (Scheffzek et al., 1997). The glutamine at position 61 is also key for GTP hydrolysis, and thus, mutations at 61 result in Ras activation (Der et al., 1986). However, these Ras mutations also require a second hit mutation that activates an oncogene like Myc or inactivates a tumor suppressor like p53 (Sinn et al., 1987; Aguirre et al., 2003; Hingorani et al., 2005).

A major unanswered question in the Ras field is why do certain mutations in particular *RAS* genes cause particular cancers? The biology of the Ras proteins discussed above may give some insight into the localization and activity of the Ras proteins; however, it is an open and active area of research. Studies of Ras signaling in development by analyzing the RASopathies may provide new insights and approaches.

1.2.7 *Drugs Targeting the Ras Signaling Pathway to Treat Cancer*

The major goal in the cancer field is to develop drugs to improve outcomes for cancer patients, and because of its importance in cancer biology, many small molecules have been developed to target components of

29

the Ras signaling pathway. These have met with varying success in clinical trials for cancer. Early efforts focused on targeting oncogenic Ras itself and its fundamental defect of persistent binding to GTP. Small molecule GAPs that would hydrolyze and inactivate mutant Ras were developed as well as GTP competitive antagonists, however these approaches failed (Cox and Der, 2010). Moving forward, researchers focused on indirect approaches. A major hope in the field was the farnesyl transferase inhibitors (FTIs), including tipifarnib (Johnson & Johnson) and lonafarnib (Schering-Plough Research Institute) that inhibit post-translational modification of the Ras proteins by farnesyl transferases and thus disrupt the ability of the Ras proteins to associate with membranes, rendering them non-functional (Reiss et al., 1990). Mouse studies found FTIs to be effective against HRAS induced mammary gland tumors (Kohl et al., 1995), however, disappointingly, they were not effective against KRAS and NRAS due to the fact that KRAS and NRAS can be alternatively modified by geranylgeranyl transferase when farnesyl transferase is inhibited and still targeted to the membrane (Whyte et al., 1997; Fiordalisi et al., 2003). The ability of the Ras proteins most common in cancer to escape FTIs by undergoing alternative prenylation explains the failure of the FTIs in clinical trials to treat cancer (Macdonald et al., 2005).

In order to disable the alternative prenylation of KRAS and NRAS, geranylgeranyl transferase type I inhibitors (GGTIs) were developed; however, GGTIs affected other geranylgeranylated proteins and were found to be lethal in a mouse model (Lobell et al., 2001). Drugs were also developed to target

downstream effectors of Ras. Sorafenib (Onyx-Bayer), a type 2 kinase inhibitor, was the first MAPK pathway inhibitor to be approved by the FDA to treat renal cell and hepatocellular carcinoma (Abou-Alfa, 2009), and it has been shown to be a multi-targeted kinase inhibitor active against CRAF but less active against BRAF. However, it is thought that its anti-tumor effect is actually due to its effect on RTK receptors for VEGF and PDGF and resultant disruption of tumor angiogenesis rather than direct effects on BRAF (Wilhelm et al., 2004). PLX4032 (Plexxikon/Roche) was developed to target BRAFV600E and has shown promise in treating patients with malignant melanoma (Bollag et al., 2010). Toxicities include fatigue, rash, and joint pain, and about one third of patients developed keratoacanthoma type skin lesions, which are a class of cutaneous squamous cell carcinomas (Bollag et al., 2010). The development of other skin carcinomas may be due to the fact that, paradoxically, inhibiting BRAFV600E results in increased activation of endogenous BRAF (Hatzivassiliou et al., 2010; Poulikakos et al., 2010).

MEK inhibitors have been developed that bind an interior hydrophobic pocket of MEK adjacent to the ATP binding site, making MEK inhibitors quite specific (Ohren et al., 2004). CI-1040 (Pfizer) was the first MEK inhibitor in clinical trials (Sebolt-Leopold et al., 1999), however, it did not show sufficient anti-tumor activity in phase II trials and was discontinued (Rinehart et al., 2004). CI-1040 spurred the development of additional MEK inhibitors with increased potency and improved pharmacological properties that are currently in clinical trial, including PD0325901 (Pfizer), AZD6244

(AstraZeneca/Array BioPharma), and GSK1120212 (GlaxoSmithKline). These MEK inhibitors have shown some efficacy in melanoma patients and minimal side effects including rash, diarrhea, and some visual disturbances (Sebolt-Leopold, 2008). Dual PI3'K-mTOR inhibitors including SF-1124 (Semafore) and XL765 (Exelixis) and pan-PI3'K inhibitors like PX-866 (Oncothyreon) (Hong et al., 2012) and GDC-0941 (Genentech) (Folkes et al., 2008) have shown potential in preclinical trials and are currently being tested in clinical trials (Courtney and Corcoran, 2010). There are also AKT inhibitors including MK-2206 (Merck), which was shown to decrease AKT levels and cause some adverse effects including rash, diarrhea, and hyperglycemia in phase I clinical trials (Yap et al., 2011).

New approaches to target Ras in cancer are currently in development. Recently, a new small molecule that inhibits the prenyl binding protein PDEδ, which facilitates KRAS diffusion to the plasma membrane, was shown to localize KRAS to endomembranes, inhibit KRAS signaling, and suppress proliferation of oncogenic KRAS induced human pancreatic ductal adenocarcinoma cells *in vitro* and *in vivo* (Zimmermann et al., 2013). Thus, disrupting the localization of Ras proteins to inhibit their activity may be a new approach to target Ras signaling in cancer. A more recent large scale, unbiased approach to target Ras is RNA interference screens based on the concept of synthetic lethality, in which two genes that when mutated alone are compatible with life but when both harbor mutations lead to death (Luo et al., 2009). Hence, screens were set up to determine genes that when mutated in

32

cells with activating mutations in *RAS* genes would be lethal. One gene identified with such a screen was STK33 (Scholl et al., 2009), however, efforts to inhibit STK33 have been shown to have no effect on KRAS-dependent cancer cell viability (Luo et al., 2012). Other genes revealed by this type of screen, like TANK-binding kinase 1 (TBK1), may have potential as therapeutic targets (Barbie et al., 2009). Thus, genetic screens may reveal new therapeutic targets of Ras in cancer, and additionally delving deeper to further understand Ras and its effectors and exploring disrupted Ras signaling in patients like CS and CFC individuals will provide new approaches to targeting Ras in cancer.

The fact that small molecules developed to target Ras and its effector pathways in the last 20 years have had little success in the treatment of cancer emphasizes the importance of determining which Ras pathway components to target. Clearly, targeting certain mechanisms like Ras farnesylation have failed or inhibiting pathway components like BRAF have had unexpected consequences, and so it is critical to further study Ras and its signaling pathways *in vivo* to develop new potential therapeutic targets and understand the repercussions of disrupting Ras signaling.

There is the possibility that small molecules developed to treat Ras in cancer may be useful in other developmental syndromes. For example, an unexpected, fortuitous outcome of FTI development is that FTIs may be useful in treating Hutchinson-Gilford Progeria Syndrome (Progeria), which is a rare, fatal genetic condition characterized by accelerated aging in children.

Progeria is caused by incomplete farnesylation of lamin A, resulting in accumulation of farnesylated lamin A called progerin, and mouse studies have shown FTIs to be effective in preventing this accumulation, and FTIs are currently in clinical trials for Progeria (Worman et al., 2009). Thus, drugs developed targeting the Ras pathway may be useful in other developmental syndromes, like the RASopathies.

1.3 The RASopathies: Dysregulation of Ras Signaling in Humans

1.3.1 *The RASopathies*

Dysregulation of Ras signaling can have major consequences during development, as exemplified by the RASopathies. The RASopathies are a group of syndromes characterized by activated Ras signaling which include Noonan syndrome (NS), LEOPARD syndrome (LS), hereditary gingival fibromatosis (HGF), neurofibromatosis type 1 (NF1), capillary malformation-arteriovenous malformation syndrome (CM-AVM), Legius syndrome, cardio-facio-cutaneous syndrome (CFC), and Costello syndrome (CS) (Tidyman and Rauen, 2009) (Figure 1.6). It is fascinating that the RASopathies, which are caused by mutations in the same Ras pathway, have both distinct and overlapping features, emphasizing the complexity of the Ras pathway in development.
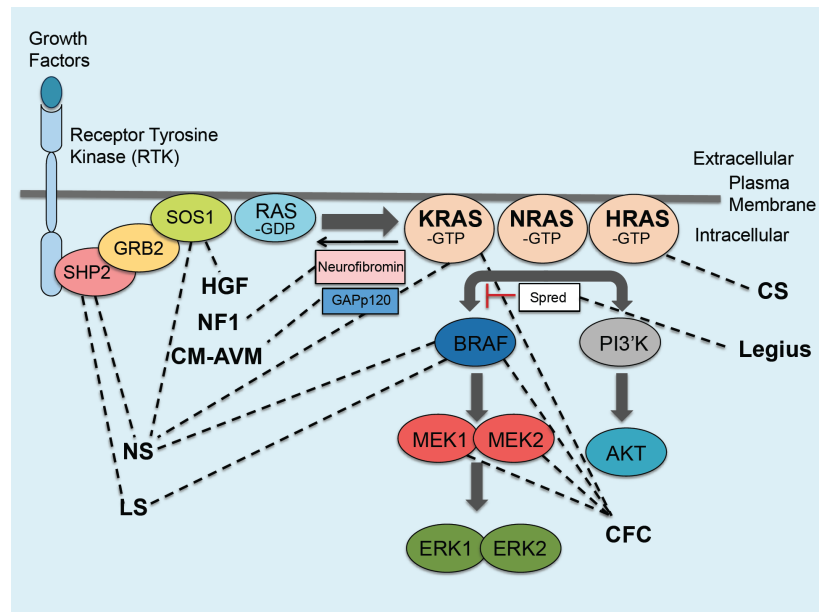
Figure 1.6 The RASopathies. Diagram of the Ras signaling pathway with dashed lines connecting the specific RASopathy with the protein in the pathway encoded by the causative mutated gene. Adapted from Tidyman and Rauen, 2009.

35

Noonan syndrome (NS) is an autosomal dominant disorder characterized by distinctive craniofacial features, short stature, congenital heart defects, renal anomalies, lymphatic malformations, bleeding disorders, and neurocognitive delay (Roberts et al., 2013). NS is caused by heterozygous *de novo* germline mutations in *PTPN11, KRAS, SOS1*, and *RAF1* (Tartaglia et al., 2001; Schubbert et al., 2006; Roberts et al., 2006b; Tartaglia et al., 2007; Pandit et al., 2007; Razzaque et al., 2007). Gain of function missense mutations in *PTPN11*, which encodes SHP2, are most commonly associated with NS, accounting for half of known cases. *PTPN11* mutations result in a SHP2 protein locked in the catalytically active state, resulting in increased Ras signaling (Tartaglia et al., 2006). *SOS1* missense mutations are the second most common, accounting for 13% of cases, and are thought to result in decrease in the auto-inhibition of the SOS1 protein and increased Ras signaling. *KRAS* mutations are only associated with <2% of cases. LEOPARD syndrome (LS) is a rare autosomal dominant disorder with a similar phenotype to NS, and the acronym LEOPARD describes the phenotype: Lentigines, EKG abnormalities, Ocular hypertelorism, Pulmonary valve stenosis, Abnormal genitalia, Retardation of growth, and Deafness (Sarkozy et al., 2008). LS, like NS, is caused by heterozygous missense mutations in *PTPN11* (Digilio et al., 2002; Legius et al., 2002); however, LS *PTPN11* mutations result in a SHP2 protein with decreased catalytic activity (Kontaridis et al., 2006) unlike gain-of-function mutations in NS, but both mutations result in increased Ras signaling. LS is also associated with *RAF1*

mutations (Pandit et al., 2007). Hereditary gingival fibromatosis (HGF) is characterized by slow growing, benign fibrous overgrowth of the keratinized gingiva. HGF is caused by a mutation in *SOS1* that results in a truncated SOS1 protein and activated RAS signaling (Hart et al., 2002; Peterkova et al., 2009). Interestingly, unlike NS, the *SOS1* mutations in HGF only cause gingival overgrowth and no other developmental anomalies.

Neurofibromatosis type 1 (NF1) is an autosomal dominant inherited disorder, and the phenotype includes café-au-lait maculae, intertriginous freckling, plexiform neurofibromas, iris Lisch nodules, osseous dysplasia, and optic pathway glioma (Rauen, 2007; Williams et al., 2009). NF1 is caused by germline mutations in *NF1* which encodes neurofibromin, a GTPase activating protein (GAP) that converts active Ras-GTP to inactive Ras-GDP, and loss of function of neurofibromin in NF1 results in constitutively active Ras-GTP and increased signaling (Tidyman and Rauen, 2009; Wallace et al., 1990; Cawthon et al., 1990; Viskochil et al., 1990). Capillary malformation-arteriovenous malformation syndrome (CM-AVM) is an autosomal dominant inherited disorder characterized by multifocal capillary malformations in many tissues including skin, muscle, bone, heart, and brain, which may be associated with arteriovenous malformations and fistulas (Tidyman and Rauen, 2009; Boon et al., 2005). Like NF1, CM-AVM is caused by inactivating mutations in a gene encoding a RasGAP, in the case of CM-AVM, a mutation in *RASA1* encoding RasGAPp120 (Eerola et al., 2003).

37

Legius syndrome (neurofibromatosis 1-like) is an autosomal dominant disorder that shares many phenotypic features with NF1, including café-au-lait maculae, axillary freckling, mild cognitive impairment, and macrocephaly. Legius syndrome is caused by heterozygous mutations in *SPRED1*, which encodes Spred1, a protein that antagonizes the Ras pathway (Brems et al., 2007). Truncation of the protein in Legius results in loss of function of Spred1 and activation of Ras signaling.

Cardio-facio-cutaneous syndrome (CFC) has a characteristic facies and congenital heart defects, including pulmonary valve stenosis, hypertrophic cardiomyopathy, and atrial septal defects (Armour and Allanson, 2008). Abnormalities of the skin, including keratosis pilaris, hyperkeratosis, and nevi; eyes, like optic nerve hypoplasia; and gastrointestinal tract are common to CFC (Roberts et al., 2006a). Individuals with CFC also have neurologic abnormalities to a varying degree, including hypotonia, motor delay, speech delay, and/or learning disabilities (Yoon et al., 2007). CFC is caused by mutations in genes encoding proteins in the MAPK pathway: BRAF, MAP2K1, MAP2K2, and KRAS (Niihori et al., 2006; Rodriguez-Viciana, 2006). The majority of CFC cases, 75%, are caused by mutations in *BRAF*, resulting in BRAF proteins with increased kinase or kinase-impaired activity; either of these cause dysregulated MAPK signaling. The remaining 25% of CFC cases are caused by activating missense mutations in MEK1 and MEK2. The association of *KRAS* mutations in CFC is unclear because individuals with NS have also been diagnosed with *KRAS* mutations.

Costello syndrome (CS) is characterized by distinct craniofacial dysmorphia, musculoskeletal anomalies including abnormal muscle fiber size and predominance of type 2 fibers, and peripheral muscle weakness (Chen et al., 2009; Tidyman et al., 2011; Stevenson et al., 2012). Dermatological abnormalities like loose redundant skin on hands and feet and cutaneous papilloma and palmoplantar keratoderma (Rasband; Siegel et al., 2012) are associated with CS. Cardiac anomalies include structural defects, hypertrophic cardiomyopathy, and arrhythmias (Karlsson, 2010; Lin et al., 2002). CS individuals also have severe failure to thrive, neurologic deficits like hypotonia and a varying degree of cognitive impairment, and increased risk of cancer development (Resende et al., 2011; Rauen, 2007). CS is caused by a heterozygous *de novo* germline mutation in *HRAS* that results in a constitutively active Ras protein (Gibson et al., 2001; Aoki et al., 2005; Fukumoto, 2004). Nearly 85% of individuals with CS have a G12S substitution caused by nt34G-A transition in codon 12 of exon 1 of the *HRAS* gene (Moffatt et al., 2008; Aoki et al., 2008; Iwasaki et al., 2005) while others have a G12A or G13D substitution. This mutation causes a change in the purine ring binding pocket of the Ras protein which affects stability of GDP binding. The GDP-bound inactive form is destabilized so that GTP binds, locking Ras in the active GTP-bound state without RasGEF and resulting in a constitutively active Ras protein (Chen et al., 2009; Zampino et al., 2007).

1.3.2 *Malignancy in the RASopathies*

The incidence and tissue specificity of malignancy vary greatly among the RASopathies. In NF1 the incidence of malignancy is estimated between 4 and 52%, and NF1 individuals develop, most commonly, malignant peripheral nerve sheath tumors (MPNSTs) and also rhabdomyosarcoma, gastrointestinal stromal tumors, neuroectodermal tumors, pheochromocytomas, and breast carcinoma (Li et al., 2012; Patil and Chamberlain, 2012). MPNSTs that usually occur in adulthood manifest earlier in life, nearly a decade earlier in the case of MPNSTs in NF1, and adult tumors occurring early in life is also observed in other RASopathies. NF1 individuals are heterozygous for an NF1 mutation, having one normal and one mutated copy of NF1, and NF1 patients develop cancer when a mutation arises in the normal NF1 copy, which is a loss of heterozygosity (LOH) (Jheon et al., 2011; Ruggieri and Packer, 2001). CM-AVM is associated with increased risk of central nervous system tumors, similar to those in NF1 (Hu et al., 2007; Eerola et al., 2003). It is estimated that 15-20% of CS individuals develop malignancy, most commonly rhabdomyosarcoma and then neuroblastoma and bladder cancer (Takamori et al., 2008; Gripp, 2005). As mentioned above, nearly all CS individuals have a G12S mutation rather than the G12V mutation found in cancer, suggesting the G12S mutation is less oncogenic than G12V, and the reason for this difference in activity is not known. The valine residue may disrupt GAP binding more and hence increase the RasGTP pool compared to the serine residue. NS is associated

with blood disorders including juvenile myelomonocytic leukemia (JMML), acute lymphoblastic leukemia (ALL), and acute myeloid leukemia (AML), and there have also been reports of solid tumors in NS patients including rhabdomyosarcoma and neuroblastoma (Tsuboi et al., 2003; Gelb, 2006). While there have been a few case reports of leukemias in LS and CFC, it is not clear at this point whether these syndromes are associated with cancer, and individuals with HGF and Legius do not appear to be at higher risk for developing malignancy.

1.3.3 *CS and CFC Mouse Models*

There are multiple mouse models for the RASopathies. These models have expanded our understanding of the syndromes, and here, CS and CFC mouse models are discussed. CS mouse models have been developed that express an $HRAS^{G12V}$ mutation (Welch et al., 2003; Chen et al., 2009; Schuhmacher et al., 2008). Although 80% of individuals with CS carry an $HRAS^{G12S}$ mutation (Huang et al., 2011; Estep et al., 2006; Gripp et al., 2005; Kerr, 2005), the $HRAS^{G12V}$ mouse model is useful because it phenocopies many aspects of the syndrome, including growth delay, macrocephaly, and craniofacial anomalies. The CS mouse model utilized in data presented in this thesis dissertation develops papillomas (Magudia et al., 2012; Chen et al., 2009), and the other mouse model develops cardiac hypertrophy and hypertension (Yoshimura et al., 2006; Schuhmacher et al., 2008). A CFC mouse model was generated by germline expression of one allele of

41

$BRAF^{V600E}$. Although $BRAF^{V600E}$ is not a mutation reported in CFC, the mouse model phenocopied some of the characteristics of CFC including reduced life span, small size, craniofacial dysmorphia, cardiomegaly, and epileptic seizures (Wodarz, 2002; Urosevic et al., 2011). However, these mice also developed neuroendocrine tumors, which are not observed in CFC patients. A more recent CFC conditional knock in mouse model that expresses a $BRAF^{L597V}$ allele reported in CFC patients was developed. This model more closely mimics the cardiac abnormalities and craniofacial dysmorphia of CFC (Sasaki, 2004; Andreadi et al., 2012).

1.3.4 *Potential Therapeutics for the RASopathies*

Many inhibitors targeting components of the Ras pathway have been developed to treat cancer (Gysin et al., 2011), and these same inhibitors may have therapeutic potential in the RASopathies (Rauen et al., 2011). Since the individual RASopathies are rare, development of treatments specifically for these syndromes would most likely not happen, so it is fortuitous that the decades of study of Ras signaling and development of small molecules targeting Ras may have potential to treat these individuals who otherwise would not have hope for a treatment. Additionally, there are many animal models for the RASopathies as described above that provide the opportunity to test the safety and efficacy of drugs in animals before treating patients in clinical trials. Animal studies have provided proof of principle for treating RASopathies with inhibitors of Ras signaling. Treating a neurofibromatosis

42

type 1 (NF1) mouse model, with conditional inactivation of *Nf1* in hematopoietic cells that develops JMML, with a MEK inhibitor (PD0325901) resulted in decreased leukocyte counts, enhanced erythropoietic function, and reduced spleen size (Steelman et al., 2004; Chang et al., 2013; Meloche and Pouysségur, 2007). In another *Nf1*^{-/-} mouse that develops neurofibromas, treatment with PD0325901 reduced neurofibroma growth and proliferation (Wang et al., 2012; Jessen et al., 2013). A NS mouse model with a *Sos1* gain-of-function mutation showed many NS phenotypes, including growth delay, craniofacial dysmorphia, hematologic abnormalities, and cardiac defects, and treatment with PD0325901 ameliorated embryonic lethality, craniofacial dysmorphia, and heart defects (Gysin et al., 2011; Chen et al., 2010). A CFC zebrafish model expressing a kinase-activating BRAF[Q257R] allele or kinase-inactivating BRAF[G596V] allele developed craniofacial anomalies, and moreover, these defects were ameliorated by treatment with low doses of MEK inhibitor at early stages of development (Rauen et al., 2011; Anastasaki et al., 2012). It is astonishing that in these RASopathy animal models, inhibition of Ras signaling reversed many of the phenotypes associated with these syndromes, providing hope for the use of these drugs to potentially treat RASopathy patients. Further work is necessary to identify the most promising drugs and dosage to treat the RASopathies, and luckily, there are animal models to do so. The potential to actually treat the RASopathies is a wonderful hope for both individuals with RASopathies and their families.

43

In the following chapters, I report the craniofacial and dental phenotypes of CFC (Chapter 2) and CS (Chapter 3) and analyze the hypoplastic enamel defect observed in CS subjects in a CS mouse model, revealing a role for Ras signaling in amelogenesis (Chapter 4). Finally, I discuss the importance of this dissertation work in advancing our understanding of Ras signaling in tooth development and the application of this knowledge to the development of teeth and other organs, the RASopathies, and cancer (Chapter 5).

CHAPTER 2:

Craniofacial and Dental Development in Cardio-facio-cutaneous Syndrome: The Importance of Ras Signaling Homeostasis

In this chapter, I report the craniofacial and dental phenotype of CFC for the first time. This work was published in Clinical Genetics, June 2013.

Alice F. Goodwin[1,2], Snehlata Oberoi[1,2], Maya Landan[1,2], Cyril Charles[1,2], Jessica Groth[1,2], Anna Martinez[3], Cecilia Fairley[1,2], Lauren A. Weiss[4,5], William E. Tidyman[1,2], Ophir D. Klein[1,2,3,5] and Katherine A. Rauen[3,5]

[1]Department of Orofacial Sciences, University of California San Francisco, San Francisco, CA

[2]Program in Craniofacial and Mesenchymal Biology, University of California San Francisco, San Francisco, CA

[3]Department of Pediatrics, Division of Medical Genetics, University of California San Francisco, San Francisco, CA

[4]Department of Psychiatry, University of California San Francisco, San Francisco, CA

[5]Institute for Human Genetics, University of California San Francisco, San Francisco, CA

2.1 ABSTRACT

Cardio-facio-cutaneous syndrome (CFC) is a RASopathy that is characterized by craniofacial, dermatologic, gastrointestinal, ocular, cardiac, and neurologic anomalies. CFC is caused by activating mutations in the RAS/mitogen-activated protein kinase (MAPK) signaling pathway that is downstream of receptor tyrosine kinase (RTK) signaling. RTK signaling is known to play a central role in craniofacial and dental development, but to date, no studies have systematically examined individuals with CFC to define key craniofacial and dental features. To fill this critical gap in our knowledge, we evaluated the craniofacial and dental phenotype of a large cohort (n=32) of CFC individuals who attended the 2009 and 2011 CFC International Family Conferences. We quantified the craniofacial features in CFC which include macrocephaly, bitemporal narrowing, convex facial profile, and hypoplastic supraorbital ridges. In addition, there is a characteristic dental phenotype in CFC that includes malocclusion with open bite, posterior crossbite, and a high-arched palate. This thorough evaluation of the craniofacial and dental phenotype in CFC individuals provides a step forward in our understanding of the role of RTK/MAPK signaling in human craniofacial development and will aid clinicians who treat patients with CFC.

2.2 INTRODUCTION

Cardio-facio-cutaneous syndrome (CFC) is a multiple congenital anomaly disorder characterized by craniofacial malformation, ectodermal abnormalities, congenital heart defects, growth delays, and neurocognitive deficits. CFC is one of the RASopathies, which also include neurofibromatosis type 1 (NF1), Noonan syndrome (NS), NS with multiple lentigines, capillary malformation-AV malformation syndrome, Legius syndrome, and Costello syndrome (CS). The common feature of the RASopathies is that they are caused by germline mutations that result in dysregulation of the Ras/mitogen-activated protein kinase (MAPK) pathway (Tidyman and Rauen, 2009). CFC is caused by heterozygous, activating, germline mutations in *KRAS*, *BRAF*, *MAP2K1* (*MEK1*), or *MAP2K2* (*MEK2*), all of which are components of the RAS/MAPK pathway (Niihori et al., 2006; Rodriguez-Viciana, 2006).

Many of the phenotypic features in these syndromes overlap, and the craniofacial phenotypes of several of the RASopathies are in fact so similar that making a definitive syndromic diagnosis can prove difficult. Careful examination of the craniofacial characteristics is critical in order to formulate an accurate diagnostic plan prior to molecular testing. However, to date, a systematic analysis of the craniofacial characteristics of each of the RASopathies in a large cohort is lacking, and such analyses will be essential for identification of unique craniofacial characteristics that may serve as useful diagnostic markers and guide genetic testing.

Receptor tyrosine kinase (RTK) signaling upstream of the Ras/MAPK pathway is known to play a central role in craniofacial and dental development. Fibroblast growth factors (FGFs), which initiate signaling through RTKs, are involved in the interactions between epithelium and mesenchyme that guide development of almost all structures of the craniofacial complex, including teeth (Pispa and Thesleff, 2003; Nie et al., 2006). In addition, mice carrying mutations in Sprouty genes, which encode proteins that negatively regulate RTK and RAS/MAPK signaling, have anomalies in both tooth number and morphology (Klein et al., 2006; 2007; Peterkova et al., 2009).

Considering the central role that RTK signaling plays in craniofacial development and the value of a detailed characterization of the craniofacial and dental phenotypes present in the different RASopathies, we sought to thoroughly examine the phenotypic features in individuals with CFC. Although previous studies have noted the major craniofacial features in CFC, no studies have systematically characterized both the craniofacial and dental phenotypic features present in CFC in a large cohort of subjects. To fill this critical gap in our knowledge and provide new insight into the effects of activated RTK/MAPK signaling in craniofacial and tooth development, we performed comprehensive craniofacial and dental exams on 32 CFC individuals.

48

2.3 MATERIALS AND METHODS

This study was approved by the UCSF Committee on Human Research. A total of 32 individuals with a clinical diagnosis of CFC were examined during the 5th International CFC Family Conference in Berkeley, California in 2009 (Anastasaki et al., 2012; Rauen et al., 2010) and the 6th CFC International Family Conference in Chicago, Illinois in 2011. The diagnoses were confirmed by a board certified medical geneticist (K.A.R. or O.D.K.) based on clinical features. Of the 32 participants enrolled in our study, 28 of the 32 (88%) had a known mutation in a gene that is causative for CFC, including *BRAF* (n=21), *MEK1* (n=2), *MEK2* (n=4), and *KRAS* (n=1). The cohort consisted of 16 males and 16 females. The average age of the cohort was 8 years, with a range of 2 to 27 years of age. The majority of the cohort reported Caucasian race (84%) but also included were Latino (6%), African (3%), and Middle Eastern (3%) individuals; the race of one subject was not reported. Written informed consent was obtained for all subjects. Complete intra- and extra-oral exams were preformed by a licensed dentist (A.F.G., S.O. or J.G.). Exams included frontal and side view craniofacial photographs (one patient declined photographs). When possible, intra- and extra-oral photographs were taken, radiographs (including panoramic, periapical, and bitewing radiographs) and dental records provided by the participant were reviewed, and alginate dental impressions were taken. The total number of patients examined for each dental characteristic is listed in Table 2. When possible, participants' parents and/or siblings were also

examined as controls (n=43). Statistical comparison between the dental phenotype of the CFC cohort and general U.S. population as determined by the NHANES III survey (Proffit et al., 2006) was made using the Fisher's exact test with 2-tailed p-value. The same statistical test was used to compare the major craniofacial and dental characteristics between individuals with *BRAF*, *MEK1*, and *MEK2* mutations.

2.4 RESULTS

2.4.1 Craniofacial phenotype of CFC

Individuals with CFC have a distinct craniofacial phenotype (Figure 2.1). The main craniofacial findings observed in ≥50% of subjects examined are summarized in Table 2.1. The majority of subjects presented with relative macrocephaly (97%), high forehead (84%), and bitemporal narrowing (84%; Figure 2.1). Most subjects had a convex (74%) facial profile (Figure 2.1). A few subjects (10%) presented with micrognathia or a small mandible, but most appeared to have a proportionally sized mandible. A significant number of subjects had hypoplasia of the superior orbital ridge (52%; Figure 2.1). Subjects also commonly had a hyperteloric (65%) and telecanthic (100%) appearance (Figure 2.1). Other common features were a short nose (71%), with a depressed nasal bridge (65%) and wide nasal tip (65%), and low-set (90%), posteriorly rotated (84%) ears with upturned lobes (52%; Figure 2.1).

Figure 2.1 Craniofacial phenotype of CFC. Frontal and profile images of individuals with CFC demonstrate the craniofacial phenotype. Note how craniofacial features change as CFC individuals age. (A) A 2 year-old girl with the common CFC craniofacial features including relative macrocephaly and short nose with depressed nasal bridge and wide nasal tip. (B) A 15 year-old female with high forehead, bitemporal narrowing, and low set, posteriorly rotated ears with upturned lobes. (C) A 12 year-old boy with hypoplasia of the superior orbital ridge. (D) A 15 year-old boy with a convex facial profile and hyperteloric and telecanthic appearance typical of CFC.

Table 2.1 Summary of craniofacial findings in a cohort of 31 individuals with cardio-facio-cutaneous syndrome (CFC).

Craniofacial Findings	n	%
Relative Macrocephaly	30	97
High Forehead	26	84
Bitemporal narrowing	26	84
Convex facial profile	23	74
Hypoplasia of superior orbital ridge	16	52
Hyperteloric appearing	20	65
Telencanthic appearing	31	100
Depressed nasal bridge	20	65
Short nose	22	71
Wide nasal tip	20	65
Low set ears	28	90
Posteriorly rotated ears	26	84
Upturned lobe	16	52

2.4.2 Dental phenotype of CFC

We next examined the dentition and found that individuals with CFC have a recognizable and characteristic dental phenotype (Table 2.2; Figure 2.2). An open bite, when the anterior teeth are not in contact when the posterior teeth are in occlusion, was a common vertical malocclusion that was observed in 37% of our cohort (Figure 2.2C). This incidence is significantly higher than the national average (3%; p=0.0001)(Proffit et al., 2006). In contrast, a deep bite, which is an increased overbite in which the maxillary anterior teeth cover the mandibular teeth by more than 2 mm, was significantly less common among our subjects (19%) than in the general population (49%; p=0.0001; Figure 2.2A)(Proffit et al., 2006). Posterior crossbite, a condition in which the maxillary posterior teeth are on the lingual (i.e. toward the tongue) side of the mandibular teeth instead of the normal buccal (i.e. toward the cheek) side, was significantly more common in the CFC cohort (19%) than in the general U.S. population (9%; p=0.032; Figure 2.2B)(Proffit et al., 2006).
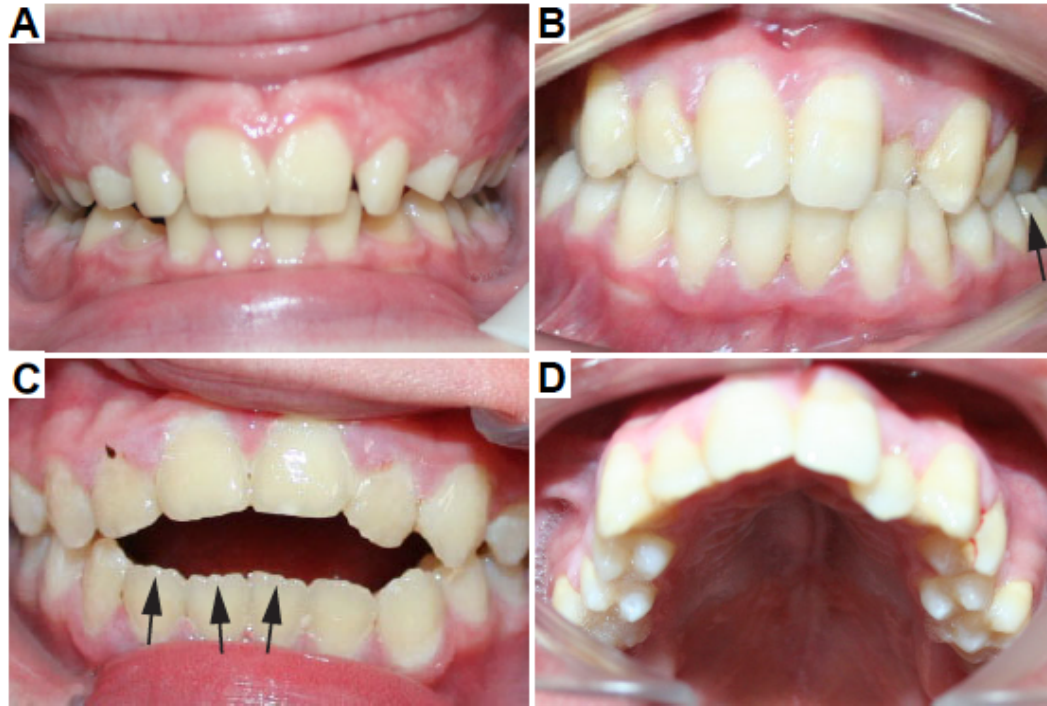
Figure 2.2 Dental phenotype of CFC. Intra-oral photographs showing the typical dental phenotypes in CFC. (A) A deep bite in which the maxillary incisors cover the mandibular incisors by more than 2 mm. (B) A posterior crossbite on the patient's left side is marked by the black arrow and is typically seen in CFC. (C) Open bite, with space between the anterior teeth while the posterior teeth are in contact. Note the mamelons or ridges on the incisal edges of the mandibular incisors (black arrows) which are normally worn down by abrasion of opposing teeth when the teeth are in contact. (D) High-arched palate.

A majority of subjects had class I molar relationship (54%), which is the ideal molar relationship according to the Angle's classification system (Riolo, 2002). In this relationship, the mesiobuccal (anterior, cheek side) cusp of the maxillary first molar aligns with the buccal side groove in the middle of the mandibular first molar so that the maxillary first molar and mandibular first molar are aligned. The percent of subjects with class I molar relationship is not significantly different from the 41% of the U.S. population with class I molar relationship (p=0.089)(Proffit et al., 2006). The percentage of subjects with class II molar relationship (46%), in which the maxillary first molar is positioned mesially (anteriorly in the mouth) to the mandibular first molar, is also similar to the national average (53%; p=0.396)(Proffit et al., 2006). No CFC individuals presented with class III molar relationship, in which the maxillary first molar is positioned distally (posteriorly) to the mandibular first molar; this is significantly less than the U.S. average (6%; p=0.029) (Proffit et al., 2006).

Dental crowding was only seen in 25% of our CFC cohort compared to about 60% of the U.S. population (p=0.0001)(Proffit et al., 2006). Only one subject presented with missing teeth (a 17 year-old male missing a maxillary central incisor), and none presented with supernumerary teeth, based on clinical examinations and review of radiographs, including periapical (n=4) and panoramic (n=2) x-rays (Table 2.2). Examination of panoramic x-rays for two CFC subjects indicated that dental development was not delayed, but followed typical timing. Eruption patterns were observed by assessing the

teeth present in relationship to the age of the individual examined and comparing to the normal eruption pattern (Pinkham et al., 2012). Most CFC individuals (87%) did not show delayed eruption patterns. The enamel appeared clinically normal. The majority of subjects had a constricted high-arched palate (80%; Figure 2.2D). The labial frenal attachment was high (62%), at the level of the unattached gingiva near the buccal fold, more often than low (38%), at the attached gingiva near the teeth, and only one subject (3%) presented with gingival hyperplasia defined as overgrowth of gingival tissue. The one subject who presented with gingival hyperplasia reported taking verapamil, a calcium channel blocker that has been reported to cause gingival swelling (Miller and Damm, 1992). Twenty-five percent of CFC individuals examined had clinical caries present, and 57% had a history of caries according to dental records. Subjects also presented with habits including a secondary tongue thrust (23%) and open mouth posture (28%). In addition, bruxism, as determined clinically by pathologic wear of the teeth, was present in 10% of our cohort.

We next compared the incidence of the major craniofacial and dental characteristics between individuals with *BRAF*, *MEK1*, and *MEK2* mutations to determine genotype-phenotype correlations. Individuals with *BRAF* mutations had a significantly higher incidence (92%) of high-arched palate compared to *MEK1*- (0%) or *MEK2*-positive individuals (0%; p=0.03). No other craniofacial or dental characteristics differed significantly between individuals with these mutations.

57

Table 2.2 Summary of the dental characteristics in cardio-facio-cutaneous syndrome (CFC).

Dental Findings	CFC			General Population[b]	p-value[c]
	Affected	Total Examined[a]	%	%	
Malocclusion					
Vertical					
Open bite	10	27	37	3	0.0001*
Deep bite	5	27	19	49	0.0001*
Transverse					
Posterior Crossbite	4	21	19	9	0.032*
Anterior/Posterior/Sagittal					
Molar relationship					
Class I	7	13	54	41	0.089
Class II	6	13	46	53	0.396
Class III	0	13	0	6	0.029*
Arch perimeter					
Crowding	8	32	25	60	0.0001*
Spacing	7	32	22	N/A[d]	
Dental development					
Missing teeth	1	31	3	N/A	
Supernumerary teeth	0	31	0	N/A	
Delayed development	0	2	0	N/A	
Delayed eruption	4	32	13	N/A	
Hard tissue					
High arched palate	16	20	80	N/A	
Soft tissue					
Frenal attachment					
High	13	21	62	N/A	

58

Low	8	21	38	N/A	
Gingival hyperplasia	1	31	3	N/A	
Pathology					
Caries present at exam	7	28	25	N/A	
History of caries	4	7	57	N/A	
Habits					
Tongue thrusting	7	31	23	N/A	
Open mouth posture	9	32	28	N/A	
Bruxism	3	31	10	N/A	

[a] Number of CFC individuals examined for each dental characteristic since dental exams were not completed on every CFC individual in the cohort

[b] Prevalence of dental characteristic in general population as determined by the NHANESIII survey (Hanna et al., 2010; Proffit et al., 2006)

[c] Comparison of incidence of dental characteristic in CFC cohort compared to general population using the Fisher's exact test with 2-tailed p-value

* significant p-value<0.05

[d] N/A Data not available

2.5 DISCUSSION

CFC is a RASopathy caused by activating mutations in *KRAS*, *BRAF*, *MEK1*, or *MEK2*. RAS/MAPK signaling is known to be critical in craniofacial and tooth development, and dysregulation of the RAS/MAPK pathway in these syndromes results in craniofacial dysmorphia. Constitutive activation of the Ras/MAPK pathway affects craniofacial development, yet the mechanism by which this happens is still unclear. It is interesting that although the RASopathies are caused by mutations in the same pathway, the different syndromes have many unique craniofacial characteristics. For example, Costello Syndrome (CS) is caused by heterozygous de novo germline mutations in the small GTPase HRAS, which is upstream of the kinases BRAF, MEK1, and MEK2, mutations in which cause CFC. However, CS and CFC have distinct craniofacial characteristics, especially as individuals age. These differences are significant enough to be useful to clinically differentiate and diagnose individuals with these syndromes. In this study, we quantified the typical CFC craniofacial features in our cohort including macrocephaly, bitemporal narrowing, convex facial profile, and hypoplastic supraorbital ridges (Table 2.1 and Figure 2.1), which lays the groundwork for the systematic analysis of the craniofacial features of the various RASopathies and provides insight into the role of RAS/MAPK signaling in craniofacial development.

This study is the first to systematically evaluate the dental phenotype of any RASopathy, and we have determined that RAS/MAPK pathway

dysregulation in CFC causes an abnormal oral phenotype. Determining the dental phenotypes associated with each of the RASopathies and correlating these phenotypes with the diverse spectrum of mutations that underlie RAS/MAPK dysregulation will be essential in furthering our understanding of this pathway in tooth development. Like individuals with CFC, mice carrying deletions in Sprouty genes have hyperactive MAPK pathway signaling. In these mice, hyperactive MAPK signaling results in supernumerary teeth (Klein et al., 2006; Charles et al., 2011). Therefore, we expected that individuals with CFC, who have activating mutations in the MAPK pathway, would similarly have supernumerary teeth. However, to our surprise, individuals with CFC did not present with anomalies in tooth number, size or morphology. In addition, these individuals had a normal pattern of tooth development and eruption, and their enamel and gingival architecture appeared normal. There were, however, abnormal dental characteristics more commonly observed in CFC than in the general population, most of which affected occlusion. Individuals with CFC had a fairly normal molar relationship, with a normal distribution of class I and class II but a significantly lower incidence of class III molar relationship compared to the general population (Table 2.2 and Figure 2.2). Individuals with CFC also had a significantly higher incidence of malocclusion than the general population, including anterior open bite and posterior crossbite (Table 2.2 and Figure 2.2). In addition, CFC individuals commonly had a high-arched palate (Figure 2.2). Thus, the primary distinguishing dental phenotypic feature in CFC is malocclusion, suggesting

61

that dysregulation of RAS/MAPK signaling disrupts normal craniofacial development, resulting in malocclusion.

Individuals with CFC also presented with abnormal oral habits. Tongue thrusting was observed in a significant number of subjects in our CFC cohort. Also, an open mouth posture was fairly common. Some evidence suggests that a tongue thrust habit may cause an altered tongue position that in turn may produce malocclusion, including open bite, posterior crossbite, and vaulting of the palate (Premkumar et al., 2011). However, a direct correlation between tongue thrust and malocclusion has not been made, and further research is required to determine how dysregulation of RAS/MAPK signaling results in the malocclusion observed in CFC.

Notably, just as activation of RAS/MAPK in humans results in craniofacial malformation, activation of the same RAS/MAPK pathways in mouse and zebrafish directly affects craniofacial phenotype. A mouse model for CFC expressing an attenuated $Braf^{V600E}$ allele (an allele that has only been identified in cancer but not in CFC) displays a rounder and shorter head as well as defects in the shape of the skull vault caused by differences in the shape of the frontal and parietal bones that form the skull vault (Urosevic et al., 2011). In addition, we determined that a zebrafish model expressing a kinase-activating $BRAF^{Q257R}$ allele, or kinase-inactivating $BRAF^{G596V}$ allele, also develops craniofacial anomalies (Anastasaki et al., 2012). Moreover, these defects were ameliorated by treatment with low doses of MEK inhibitor at early stages of development. These animal models of CFC provide a

powerful tool to further understand the role of RAS/MAPK signaling in craniofacial development.

This study, which describes the dental phenotype of CFC, establishes a first step towards understanding the role of RAS/MAPK signaling in dental development, and it provides a tool for clinicians who care for individuals with CFC. CFC individuals do not present with unique dental pathologies requiring specific treatment. Like the general population, patients with CFC require routine dental examinations and appropriate hygiene and restorative care. Careful oral hygiene instructions to patients and their families are necessary, since individuals with CFC may not have meticulous oral hygiene habits. Some individuals with CFC may be anxious dental patients due to cognitive delay and oral aversion, and thus, these individuals should be seen early and often by the dentist to accustom them to dental treatment. In addition, dentists should be aware and monitor the development of malocclusion in individuals with CFC and be prepared to refer patients to an orthodontist for treatment if necessary. In summary, thorough characterization of the craniofacial and dental phenotypes of CFC and other RASopathies will not only help guide clinicians in treating these patients, but will also provide insight into the complex role of the RAS/MAPK pathway during craniofacial development.

CHAPTER 3:

**Craniofacial and Dental Development in Costello Syndrome; HRAS
Dysregulation in the Craniofacial Complex**

In this chapter, I report the craniofacial and dental phenotype in a large CS
cohort for the first time and compare to CFC.

Alice F. Goodwin[1], Snehlata Oberoi[1], Maya Landan[1], Cyril Charles[1], Jessica
Massie[1], Cecilia Fairley[1], Katherine A. Rauen[2] and Ophir D. Klein[1,2]

[1]Department of Orofacial Sciences and Program in Craniofacial and
Mesenchymal Biology, University of California San Francisco, San Francisco,
CA

[2]Department of Pediatrics and Institute for Human Genetics, University of
California San Francisco, San Francisco, CA

3.1 ABSTRACT

Costello syndrome (CS) is a RASopathy characterized by a wide range of cardiac, musculoskeletal, dermatological, and developmental abnormalities. The RASopathies are defined as a group of syndromes caused by activated RAS/mitogen-activated protein kinase (MAPK) signaling. Specifically, CS is caused by activating mutations in *HRAS*. Receptor tyrosine kinase (RTK) signaling, which is upstream of RAS/MAPK, is known to play a central role in craniofacial and dental development, yet the key craniofacial and dental features of CS have not been systematically defined. To fill this critical gap in our knowledge, we evaluated the craniofacial and dental phenotype of a large cohort (n=41) of CS individuals. We found that the craniofacial features common in CS include macrocephaly, bitemporal narrowing, convex facial profile, full cheeks, and large appearing mouth. Additionally, CS patients have a characteristic, abnormal dental phenotype that includes malocclusion, with open bite and posterior crossbite, enamel hypo-mineralization, delayed tooth development and eruption, gingival hyperplasia, thickening of the alveolar ridge, and high-arched palate. Comparison of the craniofacial and dental phenotype in CS with other RASopathies, such as Cardio-facio-cutaneous syndrome (CFC), provides insight into the complexities of RAS/MAPK signaling in human craniofacial and dental development.

3.2 INTRODUCTION

Costello syndrome (CS) is characterized by craniofacial malformations, dermatologic anomalies, cardiac defects, musculoskeletal abnormalities, growth delay, and cognitive deficits (Rauen, 2007). CS is one of the RASopathies, a group of syndromes that includes neurofibromatosis type 1 (NF1), Noonan syndrome (NS), NS with multiple lentigines, capillary malformation-AV malformation syndrome, Legius syndrome, and Cardio-facio-cutaneous syndrome (CFC) (Tidyman and Rauen, 2009). The RASopathies are all caused by mutations that increase signaling through the RAS signaling pathway, including its main effector pathways, mitogen-activated protein kinase (MAPK) and phosphatidylinositol 3-kinase (PI3'K) (Tidyman and Rauen, 2009). In the case of CS, all known patients have a heterozygous, de novo germline mutation in *HRAS* that results in a constitutively active RAS protein (Aoki et al., 2005).

The RASopathies, which are due to distinct mutations in the RAS/MAPK pathway, have both unique and overlapping phenotypic features, especially in the craniofacial complex. Geneticists rely on craniofacial characteristics to clinically diagnose and guide genetic testing; however, distinguishing between RASopathies, such as CS and CFC, can prove difficult because of the shared phenotypic features. Thus, it is critical to carefully delineate the specific craniofacial characteristics of each of the RASopathies.

Receptor tyrosine kinase (RTK) signaling upstream of RAS/MAPK is known to play a crucial role in craniofacial and dental development. For example, Fibroblast growth factors (FGFs) that initiate signaling through RTK are involved in the crosstalk between epithelium and mesenchyme that guide the formation of nearly the entire craniofacial complex, including the teeth (Pispa and Thesleff, 2003; Nie et al., 2006). Comparing the craniofacial and dental phenotypes of the RASopathies will further our understanding of the role of RAS/MAPK signaling in craniofacial and dental development. We recently reported the craniofacial and dental findings in CFC subjects (Goodwin et al., 2012). In order to improve the phenotypic understanding of the RASopathies and to further our understanding of RAS/MAPK signaling in the craniofacial complex, we examined the craniofacial and dental features in a large cohort of 41 CS individuals.

3.3 MATERIALS AND METHODS

This study was approved by the UCSF Committee on Human Research (UCSF Committee on Human Research, IRB # 10-01426). A total of 41 individuals with a clinical diagnosis of CS were examined during the 6th International Costello Syndrome Conference in Berkeley, California in 2009 (Rauen et al., 2010) and the 7th International Costello Syndrome Family Forum in Chicago, Illinois in 2011. The diagnosis was confirmed by a board certified medical geneticist (K.A.R. or O.D.K.) based on clinical features. All of the 41 participants (21 males and 20 females) enrolled in our study were *HRAS* mutation positive. The average age of the cohort was 11 years, with a range of 1 to 35 years of age. The majority of the cohort reported Caucasian race (80%) but also included were Latino (10%), African (5%), Asian (2%), and Middle Eastern (2%) individuals. Written informed consent was obtained for all subjects. Complete intra- and extra-oral exams were performed by a licensed dentist (A.F.G., S.O., or J.M.). Exams included extra-oral frontal and profile view facial photographs. When possible, intra-oral photographs were taken, radiographs (including panoramic, periapical, and bitewing radiographs) and dental records provided by the participant were reviewed, and alginate dental impressions were taken. The total number of patients examined for each dental characteristic is listed in Table 2. When possible, participants' parents and/or siblings were also examined as controls (n=43). Statistical comparison between the dental phenotype of the CS or CFC cohort and general U.S. population as determined by the NHANES III survey (Proffit

et al., 2006) was made using the Fisher's exact test with 2-tailed p-value.

3.4 RESULTS

3.4.1 Craniofacial phenotype of CS

Individuals with CS have a characteristic craniofacial phenotype (Table 3.1, Figure 3.1). The majority of subjects presented with relative macrocephaly (93%), high forehead (85%), and bitemporal narrowing (98%). Most subjects had a convex facial profile (85%) and micrognathia (51%) or a relatively small mandible. Subjects also commonly had a hyperteloric (56%) and telencanthic (83%) appearance. Other common features were a short nose (73%), with a depressed nasal bridge (73%) and wide nasal tip (90%). Individuals with CS also had full cheeks (71%), a large appearing mouth (76%), and thick appearing lips (95%), often with a tented upper lip (76%). Commonly in CS, ears were low-set (93%) and posteriorly rotated (73%) with upturned lobes (66%).
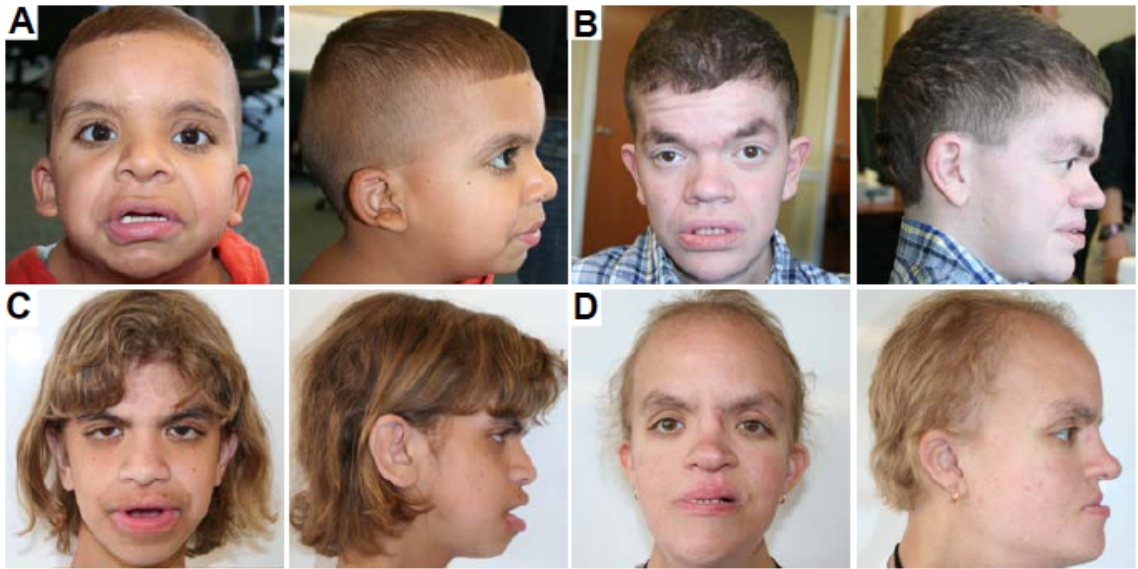
Figure 3.1 Craniofacial phenotype of CS.

Frontal and profile images of individuals with CS demonstrate the craniofacial phenotype. (A) A 6 year-old boy with common CS craniofacial features including relative macrocephaly and short nose with depressed nasal bridge and wide nasal tip. (B) A 20 year-old male with a convex facial profile, micrognathia, and low-set, posteriorly rotated ears with upturned lobes. (C) A 14 year-old female with full cheeks and a large appearing mouth with thick appearing lips. (D) A 23 year-old female with a high forehead, bitemporal narrowing, and hyperteloric and telecanthic appearance typical of CS.

Table 3.1 Summary of craniofacial findings in a cohort of 41 individuals with Costello syndrome (CS).

Craniofacial Findings	n	%
Relative macrocephaly	38	93
High forehead	35	85
Bitemporal narrowing	40	98
Convex facial profile	33	85
Micrognathia	21	51
Hyperteloric appearing	23	56
Telencanthic appearing	34	83
Depressed nasal bridge	30	73
Short nose	30	73
Wide nasal tip	37	90
Full cheeks	29	71
Large appearing mouth	31	76
Thick appearing lips	39	95
Tented upper lip	31	76
Low set ears	38	93
Posteriorly rotated ears	30	73
Upturned lobes	27	66

3.4.2 Dental phenotype of CS

Individuals with CS have a recognizable and characteristic dental phenotype (Table 3.2, Figure 3.2). An open bite, when the anterior teeth are not in contact with the posterior teeth in occlusion, was a common vertical malocclusion that was observed in 41% of our cohort (Figure 3.2B). This incidence is significantly higher than the national average (3%; p=0.0001). In contrast, a deep bite, in which the maxillary anterior teeth overlap the mandibular teeth by greater than 2 mm, was significantly less common among our subjects (9%) than in the general population (49%; p=0.0001). Posterior crossbite, a condition in which the maxillary posterior teeth are positioned lingually (i.e. toward the tongue) relative to mandibular teeth (normally, maxillary teeth are placed bucally (i.e. toward the cheek)), was significantly more common in the CS cohort (35%; Figure 3.2B) than in the general U.S. population (9%; p=0.0001).

73
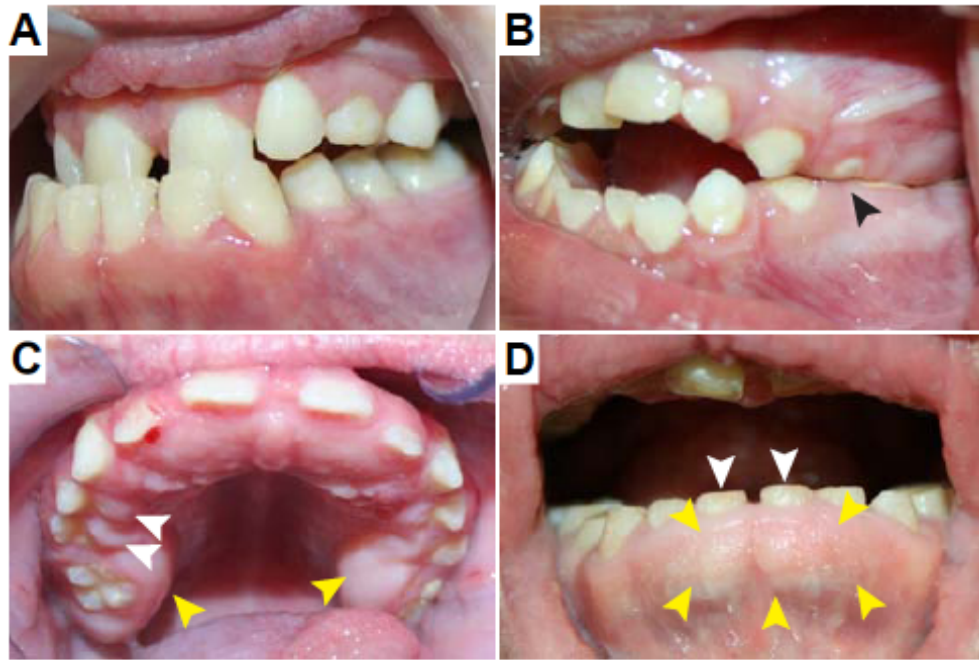
Figure 3.2 Dental phenotype of CS. Intra-oral photographs show the typical dental phenotype in CS. (A) Class III malocclusion. (B) Open bite and posterior crossbite on the patient's left side marked by the black arrow. (C) High-arched palate with thickening of the posterior maxillary alveolar ridge (yellow arrows) and gingival hyperplasia (white arrows) typical of CS. (D) Thickening of the anterior mandibular alveolar ridge (yellow arrows) and heavy incisal wear on the mandibular central incisors (white arrows).

The percentage of subjects with class I molar relationship (30%), which is the ideal molar relationship according to the Angle's classification system (Riolo, 2002), in which the mesiobuccal (anterior, cheek side) cusp of the maxillary first molar aligns with the buccal side groove in the middle of the mandibular first molar so that the maxillary first molar and mandibular first molar are aligned, was not significantly different from the 41% of the U.S. population with class I molar relationship (p=0.139). The percentage of subjects with class II molar relationship (33%), in which the maxillary first molar is positioned mesially (anteriorly in the mouth) to the mandibular first molar, was significantly greater than the national average (53%; p=0.006). Class III molar relationship (37%), in which the maxillary first molar is positioned distally (posteriorly) to the mandibular first molar, was significantly greater than the U.S. average (6%; p=0.0001; Figure 3.2A).

Dental crowding was only observed in 39% of our CS cohort compared to about 60% of the U.S. population (p=0.004). None of the CS subjects presented with missing teeth, and only one subject presented with supernumerary teeth (lateral incisor), based on clinical examination and review of radiographs. Examination of panoramic x-rays for 6 CS patients indicated that dental development was delayed in 5 of the subjects. Eruption patterns were determined by assessing the teeth present in relationship to the age of the individual examined and comparing to the normal eruption pattern. Most CS individuals (93%) showed delayed eruption patterns. The majority of subjects had a constricted high-arched palate (84%; Figure 3.2C). CS

75

patients also presented with a thickening of the posterior maxillary alveolar ridge (30%; Figure 3.2C), and 2 patients had a striking thickening of the anterior mandibular alveolar ridge (Figure 3.2D). Most CS individuals had gingival hyperplasia (64%), or overgrowth of the gingival tissue. Only 25% of CS individuals presented with clinical caries at exam; however, 57% had a history of caries according to dental records. Nearly all of the CS subjects presented with an enamel defect (88%), which was characterized clinically by demineralized white focal and striation lesions in the enamel. The subjects who presented with enamel defects were 5-35 years of age while those who did not present with enamel defects tended to be younger, between the ages of 2 and 8. Subjects also presented with habits including a secondary tongue thrust (28%) and open mouth posture (55%). In addition, bruxism, as determined clinically by pathologic wear of the teeth, was present in 56% of our cohort.

Table 3.2 Summary of the dental characteristics in Costello syndrome (CS).

Dental Findings	CS			CFC			General Population[b]	CS p-value[c]	CFC p-value[c]	CFC vs CS p-value[d]
	Affected	Total Examined[a]	%	Affected	Total Examined[a]	%	%			
Malocclusion										
Vertical										
Open bite	13	32	41	10	27	37	3	0.0001*	0.0001*	0.79
Deep bite	3	34	9	5	27	19	49	0.0001*	0.0001*	0.44
Transverse										
Posterior crossbite	12	34	35	4	21	19	9	0.0001*	0.032*	0.23
Anterior/ Posterior/ Sagittal										
Molar relationship										
Class I	8	27	30	7	13	54	41	0.139	0.089	0.17
Class II	9	27	33	6	13	46	53	0.006*	0.396	0.50
Class III	10	27	37	0	13	0	6	0.0001*	0.029*	0.016*
Arch perimeter										
Crowding	13	33	39	8	32	25	60	0.004*	0.0001*	0.29
Spacing	14	33	42	7	32	22	N/A[e]			0.11
Dental development										
Missing teeth	0	31	0	1	31	3	N/A			1.00
Supernumerary teeth	1	31	3	0	31	0	N/A			1.00
Delayed development	5	6	83	0	2	0	N/A			0.11
Delayed eruption	27	29	93	4	32	13	N/A			0.0001*

Hard tissue

High arched palate	27	32	84	16	20	80	N/A			0.72
Thickening of the posterior maxillary alveolar ridge	10	33	30	0	31	0	N/A			0.0009*
Thickening of the anterior mandibular alveolar ridge	2	33	6	0	31	0	N/A			0.49
Soft tissue										
Gingival hyperplasia	21	33	64	1	31	3	N/A			0.0001*
Pathology										
Caries present at exam	9	35	26	7	28	25	N/A			1.00
History of caries	10	14	71	4	7	57	N/A			0.64
Enamel defect	29	33	88	4	13	31	N/A			0.0003*
Habits										
Tongue thrusting	9	32	28	7	31	23	N/A			0.77
Open mouth posture	22	40	55	9	32	29	N/A			0.03*
Bruxism	18	32	56	3	31	10	N/A			0.0001*

[a] Number of CS individuals examined for each dental characteristic since dental exams were not completed on every CS individual in the cohort

[b] Prevalence of dental characteristic in general population as determined by the NHANESIII survey

[c] Comparison of incidence of dental characteristic in CS cohort compared to general population using the Fisher's exact test with 2-tailed p-value

* significant p-value<0.05

[d] Comparison of incidence of dental characteristic between CS and CFC using the Fisher's exact test with 2-tailed p-value

[e] N/A Data not available

3.5 DISCUSSION

The RASopathies are a group of syndromes caused by dysregulation of the Ras/MAPK pathway in which affected individuals commonly present with craniofacial dysmorphia. Each syndrome is characterized by distinct facies that are used to clinically differentiate and diagnose the many RASopathies. We have previously reported that CFC, caused by activating mutations in *KRAS*, *BRAF*, *MEK1*, or *MEK2* (Rodriguez-Viciana, 2006; Niihori et al., 2006)*,* is characterized by a distinct craniofacial phenotype including macrocephaly, bitemporal narrowing, convex facial profile, and hypoplastic supraorbital ridges (Goodwin et al., 2012). Here, we have thoroughly examined the craniofacial findings in CS, which is caused by heterozygous de novo germline mutations in the small GTPase HRAS that functions upstream of the kinases BRAF, MEK1, and MEK2. CS shares craniofacial features with CFC, including macrocephaly, bitemporal narrowing, and convex facial profile, but also possesses additional, unique characteristics including micrognathia, full cheeks, large appearing mouth, and thick appearing lips. The "coarser" appearance of CS individuals may be attributed to these "fuller" features, which are distinguishable from CFC, especially as individuals age. Analyzing the craniofacial features of the RASopathies provides specific craniofacial criteria that are useful in clinical diagnosis of the RASopathies, and further study may elucidate the role of Ras/MAPK signaling in craniofacial development.

There are many striking differences between the dental phenotypes of CS and CFC (Table 3.2), and analysis of the dental phenotypes of the RASopathies caused by mutations at different points along the Ras pathway will provide insight into the role of Ras and its effector pathways in tooth development. We identified some overlapping dental characteristics between CS and CFC, but overall, CS had more dysmorphic dental characteristics compared to CFC. Malocclusion, including anterior open bite and posterior crossbite, was a common dental finding in both CFC and CS, and there was no statistical significance in the incidence between CS and CFC in either (p=0.79, p=0.23, respectively, Table 3.2). However, individuals with CS also had a significantly increased incidence of class III molar relationship compared to the CFC cohort and general population (p=0.016, p=0.0001, respectively). Similar to individuals with CFC, those with CS did not have anomalies in tooth number or morphology. Although we did not observe differences in size of the teeth clinically or based on dental casts (n=3) in our CS cohort, it was recently reported in a small cohort of 4 CS individuals that primary lateral incisors and first and second molars and permanent first molars were small in size, based on multi-detector row computed tomography (MDCT) (Takahashi and Ohashi, 2012).

Our previous analyses of mice carrying mutations in RTK antagonists revealed the formation of supernumerary teeth and changes in tooth morphology due to hyperactive MAPK signaling (Klein et al., 2006; 2007; Peterkova et al., 2009). We therefore had predicted that individuals with CS

and CFC would have supernumerary or malformed teeth, and our finding of normal tooth number and shape was surprising. Another surprising finding was that in CS individuals the enamel structure was severely disrupted. Individuals with CS frequently presented white focal lesions and striations (88%) compared to CFC individuals (31%; p=0.0003). CS individuals also had increased incidence of bruxism (56%) compared to CFC individuals (10%; p=0.03), indicative of pathologic wear, most likely due to decreased mineralization of CS enamel. Indeed, the structure of CS enamel was less densely mineralized and disorganized according to scanning electron microscopy (SEM; See Chapter 4). Interestingly, SEM imaging of CFC enamel revealed normal structure (Goodwin et al., 2012) data not shown.

In addition to structural defects, CS individuals also had delayed tooth development and eruption, unlike CFC individuals. The difference in incidence of delayed tooth eruption was statistically significant between the CS and CFC cohorts (p=0.0001), however there was not a clear statistical significance in delayed development (p=0.11), most likely due to the small sample size of the cohorts (5/6 and 0/2, respectively; Table 3.2). The delayed eruption in CS individuals may be due to dysfunction of osteoclasts, which resorb alveolar bone around the developing tooth to allow eruption (Wise, 2009). CS and CFC individuals have been shown to have increased urinary pyridinium crosslinks (breakdown product of mature collagen), suggestive of increased osteoclastic activity (Stevenson et al., 2011). However, activity of CS or CFC osteoclasts has not been assessed *in vitro* or *in vivo*. In addition

81

to the osteoclast activity in the coronal region of the erupting tooth, there must also be osteogenic activity near the roots of the tooth to force the tooth to erupt and maintain alveolar bone around the tooth. Thus, tooth eruption requires both osteoclastic and osteogenic activity, and it may be that an imbalance in bone remodeling in the activated Ras signaling environment results in impairment of tooth eruption.

CS individuals presented with distinct hyperplasia of the oral tissues not observed in CFC; about 65% of our CS cohort and only 3% of our CFC cohort presented with gingival hyperplasia (p=0.0001, Table 3.2). A significant number (30%) of CS individuals also had thickening of the maxillary posterior alveolar ridge not observed in CFC (0%; p=0.0009), and there were two CS individuals who presented with a thickening of the mandibular anterior alveolar ridge. It is intriguing that only CS and not CFC individuals presented with this tissue hyperplasia phenotype. Since CFC is mainly caused by mutations in MAPK (*BRAF*, *MEK1*, *MEK2*) and CS is caused by upstream activating mutations in HRAS, it is possible that Ras is signaling through PI3'K, rather than MAPK, to increase oral tissue proliferation in CS. This hypothesis is supported by case reports in Proteus Syndrome, a rare hamartoma syndrome that includes gingival hypertrophy and can be caused by mutations in the PI3'K/AKT pathway (Becktor et al., 2002; Sakamoto et al., 2010). Additionally, gingival fibromas have been reported in individuals with Tuberous Sclerosis caused by mutations in *TSC1* or *TSC2*, which encode proteins downstream of AKT (Sparling et al., 2007). Activation upstream of

Ras signaling has also been implicated in gingival hypertrophy. Hereditary Gingival Fibromatosis Type 1 (HGF1), which is caused by activating mutations in *SOS-1* that encodes a protein that recruits Ras to the membrane for activation, is characterized by benign, slowly progressive, non-hemorrhagic, fibrous enlargement of maxillary and mandibular keratinized gingiva (Hart et al., 2002). These patient data point to differences in the roles of the multiple effector pathways of Ras such as MAPK and PI3'K in the presentation of RASopathies.

Like individuals with CFC, CS individuals do not present with dental features requiring special treatment. CS individuals should undergo regular dental exams and treatment. Dentists should pay special attention to the oral hygiene of CS patients since hyperplasia of the gingival tissue may make proper cleaning of the teeth difficult. Although the caries incidence in our cohort was not strikingly high, CS individuals may be at higher risk due to hypo-mineralized enamel. Additionally, hypo-mineralized enamel may lead to increased pathologic wear of the teeth, and increased fluoride treatment, whether in office fluoride varnish or at home fluoride rinse in addition to fluoride toothpaste, may be recommended. For severe tooth abrasion, a custom mouthguard may be considered. Delayed tooth development and eruption should be explained to patients and their families to alleviate any concerns. If there is a significant delay, panoramic x-rays are recommended to determine tooth development stage. In addition, CS individuals are likely to

develop malocclusion, and so early referral to an orthodontist is recommended.

Together, the data we present here add to the study of the craniofacial and dental phenotypes in the RASopathies, and this information is useful for clinicians treating CS patients. Additionally, by comparing the RASopathies and focusing on the differences between the syndromes, we can begin to dissect the roles of the Ras pathway and its multiple effectors in craniofacial and dental development.

CHAPTER 4:

Abnormal Ras Signaling Negatively Regulates Enamel Formation

In this chapter, I thoroughly evaluate the hypoplastic enamel defect observed clinically in CS patients, and further analyze the enamel defect in a CS mouse model, revealing an important role for Ras in amelogenesis.

Alice F Goodwin[1], William E Tidyman[1,§], Andrew H Jheon[1,§], Amnon Sharir[1], Xu Zheng[1,2], Cyril Charles[1], James A Fagin[3], Martin McMahon[4], Thomas GH Diekwisch[5], Bernhard Ganss[6], Katherine A Rauen[4,7], and Ophir D Klein[1,4,7]

[1] Department of Orofacial Sciences and Program in Craniofacial and Mesenchymal Biology, University of California, San Francisco, San Francisco, CA

[2] Department of Stomatology, Peking University Third Hospital, Bejing, China

[3] Human Oncology and Pathogenesis Program, Memorial Sloan Kettering Cancer Center, New York, NY

[4] Helen Diller Family Comprehensive Cancer Center, University of California, San Francisco, San Francisco, CA

[5] Brodie Laboratory for Craniofacial Genetics, College of Dentistry, University of Illinois at Chicago, Chicago, IL

[6] Matrix Dynamics Group, Faculty of Dentistry, University of Toronto, Ontario, Canada

[7] Department of Pediatrics and Institute for Human Genetics, University of California, San Francisco, San Francisco, CA

[§] Equal co-second authors

4.1 ABSTRACT

RASopathies are syndromes caused by gain-of-function mutations in the Ras signaling pathway. One of these conditions, Costello syndrome (CS), is caused by an activating germline mutation in *HRAS* and is characterized by a wide range of cardiac, musculoskeletal, dermatological, and developmental abnormalities. We report that a majority of individuals with CS have hypo-mineralization of enamel, the outer covering of teeth, and that similar defects are present in a CS mouse model. Comprehensive analysis of the mouse model revealed that ameloblasts, the cells that generate enamel, lacked polarity, and the ameloblast progenitor cells were hyperproliferative. Ras signals through two main effector cascades, the mitogen-activated protein kinase (MAPK) and phosphatidylinositol 3-kinase (PI3'K) pathways. To determine through which pathway Ras affects enamel formation, inhibitors targeting either PI3'K or MEK1/2, a kinase in the MAPK pathway, were utilized. MEK1/2 inhibition rescued the hypo-mineralized enamel, normalized the ameloblast polarity defect, and restored normal progenitor cell proliferation. In contrast, PI3'K inhibition only corrected the progenitor cell proliferation phenotype. We demonstrate for the first time the central role of Ras signaling in the teeth of CS individuals, and we present the mouse incisor as a model system to dissect the roles of the Ras effector pathways *in vivo*.

4.2 INTRODUCTION

The role of Ras signaling has been extensively studied in development and disease, particularly in cancer, yet its function in tooth development is not yet known. Receptor tyrosine kinase (RTK) signaling upstream of Ras is activated by fibroblast growth factors (FGFs), which are known to regulate epithelial-mesenchymal interactions in the developing tooth (Nie et al., 2006). We have previously reported that deletion of Sprouty genes, which encode proteins that antagonize the Ras/mitogen-activated protein kinase (MAPK) pathway, results in changes in tooth number and morphology (Klein et al., 2006; 2007; Peterkova et al., 2009), suggesting that Ras signaling is important in developing teeth. However, the role of Ras and its downstream effectors, including the MAPK and phosphoinositide 3-kinase (PI3'K) pathways, has not yet been explored in tooth development and renewal.

Costello syndrome (CS) provides an ideal model to study the effects of activated Ras signaling in development. CS is characterized by craniofacial malformations, dermatologic anomalies, cardiac defects, musculoskeletal abnormalities, growth delay, and cognitive deficits (Rauen, 2007). CS is one of a number of RASopathies, a group of syndromes that includes neurofibromatosis type 1 (NF1), Noonan syndrome (NS), NS with multiple lentigines, capillary malformation-AV malformation syndrome, Legius syndrome, and Cardio-facio-cutaneous syndrome (CFC) (Tidyman and Rauen, 2009). The RASopathies are caused by mutations that increase signaling through the Ras/MAPK pathway (Tidyman and Rauen, 2009). In CS,

individuals have heterozygous, germline mutations in *HRAS* that result in the constitutive activation of Ras (Aoki et al., 2005).

Multiple mouse models have been developed to study the RASopathies. Here, we have utilized a CS mouse model expressing an *HRas*[G12V] mutation (Chen et al., 2009). Although 80% of individuals with CS carry an *HRAS*[G12S] mutation (Estep et al., 2006; Gripp et al., 2005; Kerr et al., 2006), the *HRas*[G12V] mouse model is useful because it phenocopies many aspects of the syndrome, including growth delay, macrocephaly, craniofacial anomalies, and papilloma development (Chen et al., 2009).

We examined the teeth of individuals with CS and in CS (*HRas*[G12V]) mice and observed that enamel was hypo-mineralized in both human and mouse CS. To systematically study the cellular mechanisms underlying this defect, we took advantage of the continuously growing mouse incisor model (Smith and Warshawsky, 1975; 1977; Harada et al., 1999; Seidel et al., 2010; Juuri et al., 2012; Biehs et al.; Jheon et al., 2012). We discovered that in CS mice, the proliferation and differentiation of enamel-producing ameloblasts and their precursors were compromised, and the inhibition of MEK1/2 (mitogen activated protein kinase kinase) or PI3'K rescued distinct aspects of the dental phenotype. Our studies demonstrate for the first time the central role of Ras signaling in tooth development, and the utilization of the mouse incisor model to dissect the roles of the distinct components of RAS signaling.

4.3 MATERIALS AND METHODS

4.3.1 Human subject craniofacial and dental exams

A total of 41 individuals with a clinical diagnosis of CS were examined during the 6th International Costello Syndrome Conference in Berkeley, California in 2009 (Rauen et al., 2010) and the 7th International Costello Syndrome Family Forum in Chicago, IL in 2011. The diagnosis was confirmed by a board certified medical geneticist (K.A.R. or O.D.K.) based on clinical features. All 41 participants enrolled in our study were *HRAS* mutation positive. The cohort consisted of 21 males and 20 females. The average age of the cohort was 11 years, with a range of 1 to 35 years of age. The majority of the cohort reported Caucasian race (80%), but also included were Latino (10%), African (5%), Asian (2%), and Middle Eastern (2%) individuals. Written informed consent was obtained for all subjects. Complete intra- and extra-oral exams were preformed by a licensed dentist (A.F.G.). Exams included frontal and side view craniofacial photographs, intra-oral photographs, review of radiographs (including panoramic, periapical, and bitewing radiographs) and dental records provided by the participant, and alginate dental impressions. UV images were taken with an Olympus E-620 camera (Center Valley, PA) and a Pentax Ultra-Achromatic Takumar Quartz lens (Denver, CO), which heightened the contrast between areas of mineralized and de-mineralized enamel.

4.3.2 Mouse husbandry and inhibitor treatment

All experiments involving mice were conducted in accordance with protocols approved by the University of California, San Francisco Institutional Animal Care and Use Committee. CS ($Hras^{G12V}$) mice were bred and genotyped as previously described (Chen et al., 2009). PD0325901 (Pfizer, New York, NY) and GDC0941 (Genentech, South San Francisco, CA) were formulated in 0.5% (w/v) (hydroxypropyl)methyl cellulose (HPMT; Sigma, St. Louis, MO). PD0325901 was administered to 3-month-old mice by oral gavage at 12.5 mg/kg and GDC0941 at 75 mg/kg per mouse once per day for 28 days.

4.3.3 Micro-computed tomography and SEM analysis of exfoliated human and mouse teeth

Micro-computed tomography (μCT) was performed on human teeth and mouse hemi-mandibles. For patient samples, 1 exfoliated primary maxillary central incisor from a CS individual and 1 age-matched control tooth were collected and stored dry at room temperature. For mouse samples, hemi-mandibles from P21 and P70 control and CS ($Hras^{G12V}$) mice were dissected, cleaned of excess tissue, and fixed overnight in 4% paraformaldehyde (PFA), followed by dehydration in 70% ethanol. Human and mouse samples were scanned using a micro-focused X-ray tomographic system (MicroXCT-200, Xradia, Pleasanton, CA), at 55 kV and 144 μA. 2000

projection images at an exposure time of 13 s with a linear magnification of 2X were taken. The final pixel size was 20.5 µm. The volume was reconstructed using a back projection filtered algorithm (XRadia, Pleasanton, CA). Following reconstruction, 3D image processing and analysis were carried out using MicroView (Version 5.2.2, GE Healthcare, Pittsburgh, PA) and Amira (Version 5.3, Visualization Sciences Group, Burlington, MA) software. A 700µm transverse section (35 slices) of the incisor, adjacent to the second molar, was used to measure the following parameters: enamel volume and enamel coverage, which is defined by the ratio of enamel area to tooth area.

Scanning electron microscopy (SEM) was performed on exfoliated patient teeth and mouse hemi-mandibles. For patient samples, 2 exfoliated primary teeth (maxillary central and lateral incisor) from 2 CS individuals and 1 exfoliated age-matched control maxillary central incisor were collected and stored dry at room temperature. For mouse samples, hemi-mandibles from 12-week old control and CS mice were dissected free of soft and connective tissue, fixed in 4% PFA in PBS overnight, then dehydrated in a graded ethanol series, and dried in a vacuum desiccator. After initial treatment, mouse and human samples were treated the same. Samples were embedded in epoxy resin (resin 105 and hardener 205 at a ratio of 5:1 w/w, WestSystem, Bay City, MI), ground to the desired thickness on a plate grinder (EXAKT 400CS, Norderstedt, Germany) using 800 grit silicon carbide paper, and polished with 2000 and 4000 grit silicon carbide paper (Hermes Abrasives,

Mississauga, ON, Canada). The exposed tissue was etched with 10% phosphoric acid for 30 seconds, rinsed with water, and dried in a vacuum desiccator. Samples were mounted on SEM stubs with carbon tape, surfaces coated with 7nm gold using a sputter coating machine (Desk II, Denton Vacuum, Moorestown, NJ), and imaged in a Philips SEM instrument (XL30 ESEM, Philips, Andover, MA) operating at a beam energy of 20 keV in secondary electron or backscatter mode. Images were processed using Adobe Photoshop CS5.1 to adjust upper and lower limits of input levels in grayscale mode, and to apply auto balance and auto contrast settings.

4.3.4 Histological analysis of mouse teeth

Post-natal day 2, 21 and 70 CS and control mice were euthanized and mandibles were removed and fixed in 4% paraformaldahyde overnight. Mandibles were then decalcified in 0.5M EDTA for 7-16 days, dehydrated, embedded in paraffin, and serially sectioned sagitally or coronally on a Leica microtome at 7 mM. Samples were stained with H&E and imaged at 20X and 40X on a Leica upright microscope. Quantification was done using ImageJ software (Rasband). Immunohistochemistry (IHC) was also performed following standard protocols using antibodies against GM-130 (Cell Signaling #2296, Danvers, MA), amelogenin (Santa Cruz #32892, Dallas, TX), and p-ERK (Cell Signaling #9101, Danvers, MA). For proliferation analysis, 10-week control and CS mice were injected intraperitoneally with 1mg of BrdU 1.5 hours prior to euthanization, and IHC was performed using an antibody

92

against BrdU (Abcam #6326, Cambridge, MA). Number of nuclei and BrdU cells in the cervical loop and transit-amplifying region was determined using pixel quantification in Adobe Illustrator.

4.3.5 RNA isolation and qPCR

Mandibular molars were removed from P11 control and CS mandibles in PBS and transferred to Dulbecco's Modified Eagle Medium (DMEM) at 4°C. RNA was extracted from the tissue using the RNeasy Mini Kit (Qiagen, Germantown, MD). RNA was then quantified using the NanoDrop 2000 (Thermo Scientific, Wilmington, DE), and cDNA was made with MMLV Reverse Transcriptase. qPCR reactions were performed using the GoTaq qPCR Master Mix (Promega, Madison, WI) in a Mastercycler Realplex (Eppendorf, Hauppauge, NY). PrimeTime qPCR primers (Integrated DNA Technologies, Coralville, IA) for each of the genes of interest were used (sequences available upon request). qPCR conditions were as follows: 95°C, 2 minutes; 40 cycles at 95°C, 15 seconds; 60°C, 15 seconds; 68°C, 20 seconds; followed by a melting curve gradient. Expression levels of the genes of interest were normalized to levels of *L19* and are presented as relative levels to control.

4.3.6 Western blot hybridization

Liver tissue was collected, snap-frozen, and homogenized in cell lysis

buffer with the addition of phosphatase inhibitor cocktail. The lysates were cleared by centrifugation and soluble protein quantified by the Bradford method. 2.5 mg of protein was subjected to PAGE on a NuPAGE Novex 4–12% Bis-Tris gradient gel (Invitrogen, Grand Island, NY) and transferred to BVDF membrane. Western blot hybridization was performed using standard protocols. Blots were probed with antibodies to p-MEK1/2 (Cell Signaling #2338, Danvers, MA), p-ERK (Cell Signaling #9101, Danvers, MA), total ERK (Cell Signaling #9102, Danvers, MA), p-AKT (Cell Signaling #9271, Danvers, MA) and total AKT (Cell Signaling #9272, Danvers, MA). Antibody to GAPDH (#AM4300, Ambion, Austin, TX) was used as a protein loading control.

4.4 RESULTS

4.4.1 Individuals with CS have defective enamel

Because of the optical properties of enamel, less dense enamel appears chalky white and opaque to the human eye, whereas normal enamel looks translucent and slightly yellow. Therefore, the presence of white lesions is suggestive of demineralized enamel (Karlsson, 2010). The enamel of nearly all CS participants examined (n=29; 88%) had focal white lesions and striations, which are not normally present in healthy enamel (Figure 4.1A,B). In addition, pathologic wear, as indicated by reduced cusps and/or cup shaped lesions on the cusps (Figure 4.1C,D), was present in 56% (n=18) of CS subjects. Such pathologic wear, not observed in unaffected individuals of the same age, suggested that CS individuals' enamel was less densely mineralized, and thus, more susceptible to abrasion (Figure 4.1C,D). In order to increase the contrast between the mineralized and demineralized enamel areas, we obtained photographs using a UV camera, which confirmed that individuals with CS had demineralized striated lesions that were not present in controls (Figure 4.1E,F).

To assess for the presence of structural enamel defects, scanning electron microscopy (SEM) was performed on etched enamel from exfoliated CS and age-matched control teeth. Healthy enamel displayed a parallel arrangement of hydroxyapatite prisms spanning from the dentin-enamel junction (DEJ) to the enamel surface (Figure 4.1G). In CS enamel, the

organized, parallel pattern of hydroxyapatite prisms was absent, and the orientation of rods was more irregular from the DEJ to the enamel surface (Figure 4.1H). More importantly, the inter-rod hydroxyapatite crystals that fill the space between enamel rods in normal enamel (Figure 4.1G') were absent in CS enamel (Figure 4.1H'). Furthermore, micro-computed tomography (μCT) analysis of exfoliated primary teeth showed that the enamel in CS subjects was thinner than in controls (Supplemental Figure 1).
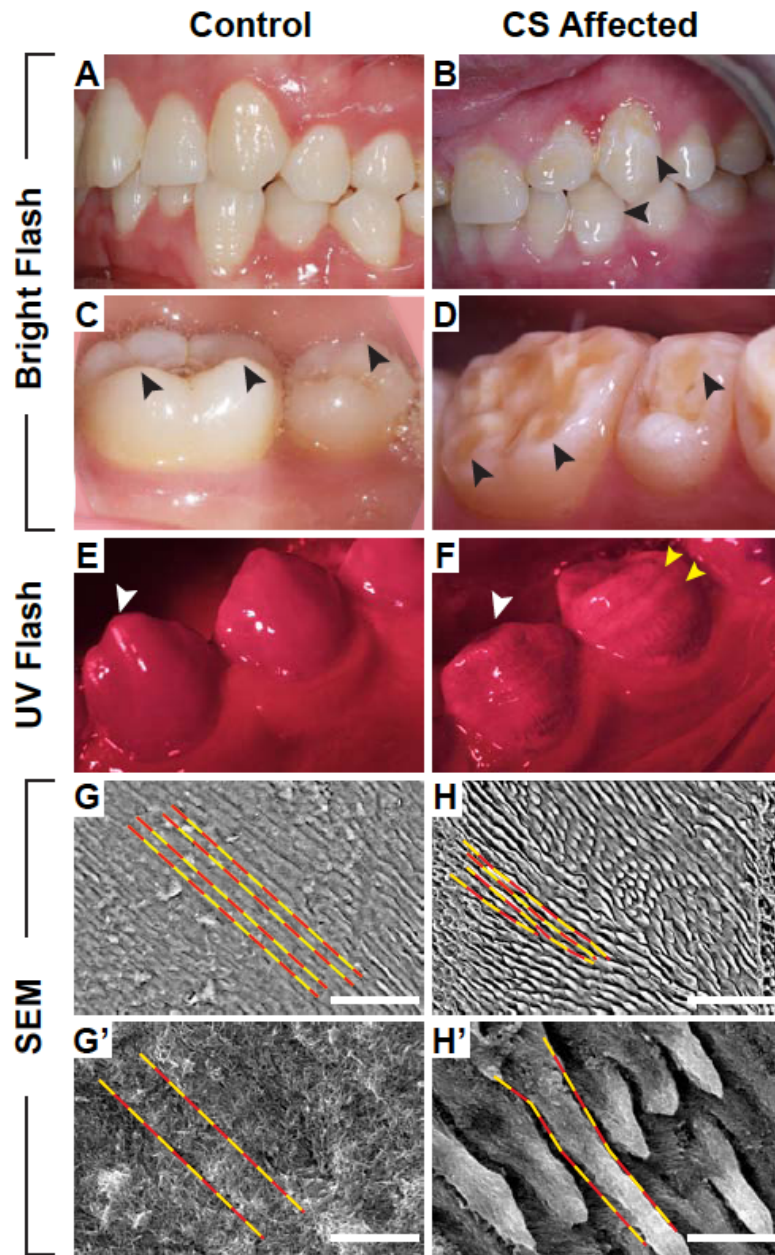
Figure 4.1 Defective enamel is a feature of CS. (A-D) Intraoral photographs. Control patient (A) had normal enamel, whereas 19 year-old CS affected female (B) had demineralized white focal lesions and striations (black arrows). Control patient (C) had normal cusps, whereas 23 year-old affected male (D) had cup-shaped lesions (black arrows) on cusps. (E,F) UV flash images of mandibular canine and first premolar in unaffected 15 year-old (E) and his 25 year-old CS affected brother with heavy wear on the cusps (F, white arrows). Alternating light and dark striations (yellow arrows) in F indicated demineralized enamel. (G,H) SEM images of enamel of exfoliated maxillary primary incisors showed that the hydroxyappetite crystals were less organized and not parallel in the affected CS individual (H) compared to control (G) as highlighted by the red and yellow dashed lines (scale bar: 50µm). Higher magnification images showed that the inter-rod enamel present in control (G') was missing from CS enamel (H') (scale bar: 5µm).

97

4.4.2 CS (*Hras*^G12V) mice have poorly mineralized and disorganized enamel

μCT was performed on hemi-mandibles of CS (*HRas*^{G12V}) mice (Figure 4.2A). Coronal images at the first molar were captured to determine the volume, distribution, and density of molar and incisor enamel (Figure 4.2A'). Normally, mice possess enamel on the crowns of the 3 molars and the labial aspect of the incisor (Figure 4.2B,B',D,D'). However, the molars of CS mice showed little to no enamel (Figure 4.2C-C",E-E"). In control mice, incisor enamel was more dense at postnatal day (P) 70 than P21 (Figure 4.2B''',D'''). In fact, at all stages analyzed, the CS incisor enamel was less densely mineralized (Figure 4.2C''',E'''). In controls, enamel covered the entire labial surface of the incisor, whereas in CS mutants, the total volume of enamel was decreased, with enamel covering a decreased percent of the tooth area (Figure 4.2C''',E''', Supplemental Figure 5).

To determine whether enamel microstructure was disrupted in CS mice, SEM analysis was performed on incisors of 12-week old (P70) animals. In controls, the enamel rods were highly organized, running parallel from the DEJ to the enamel surface (Figure 4.2F,F') similar to that observed in human teeth (Figure 4.1G). This interdigitated and highly organized pattern was lost in CS incisors, and the enamel rods intersected at irregular angles and did not completely span the DEJ to the enamel surface (Figure 4.2G,G'), similar to what we observed in human CS teeth (Fig. 4.1H).

98

µCT imaging of CS mice also revealed large cysts in the bone in the region of the 3rd molar at P21 as compared to control (n=3; Figure 4.2B,C). Histological examination of the cysts at P21 revealed that they were lined by epithelium infiltrated by ghost cells, or aneucleic cells with basophilic granules (data not shown). The cysts were near, but not associated with, the 3rd molar, which is suggestive of calcifying odontogenic cysts (Resende et al., 2011). Interestingly, these cysts were not observed at P70, indicating that they resolved in adulthood (n=3; Figure 4.2E).
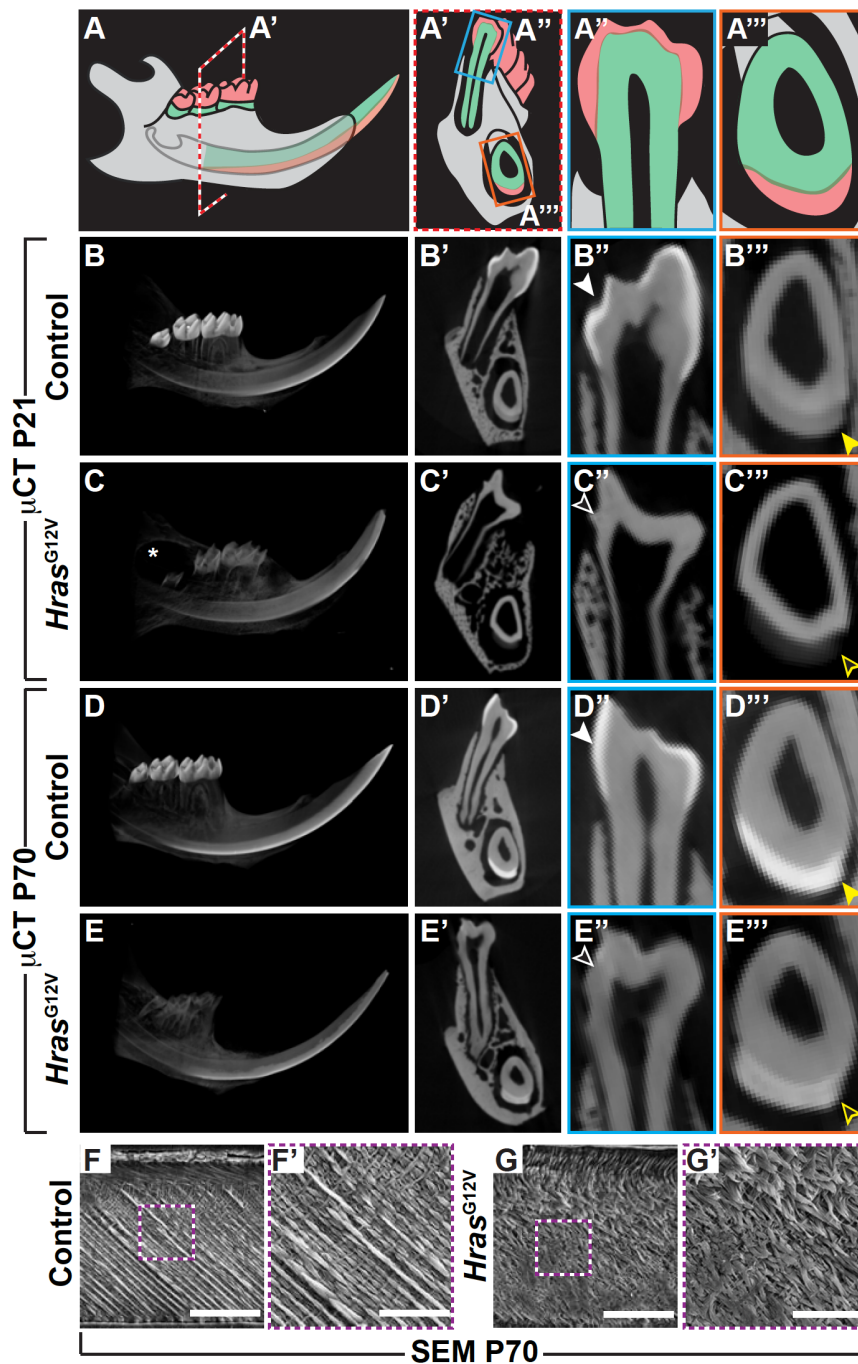
Figure 4.2 CS (*Hras*^G12v) mice have less densely mineralized, disorganized enamel. Micro-CT (μCT) images of the entire mouse mandible (A) and first molar and incisor (A') (red dashed plane). (A", A''') Magnified view of the molar and incisor. Enamel is colored red, dentin is green, and bone is gray. (B,C,D,E) In control, enamel was present on the molars (B',B",D',D"; white arrows) and labial aspect of the incisor (B',B''',D',D'''; yellow arrows) while CS mutant had little to no enamel on the molars (C',C",E',E"; open white arrows) and less dense and abnormally distributed enamel on the labial aspect of the incisor at P21 (C',C''') and P70 (E',E'''; open yellow arrows). Note the large cyst structure in the region of the 3rd molar in the CS mutant (marked by asterisk) at P21 (C) that was resolved at P70 (E). (F,G) SEMs showed that control enamel rods were parallel and ran continuously from the DEJ (bottom of image) to enamel surface (top of image) (F') while the CS mutant enamel rods were disorganized and intersected (G') (scale bar: G,H; 50μm G',H'; 10μm).

100

4.4.3 CS (*Hras*[G12V]) ameloblasts are disorganized and have abnormal cell polarity at the secretory and maturation stages

In order to determine the cause of the enamel defects in the CS (*Hras*[G12V]) mice, the ameloblasts were examined using the mouse incisor model. The rodent tooth is remarkable in that the ameloblast progenitor cells exit the stem cell-containing cervical loop (CL), proliferate as they move into the transit-amplifying (TA) region, and differentiate into ameloblasts. As the ameloblasts move along the incisor, they transition from the secretory stage, during which they secrete enamel proteins including amelogenin (AMEL) and ameloblastin (AMBN) to form the enamel matrix (Gibson et al., 2001; Fukumoto, 2004), to the maturation stage, when ameloblasts secrete proteins such as odontogenic ameloblast associated protein (ODAM/APIN) and amelotin (AMTN) that enable the mineralization of the enamel matrix (Moffatt et al., 2008; Iwasaki et al., 2005). Thus, the distinct steps of amelogenesis can be observed in a "conveyor belt-like" fashion along the length of the mouse incisor.

Normally, ameloblasts are highly organized in a single cell layer on the labial aspect of the incisor (Figure 4.3A-A"). Hematoxylin and eosin (H&E) stained coronal sections in the region of the 1st molar from P70 control mice showed that the ameloblasts and underlying stratum intermedium (SI) cells were separated by a clear border (Figure 4.3B,B'). In addition, control ameloblasts were polarized, with the nuclei located in the basal portion of the cell (Figure 4.3B,B'). In contrast, CS ameloblasts and the underlying SI and

101

stellate reticulum (SR) were disorganized, and there appeared to be a loss of the well-defined border between ameloblasts and SI (Figure 4.3C,C'; (Chen et al., 2009)). CS ameloblasts appeared crowded (Figure 4.3C'), and there was an increased number of CS ameloblasts at both the secretory and maturation stages (Figure 4.3E). Furthermore, the nuclei in CS ameloblasts were located in the apical two-thirds of the cell significantly more often than in controls at both the secretory and maturation stages (Figure 4.3B',C',D). This mis-orientation of nuclei indicated a loss of cell polarity. In control ameloblasts, the Golgi apparatus is positioned apically with respect to the nuclei. However, in a significant number of CS ameloblasts the Golgi apparatus was mis-oriented basally relative to the nucleus, demonstrating a lack of CS ameloblast polarity (Supplemental Figure 2). Interestingly, there were no differences between control and CS mice in expression of the hemi-desmosomal protein E-cadherin (Li et al., 2012) or the desmosome-associated protein PERP that are important in ameloblast-SI attachment ((Jheon et al., 2011); data not shown).

When ameloblasts reach the maturation stage, the enamel protein matrix is normally removed to allow proper mineralization (Hu et al., 2007). In demineralized samples from control mouse incisors, the empty enamel space between the ameloblasts and dentin confirmed the complete removal of enamel matrix (Figure 4.3B). In contrast, CS mice showed residual enamel matrix, indicating that CS ameloblasts did not completely remove the enamel matrix to form properly mineralized enamel (Figure 4.3C). Furthermore, qPCR

102

showed that maturation stage molars at P11 expressed decreased levels of

Amtn and *Apin*/*Odam* (Supplemental Figure 3).
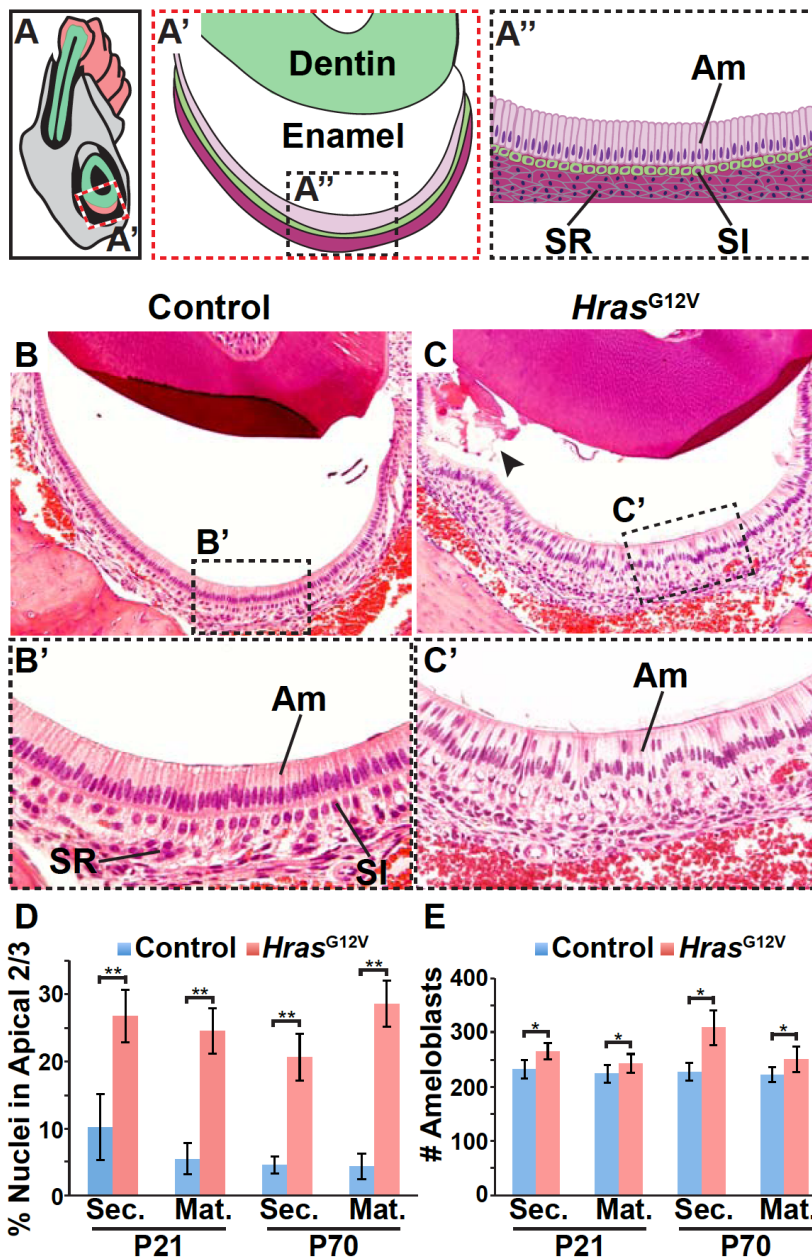
Figure 4.3 CS (*Hras*^G12V) ameloblasts are disorganized and lose cell polarity. Coronal sections of the mouse mandible at the plane of the first molar, as shown in A, were stained with H&E. Images were taken of the labial aspect of the incisor at 20X (A') and 40X (A"). (B, B') In control, the ameloblasts (Am) were highly organized, with their nuclei in the basal aspect of the cell, and there was a clear border between the ameloblasts and underlying stratum intermedium (SI) and stellate reticulum (SR). (C, C') In the CS mutant, the ameloblasts were crowded, the nuclei were in the apical 2/3 of cells, and there was no clear boundary between the ameloblasts and SI/SR. The enamel space in the control was empty (B) while there was pink stained enamel matrix protein (marked by the arrow) in the CS mutant (C). The percent of nuclei in the apical 2/3 of the cell (D; **$p<0.0025$) and number of ameloblasts in the labial aspect of the incisor (E; *$p<0.025$) at secretory (Sec.) and maturation (Mat.) stage are quantified.

104

4.4.4 Treatment with MEK and PI3'K inhibitors enhances enamel deposition in control mice

In order to determine through which effector pathway HRAS acts to regulate amelogenesis, mice were treated with MEK1/2 (PD0325901, Pfizer, New York, NY) or PI3'K (GDC-0941, Genentech, South San Francisco, CA) inhibitors. The systemic inhibition of the signaling pathways by the specific inhibitors was confirmed by performing western blot analysis on protein isolated from the liver (Supplemental Figure 4). We first tested the effects of these inhibitors in control adult (P70) mice. Coronal µCT images showed that mice treated with MEK or PI3'K inhibitors for 28 days had normal enamel density (Figure 4.4A',E',I'); however, the enamel formed earlier after treatment with either of the inhibitors compared to vehicle-treated control mice. In control mice, enamel was visible near the 1st molar, whereas enamel appeared near the 2nd molar with MEK inhibition and near the 3rd molar with PI3'K inhibition (Figure 4.4A,E,I). Although the timing of enamel deposition differed, the enamel structure analyzed by SEM was the same with vehicle, MEK and PI3'K inhibitor treatments (Figure 4.4B,F,J).
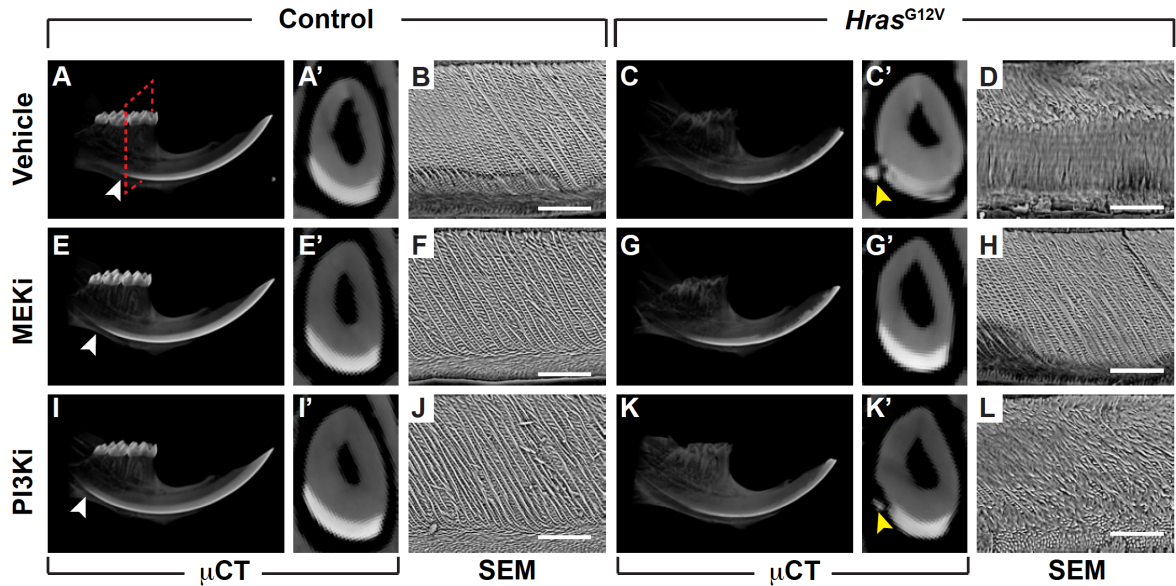
Figure 4.4 HRAS signaling negatively regulates enamel formation. Micro-CT (μCT) and SEM images of control and CS (*Hras*[G12V]) incisors treated with vehicle, MEK1/2 inhibitor (MEKi), or PI3'K inhibitor (PI3Ki) for 28 days. (A,E,I) Coronal μCT images of the incisor in the plane of the 1st molar indicated by the red dashed rectangle showed that enamel density and distribution was similar in control treated with MEKi (E') or PI3Ki (I') compared to vehicle (A'), but enamel mineralization began earlier as noted by white arrowheads. (C,G,K) The CS incisor treated with MEKi (G') appeared to have denser enamel than the CS incisor treated with vehicle (C') or PI3Ki (K'), similar to the control treated with vehicle (A'). Note MEKi (G'), but not PI3Ki (K'), treatment rescued CS enamel distribution pattern, including enamel pearl phenotype (marked by yellow arrowhead) (C'). (D,H,L) SEM images showed that the highly organized pattern of enamel rods in the control (B) was rescued in the CS incisor treated with MEKi (H), but not PI3Ki (L) (scale bar: 50μm).

4.4.5 MEK inhibition of CS (*Hras*^{G12V}) mice rescues the enamel defect

We next assessed the effects of the pathway specific inhibitors in CS adult mutant mice. Treatment of CS mice with the MEK inhibitor rescued the density, patterning and structure of enamel, whereas PI3'K inhibition only partially rescued the enamel density and had no effect on the patterning or structure of enamel. CS mice treated with MEK inhibitor produced densely mineralized enamel that covered the entire aspect of the labial incisor, similar to vehicle-treated control mice (Figure 4.4A',G'). In fact, the enamel volume and percent of tooth covered by enamel was not significantly different between MEK inhibitor treated CS and vehicle treated control incisors (Supplemental Figure 5). MEK inhibition not only rescued the density and patterning of enamel but also restored the enamel microstructure comparable to the control (Figure 4.4B,H). Treatment with PI3'K inhibitor resulted in the formation of enamel with slightly increased mineral density compared to CS enamel but less dense than control incisor, and thus, the rescue appeared to be less than with MEK inhibition (Figure 4.4C',G',K'). PI3'K inhibition failed to rescue the distribution of enamel, as the enamel did not cover the entire labial aspect of the incisor, or the enamel structure, because the enamel rod pattern was disorganized similar to CS enamel (Figure 4.4D,L). These studies using highly specific antagonists demonstrate that hyperactive HRAS signals primarily through MAPK to dysregulate enamel formation.

Underlying the rescue of the enamel mineralization defect was the normalization of the morphology of the enamel-producing ameloblasts. CS

107

ameloblasts treated with MEK inhibitor were normally polarized, with nuclei in the basal portion of the cell similar to control mice (Figure 4.5A',G',M). In contrast, PI3'K inhibition did not rescue polarity of CS ameloblasts (Figure 4.5D',J',M). Also, in both vehicle treated and PI3'K inhibited CS incisors, there was residual enamel matrix in the enamel space (Figure 4.5D,J). In 75% of samples, areas of sequestered enamel matrix were surrounded by disorganized ameloblasts (Figure 4.5D) on the labial aspect of the CS incisor. These sequestered areas of matrix were presumably precursors of ectopic enamel pearls observed near the lateral aspect of CS incisors (Figure 4.4C'). In contrast, areas of sequestered enamel matrix were not observed in CS incisors treated with MEK inhibitor, although they were present in incisors treated with PI3'K inhibitor (Figure 4.5G,J).

MEK inhibition also appeared to rescue the ability of CS ameloblasts to differentiate and secrete enamel proteins. In CS mice, there was a delay in ameloblast secretion of enamel proteins such as AMEL and AMBN, as indicated by the increased distance between the cervical loop (CL) region and the appearance of enamel proteins compared to controls (Figure 4.5B,E,N). Treatment with MEK inhibitor rescued this delayed expression, and CS ameloblasts began to secrete AMEL at the same location as control (Figure 5H,N). In contrast, PI3'K treatment of CS mice did not rescue the delay in appearance of enamel proteins (Figure 4.5K,N).

To determine differences in Ras/MAPK signaling in the CS incisor compared to control, p-ERK immunostaining was done. p-ERK expression in

the control incisor was low compared to high levels of p-ERK activation along the length of the CS incisor (Figure 4.5C,F). MEK inhibitor treatment of the CS incisor decreased the p-ERK levels to control, and PI3'K inhibition did not affect p-ERK expression in the CS incisor (Figure 4.5I,L).
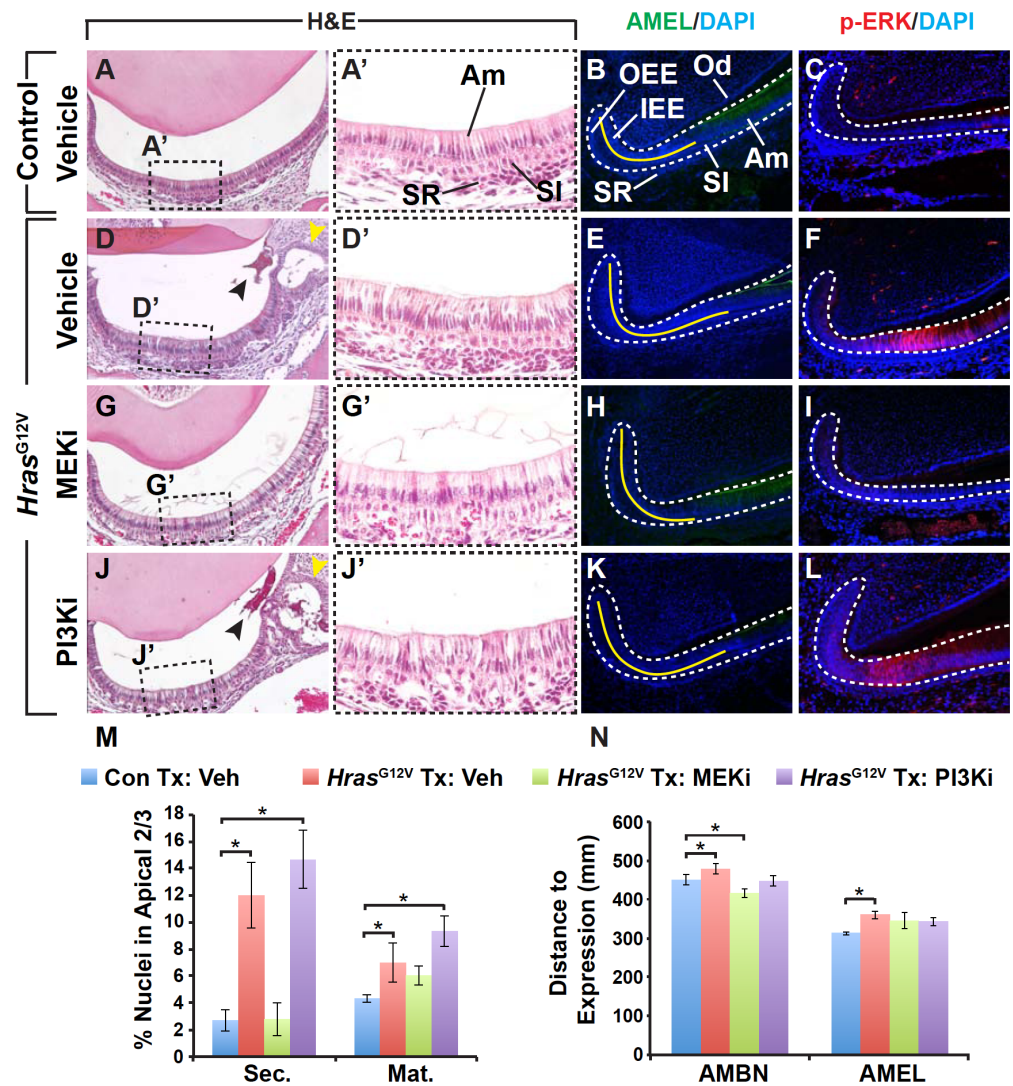
Figure 4.5 MEK inhibition rescues CS (*Hras*[G12V]) ameloblast cell polarity and protein expression. Images of H&E stained coronal sections showed CS ameloblasts treated with MEK inhibitor (MEKi) (G, G') were polarized with nuclei in the basal portion of the cell, similar to control (A, A') while the PI3'K inhibitor (PI3Ki) treated CS ameloblasts (J, J') showed loss of polarity like the CS ameloblasts treated with vehicle (D, D'). Sagittal sections of mouse incisors stained with antibodies against amelogenin (AMEL) showed that expression of the secretory stage enamel protein was delayed and detected at a greater distance from the cervical loop in CS incisor (E) compared to control (B). Treatment with MEKi (H) decreased the distance similar to control (B), unlike treatment with PI3Ki (K). Immunostaining on sagittal sections with an antibody against p-ERK showed high levels of expression along the length of the CS incisor (F) compared to control (C). Treatment of CS incisor with MEKi (I) reduced expression levels to that of control (C) while PI3Ki did not affect p-ERK expression (L). Quantification of the percentage of nuclei in the apical 2/3 of the ameloblasts (M; *$p<0.05$) and distance from the cervical loop to the start of enamel protein expression (N; *$p<0.05$) is shown in the graphs. (ameloblast, Am; stellate reticulum, SR; stratum intermedium, SI; outer enamel epithelium, OEE; inner enamel epithelium, IEE; odontoblast, Od)

110

4.4.6 MEK or PI3'K inhibition rescues the hyperproliferative progenitor phenotype in CS (*Hras*^{G12V}) mice

The increase in ameloblast number at the secretory and maturation stages in CS mice was correlated with increased proliferation of progenitor cells in the CL and transit-amplifying (TA) region compared to control (Figure 4.6B,C). In the CS mouse CL/TA region, 25% of cells were proliferative, compared to 12% of cells in control mice (Figure 4.6B,C,H). In addition, the length of the TA region was significantly shorter in CS mice compared to controls (Figure 4.6B,C,I). In control mice, MEK and PI3'K inhibition decreased proliferation in the CL/TA and decreased the length of the TA region significantly (Figure 4.6B,D,F). There was no significant difference in proliferation or TA zone length between MEK and PI3'K treated control mice (Figure 4.6H,I). MEK inhibition of CS mice rescued the hyperproliferative phenotype, reducing proliferation to levels observed in control mice (Figure 4.6B,E). However, the length of the TA region was not rescued (Figure 4.6I). PI3'K-treated CS mice showed reduced proliferation levels even below that of controls (Figure 4.6B,G), and the TA region was significantly shorter than vehicle-treated control and CS mice (Figure 4.6I).

111
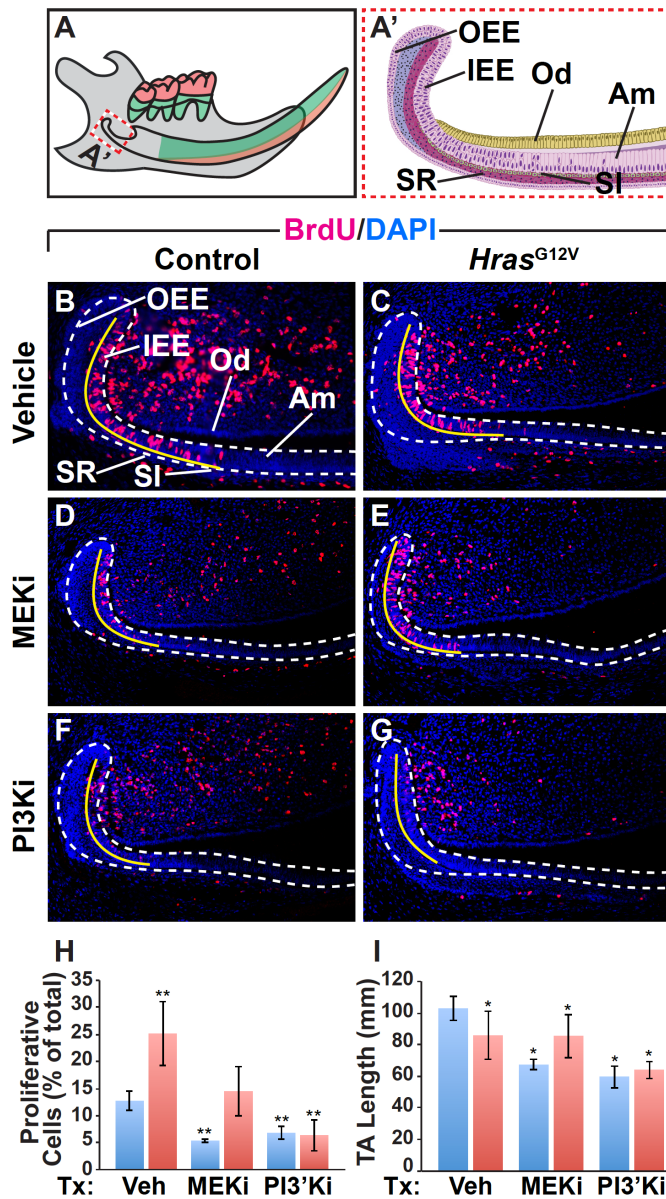
Figure 4.6 MAPK or PI3'K inhibition rescues progenitor cell hyperproliferation in CS (*Hras*^{G12V}) mouse incisor. Immunostaining with anti-BrdU antibody (red) and DAPI (blue) counterstain in the cervical loop (CL) (A') at the proximal end of the incisor (A) revealed an increase in the number of proliferative cells in the CS incisor (C) compared to control (B) in the CL and transit amplifying (TA) region (outlined by the white dashed line). Proliferation was decreased in the control by treatment with MEK1/2 (MEKi) (D) and PI3'K (PI3Ki) inhibitor (F), and the length of the TA zone was shortened (labeled with yellow line). Treatment of CS mice with MEKi (E) decreased the proliferation to control levels, and treatment with PI3Ki (G) reduced it below control levels; however, treatment with neither MEKi nor PI3Ki rescued the TA region length. The percent of BrdU positive cells (H; **p<0.01) and TA length (I; *p<0.05) are quantified in the graphs (significant compared to vehicle treated control). (ameloblast, Am; stellate reticulum, SR; stratum intermedium, SI; outer enamel epithelium, OEE; inner enamel epithelium, IEE; odontoblast, Od)

112

4.5 DISCUSSION

The RASopathies are a group of syndromes estimated to affect 1 in 1,000 live births. There are numerous morbidities associated with these syndromes, and presently, effective therapies are lacking. Although the role of Ras signaling has been studied in development of several organs, almost nothing is known about its role during tooth development and renewal. Our analyses of both humans with CS and a CS mouse model revealed that activated HRAS negatively regulates enamel formation. Specifically, CS individuals with activated Ras signaling presented with hypo-mineralized, disorganized enamel, and a similar enamel phenotype was observed in CS mice. CS ameloblast progenitor cells were hyperproliferative, and CS ameloblasts lacked cell polarity. Furthermore, attenuation of the MAPK pathway led to the rescue of the enamel and ameloblast phenotypes, whereas modulation of either MAPK or PI3'K signaling prevented progenitor cell hyperproliferation in CS mice.

The role of RTK, and particularly FGF, signaling has been studied previously in tooth development, but the focus has been on tooth morphogenesis. Only a few studies have explored FGF signaling in enamel formation, and thus, little is known about the role of RTK or downstream Ras signaling in enamel formation. Inactivation of *Fgfr1* in the epithelium resulted in dysfunctional ameloblasts that produced disorganized enamel (Takamori et al., 2008). Overexpression of *Fgf2* in cultured embryonic molars resulted in decreased expression of amelogenin, while inhibition of FGF2 increased

113

amelogenin expression and enamel formation (Tsuboi et al., 2003). Interestingly, other Ras superfamily members have been shown to play a role in amelogenesis, including Rac, a GTPase involved in cytoskeletal remodeling that is directly activated by PI3'K (Welch et al., 2003). Conditional inactivation of *Rac1* in the epithelium resulted in ameloblasts that expressed decreased levels of amelogenin and lost attachment to the secreted enamel matrix, resulting in hypo-mineralized enamel (Huang et al., 2011). Thus, it is possible that activated HRAS disrupts Rac1 signaling, which may result in ameloblast dysfunction and hypo-mineralized enamel in CS.

Ras is thought to play an important role in cell polarity, proliferation, and differentiation, but studies to address the mechanistic role of Ras have largely been performed *in vitro*. For example, tissue culture studies have shown that activation of KRAS and BRAF in a colon cancer cell line perturbs the polarity of cyst structures (Magudia et al., 2012), and activation of HRAS in neuronal cell culture causes loss of polarity and multiple axon formation (Yoshimura et al., 2006). To establish polarity in mammalian epithelial cells, a PAR-3/PAR-6/aPKC/Cdc42 complex localizes to the apical end of the cell, where adherens junctions and then tight junctions form that divide the apical and basolateral regions of the cell (reviewed in (Wodarz, 2002)). PI3'K signaling has been shown to localize Rac and Cdc42 to the leading edge of cells undergoing chemotaxis to induce actin polymerization there (Sasaki, 2004), and in breast epithelial tumor cells, PI3'K activates Rac, which results in loss of polarity (Liu, 2004). Only recently have investigators begun to study

Ras function *in vivo*. A recent study showed that ERK controls spindle orientation during cell division in the developing lung (Tang et al., 2011). In our study, the loss of ameloblast polarity in CS mice was rescued by treatment with MEK but not PI3'K inhibition, suggesting that, in the incisor, hyperactive Ras disrupts ameloblast polarity through MAPK. The mechanistic role that Ras plays in epithelial cell polarity is still unclear, and ameloblasts may serve as a useful model to further understand the role of Ras in the establishment and maintenance of epithelial cell polarity *in vivo*.

In vitro studies have shown that p-ERK and p-AKT regulate proliferation by decreasing p27^{kip1} and p21^{cip1} levels to allow progression from G_0 to S phase (Steelman et al., 2004; Meloche and Pouysségur, 2007). In the mouse CS incisor, proliferation in the cervical loop (CL) and transit-amplifying (TA) region was increased. MEK inhibition reduced proliferation to control levels, and PI3'K inhibition reduced it even further. Thus, both MAPK and PI3'K signaling are important in proliferation, and in CS, PI3'K may have a larger role than MAPK in proliferation. Ras may also play a role in cell differentiation, as in the case of a *Nf1$^{-/-}$* mouse model, in which increased differentiation of neuroblasts into glial cells was observed, and the increased differentiation was rescued by inhibiting ERK (Wang et al., 2012). In this study, we found that p-ERK levels were high in the CS incisor compared to the low levels in control incisors, indicating that the low level of p-ERK may be necessary for the ameloblast progenitors to exit the cell cycle and differentiate. MEK inhibition rescued the delay in ameloblast differentiation in CS mice.

Thus, in the CS mutant, consistently high levels of p-ERK result in hyper-proliferative progenitor cells and delay in ameloblast differentiation.

A number of inhibitors have been developed to target Ras and its effectors to treat cancer (reviewed in (Gysin et al., 2011)). These same inhibitors are potentially useful for treating the RASopathies (Rauen et al., 2011), and our study is the first to report modulation of the Ras pathway with inhibitors in CS. This concept has recently been explored in animal models of other RASopathies. For example, treatment of neurofibromatosis type 1 (NF1) mouse models with a MEK inhibitor (PD0325901) reduced the growth and proliferation of neurofibromas (Jessen et al., 2013) and abrogated the myeloproliferative disease in these mice (Chang et al., 2013). In a Noonan syndrome (NS) mouse model with an activating mutation in *SHP2*, MEK inhibition with U0126 ameliorated craniofacial defects and rescued skull shape and size (Nakamura et al., 2009), and in another SOS gain-of-function NS mouse model, treatment with MEK inhibitor (PD0325901) reduced embryonic lethality and rescued heart defects (Chen et al., 2010). A CFC zebrafish model expressing a kinase-activating BRAF[Q257R] allele or kinase-inactivating BRAF[G596V] allele developed craniofacial anomalies, and moreover, these defects were ameliorated by treatment with low doses of MEK inhibitor at early stages of development (Anastasaki et al., 2012). Interestingly, these studies focused on the role of MAPK signaling in NF1, NS, and CFC, and very little work has been done to examine PI3'K/AKT signaling in any of the RASopathies.

116

By comparing the distinct dental phenotypes found in the various RASopathies, we can obtain further insights into the role of the Ras pathway in human teeth. For example, whereas activating mutations in HRAS cause CS, individuals with CFC harbor activating mutations in the kinases BRAF, MEK1 or MEK2, which function downstream of HRAS (Niihori et al., 2006; Rodriguez-Viciana, 2006). Our inhibitor studies in the CS mouse model revealed that modulating the MAPK pathway rescued the enamel phenotype, which would suggest that CFC individuals with activating mutations in the MAPK pathway would have an enamel defect. However, in contrast to the enamel defects in CS individuals, CFC enamel appeared clinically normal (Goodwin et al., 2012), and SEM data showed that the structure of CFC enamel was normal (data not shown). Thus, hyperactivation of Ras signaling in CS versus hyperactivation of MAPK signaling in CFC individuals has different effects on cells in the developing tooth, and whether this is due to quantitative differences in the levels of signaling or to qualitative differences in signaling outputs will be important future topics to explore. Data from clinical studies of other RASopathies indicate that additional pathways downstream of Ras, including PI3'K, or pathways that crosstalk with the RAS/MAPK pathway also play a role in amelogenesis. For example, individuals with Tuberous Sclerosis, which is caused by mutations in the AKT targets *TSC1* or *TSC2*, have de-mineralized pits in the enamel surface (Sparling et al., 2007); interestingly, this phenotype is different from the generalized hypo-mineralized enamel defect in CS. These data suggest a role for PI3'K in tooth

117

development and that dysregulation of PI3'K signaling may disrupt enamel formation. Further studies of RASopathies, both in terms of clinical phenotyping of patients and through utilization of mouse models for mechanistic studies, will help to dissect the role of Ras signaling in amelogenesis and other tissues.

Because the tooth, like most other organs, develops through reciprocal epithelial-mesenchymal interactions (Tucker and Sharpe, 2004; Jernvall and Thesleff, 2000), knowledge gained by studying tooth development may be generalizable to other organs. Thus, dissecting the function of the Ras pathway and its many effectors, including MAPK and PI3'K, in the teeth of both humans and mice will not only advance our knowledge of signaling in the tooth, but also will provide information about the intricacies of Ras signaling in general, which will in turn advance progress towards treatment of the RASopathies.

CHAPTER 5:

Summary, Conclusion, and Future Perspective

In this chapter, I summarize the findings of this thesis dissertation exploring the role of Ras in tooth development utilizing the RASopathies. The work presented in this thesis elucidates the role of Ras in amelogenesis, which will be useful in advancing our efforts to bioengineer teeth. Also, the knowledge gained by studying Ras in the tooth may further our understanding of the functions of Ras and its effector pathways in the RASopathies and cancer.

Summary

The role of Ras signaling in tooth development was analyzed using the RASopathies as a model. I analyzed the craniofacial and dental phenotypes in Costello syndrome (CS) and cardio-facio-cutaneous syndrome (CFC) and found that these syndromes have both unique and shared characteristics. CS and CFC have in common craniofacial characteristics including macrocephaly, bitemporal narrowing, and convex facial profile. Additionally, individuals with CFC have hypoplastic supraorbital ridges, and CS individuals have characteristic micrognathia, full cheeks, large appearing mouth, and thick appearing lips. It is these differences in craniofacial phenotype that give CFC its "delicate" features and CS its "coarser" appearance.

119

The data presented in this thesis are the first analyses of the dental phenotype of any of the RASopathies. Neither CS nor CFC had changes in tooth number or shape. Common to both CS and CFC was malocclusion, including open bite and posterior crossbite. CS and CFC also both had minimal dental crowding, similar caries incidence, and similar habits, like tongue thrusting and open mouth posture. The molar relationship differed between CS and CFC since CFC individuals tended to have class I or class II molar relationship while CS had class III. Overall, the CS dental phenotype was more dysmorphic, with thickening of the posterior maxillary and anterior mandibular alveolar ridge and gingival hyperplasia. CS individuals also had delayed tooth development and eruption. Strikingly, CS individuals had hypoplastic enamel with decreased enamel density and disorganized enamel rod pattern with missing inter-rod enamel that was not present in CFC.

The hypoplastic enamel phenotype in CS provided an excellent opportunity to explore the role of Ras signaling in amelogenesis, and we obtained a CS mouse model for further analysis. The CS enamel phenotype was phenocopied in the CS mouse with missing enamel on the molars and less densely, improperly distributed enamel with disorganized, intersecting enamel rods on the labial aspect of the incisor. Further analysis revealed that the progenitor cells in the cervical loop were hyperproliferative, and the ameloblasts lacked cell polarity and had delayed enamel protein expression, resulting in the enamel phenotype.

To determine the mechanism by which Ras affects amelogenesis, I utilized MEK1/2 (PD0325901) and PI3'K (GDC-0941) inhibitors. Interestingly, MEK inhibition rescued the ameloblast loss of polarity and delayed differentiation while MEK or PI3'K inhibition rescued the hyperproliferation phenotype.

Conclusion and Future Perspectives

The data presented in this thesis dissertation advance our understanding of Ras signaling in craniofacial and dental development. The studies presented here are the first to analyze the craniofacial and dental phenotype in a large cohort of CS and CFC subjects. This data is useful in aiding in clinical diagnosis to guide genetic testing. Also, this thesis provides a primer for dentists treating CS and CFC patients. Additionally, further craniofacial phenotyping of other RASopathies and analysis and manipulation of dental and craniofacial phenotypes in animal models will further our understanding of Ras signaling in craniofacial and tooth development.

In particular, comparison of dental findings in CS and CFC revealed a striking role for Ras in amelogenesis. In the CS mouse model with activated HRAS signaling, ameloblasts were disorganized and lost cell polarity, which may have resulted in inability of the ameloblasts to properly secrete enamel proteins. Delayed expression in secretory enamel proteins and decreased levels of maturation stage protein resulted in a thin matrix that was not

properly mineralized. How Ras affects secretion remains unclear, but Ras may have direct effects on cytoskeletal modeling through Rac or target components of the vesicular trafficking apparatus. Cell culture would be quite useful to observe protein trafficking in ameloblasts using fluorescently labeled enamel proteins, however, the availability of ameloblast cell lines are limited. There are LS8 and HAT7 cell lines which are ameloblast progenitor cells cultured from mouse cervical loops (Chen et al., 1992; Kawano et al., 2002). However, these cells do not necessarily behave like ameloblasts; for example, they do not secrete enamel proteins in appropriate stages or produce mineralized matrices. Currently, our lab is isolating and characterizing mouse incisor stem cells that may be a more useful cell model to understand the direct effects of Ras on amelogenesis (Chavez et al., 2013).

Also, our data suggest that Ras is necessary to maintain ameloblast cell polarity. Much work is necessary to determine direct targets of Ras in establishing and maintaining epithelial cell polarity. I performed many experiments to determine the expression of tight junction proteins like Par3/Par6 and ZO-1, and hemi-desmosomal components like E-cadherin and PERP *in vivo*; however, I did not observe clear differences in localization of these cellular junctions that may have disrupted polarity in the HRAS activated mutant. Further work is now being done to determine whether there are changes in mitotic spindle orientation in the HRAS activated cells that may contribute to the lack of polarity. *In vitro* cell culture would be useful to further explore the effects of Ras signaling on cell polarity. I attempted to

122

culture Madin-Darby canine kidney epithelial cells (MDCKs), a classic epithelial cell line, on multiple substrates, like Matrigel and transwell filters, to induce polarization, and I had some success inducing MDCKs to polarize on transwell filters, but I was unable to transfect these cells with mutated HRAS plasmids to explore the effect of activated Ras signaling on polarity. Wounding assays, in which a scratch is made in a confluent layer of cells, and the way in which the cells orient and migrate at the wound is observed, with HRAS transfected cells would have been another way to explore Ras effects on cell polarity, however, wounding assays are mimicking cell migration which is not necessarily the same as establishment and maintenance of cell polarity. Thus, the role of Ras in cell polarity is an unanswered question that could have major implications in cancer treatment since prevention of Ras induced loss of polarity could impede metastasis. Further experiments in the effect of Ras on polarity in the tooth may provide generalizable knowledge about Ras and epithelial cell polarity.

Mechanistically, high levels of p-ERK expression were observed along the entire length of the CS incisor compared to control, and high levels of p-ERK may have prevented proliferative progenitor cells from exiting the cell cycle and differentiating into ameloblasts in the incisor. The expression of p-AKT in the incisor is not shown in this thesis, however, preliminary data indicates that p-AKT is indeed expressed in cervical loop where progenitor cells reside, and p-AKT may control progenitor proliferation there. Work is in progress to determine the expression patterns of the Ras effectors in the

tooth, and it will be quite interesting to explore the effect of regulators like Sprouty proteins and upstream FGFs on expression of Ras effectors in the tooth. These types of experiments may be done in mouse models *in vivo*, in Sprouty-null or Fgf3/10 knock out mice for example, or cervical loop cultures may be manipulated with Ras pathway inhibitors or agonists to determine the effects of Ras signaling dysregulation on progenitor cell proliferation and ameloblast differentiation *in vitro*. Our data suggest Ras controls differentiation of ameloblasts through MAPK and regulates proliferation of the progenitor cell population through MAPK and PI3'K. The exact role of MAPK and PI3'K in proliferation and differentiation is a major unanswered question, and the tooth provides an excellent model to dissect the roles of the multiple effector pathways of Ras, and what is learned about Ras signaling in the tooth will be applicable to our understanding of Ras in the RASopathies and cancer.

A major goal in craniofacial biology and clinical dentistry is to bioengineer teeth to alleviate the morbidities of tooth loss in patients, and information gained about Ras signaling in tooth development may aid in this endeavor. There are currently many approaches to replacing adult human teeth under consideration. Humans develop a secondary, permanent dentition from the dental lamina of the primary dentition (Järvinen et al., 2009). There is some information known about the signaling necessary to activate and maintain the dental lamina, including the importance of Wnt signaling (Järvinen et al., 2009; Wang et al., 2009). However, adult secondary dentition

124

does not have a dental lamina, so the potential to grow another replacement set of teeth in adult humans is minimal. There are also stem cells (SCs) in the human tooth that may be used to grow teeth including mesenchymal dental pulp stem cells (DPSCs), periodontal ligament stem cells (PDLSCs), stem cells from exfoliated deciduous (SHED) and 3rd molars, and epithelial SCs in the rests of Malassez that all have varying capacity to produce dentin, cementum, and enamel- and PDL- like structures (Gronthos et al., 2000; Seo et al., 2004; Lozano and Bueno, 2011; Shinmura et al., 2008). However, these cells have limited potential and most likely could not undergo tooth morphogenesis *in vivo*. A more realistic approach may be to engineer a tooth *in vitro* and implant it into the patient's mouth. Tooth bud tissue recombination experiments have been done in mouse, and recombining dissociated embryonic dental epithelial and mesenchymal cells and implanting them in the adult mouse jaw can generate a functional tooth (Nakao et al., 2007; Oshima et al., 2011). In patients, human embryonic or induced pluripotent stem cells could be reprogrammed and differentiated along epithelial and mesenchymal cell fates (Hanna et al., 2010). However, at this stage, the molecular signatures of the dental epithelial and mesenchymal lineage are not well understood, and many labs are working to understand the critical signaling in dental stem cells and how to culture them. Another approach, once the signaling to program progenitor cells to differentiate along the epithelial or mesenchymal lineage and undergo tooth morphogenesis is understood, would be to apply these factors directly to the tissue to induce

125

tooth development. Undoubtedly, much work is required to make bioengineered teeth a reality, but an improved understanding of critical signaling cascades will be an important feature of the foundation for such approaches. Therefore, my finding that Ras is important in amelogenesis and that MAPK signaling may be required for ameloblasts to differentiate and produce enamel may help advance progress towards replacement teeth.

It is also critical to understand activated Ras signaling in the context of the RASopathies as progress is made toward clinical trials to treat the RASopathies, and the tooth may serve as a useful model to do so. Understanding how activating mutations in CS and CFC affect the Ras signaling pathway is necessary to select potential drug therapies. There are several drugs targeting specific proteins affected in CS and CFC that may have potential in treating these syndromes. Farnesyl transferase inhibitors (FTIs), like tipifarnib (Johnson & Johnson) and lonafarnib (Schering-Plough Research Institute), were quite successful in inhibiting HRAS, and since CS is caused by activation of HRAS, FTIs may be effective in treating CS. Also, MEK inhibitors like PD0325901 (Pfizer) may be useful in treating CFC. Specific BRAF inhibitors may be less useful in CFC because they are targeted to BRAFV600E and, surprisingly, appear to have opposite effects on endogenous BRAF signaling, increasing signaling. The Ras signaling pathway must be clearly understood in order to know which components to target because in the case of inhibitors in cancer, manipulation of the Ras pathway had surprising consequences. Paradoxically, BRAF inhibitors have

126

been shown to activate MEK possibly due to negative feedback that decreases inhibitory autophosphorylation and increases Raf signaling. Inhibition of MEK decreases MAPK signaling as expected; however, it can also activate upstream signaling through negative feedback and activate alternative pathways, including PI'3K. Therefore, it will be important to determine appropriate doses of these inhibitors to ameliorate rather than totally ablate the MAPK signaling pathway and avoid negative feedback, or consider dosing drugs in combination. Also, appropriate dosing is critical to minimize side effects, especially if patients will be taking low doses over long periods of time.

To move forward with clinical trials in CS and CFC, it will be important to identify clear endpoints for a clinical trial. It is necessary to identify which characteristics to target with drug treatment and develop parameters to test the efficacy of treatment. Endpoints for clinical trials of CS and CFC may include cardiomyopathy, short stature, neurocognition, and hypotonia (Rauen et al., 2011). Recruitment criteria for clinical trials are important as well. CS and CFC are both rare syndromes with only a few hundred reported cases, but it is still important to select age, sex, and ethnicity matched individuals who would benefit most from a trial. Fortunately, both CS and CFC have strong family networks (CS Family Network and CFC International, respectively), which may aid in identifying and recruiting participants. Thus, although there are many hurdles to clinical trials to treat CS and CFC, there is potential to bring effective treatment to patients.

127

In addition, what is learned by studying the RASopathies and the effects of Ras signaling, using the tooth as a model, may be applicable to further understanding Ras signaling in cancer and developing new approaches to cancer treatment. Considering the high prevalence of *RAS* mutations in cancer, it is fascinating that although individuals with the RASopathies have mutations that increase Ras/MAPK signaling in every cell of their body, they do not necessarily develop cancer. An explanation could be that the mutations in the RASopathies activate the cascade less strongly than those in cancer. For example, the most common *BRAF* mutation in cancer is the highly activating *BRAF*^{V600E} mutation implicated in malignant melanoma, papillary thyroid cancer, and colorectal cancers, as well as ovarian, breast and lung cancers (Cantwell-Dorris et al., 2011); however, there are no reports of germline *BRAF*^{V600E} mutations, most likely because this highly oncogenic mutation is incompatible with life. CFC is caused by a heterogenous group of missense mutations in *BRAF* that result in kinase-active and –inactive BRAF proteins that activate downstream p-MEK and p-ERK to varying degrees (Rodriguez-Viciana, 2006), including BRAF activity similar to that induced by *BRAF*^{V600E}. However, even though BRAF mutations in CFC activate MAPK signaling to a high level, it does not necessarily result in tumorigenesis. An explanation may be that a second hit mutation in a tumor suppressor like p53 may be required to induce tumorigenesis in cells with less activating *RAS* mutations (Santoriello et al., 2009). Another explanation is that constant increased Ras signaling in the RASopathies may result in elevation

in negative regulatory mechanisms. For example, increased Sprouty or Spred protein expression may increase negative regulation of Ras, ultimately resulting in decreased Ras signaling, although this hypothesis must be proven experimentally. Activated Ras signaling in the RASopathies may also signal through alternative effector pathways, increasing cross talk and negative regulation between pathways. It is fascinating that RASopathy patients are somehow able to manage constant Ras activation, and understanding the mechanisms that underlie this regulation could be useful in managing activated Ras in cancer.

Thus, the RASopathies provide an opportunity to study Ras signaling in humans, and in particular, the tooth serves as an excellent model organ to dissect the intricacies of Ras signaling. Indeed, information gained about Ras signaling in the tooth may not only be useful in understanding tooth development, but applied to efforts to bioengineer teeth and also understand Ras in development of other organs and in cancer.
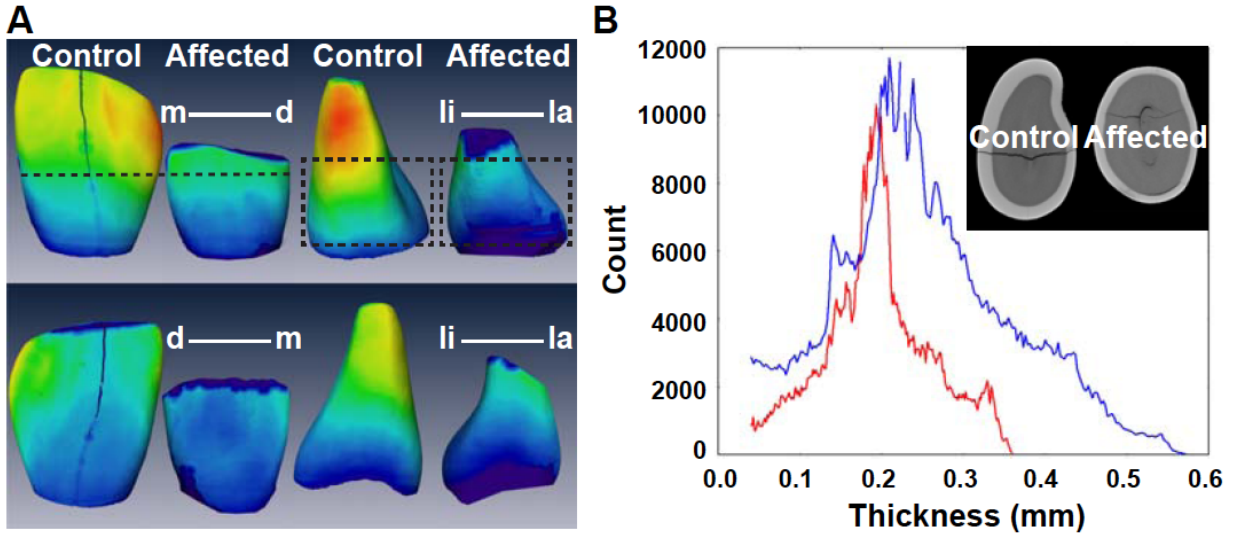
Supplemental Figure 1 Individuals with CS have decreased enamel thickness compared to controls. (A) Micro-CT (µCT) images of labial (la), mesial (m), lingual (li), and distal (d) surfaces of affected CS and age-matched control teeth (primary maxillary incisors). The color of each pixel represents the enamel thickness at that point of the tooth; blue is decreased and red is increased thickness. (B) Graph of the quantification of colored pixels (y-axis) corresponding to enamel thickness (x-axis) in the volume of the tooth, indicated by the dashed box in (A). *Inset*, µCT scan of control and affected teeth at the level of the dashed line in (A).
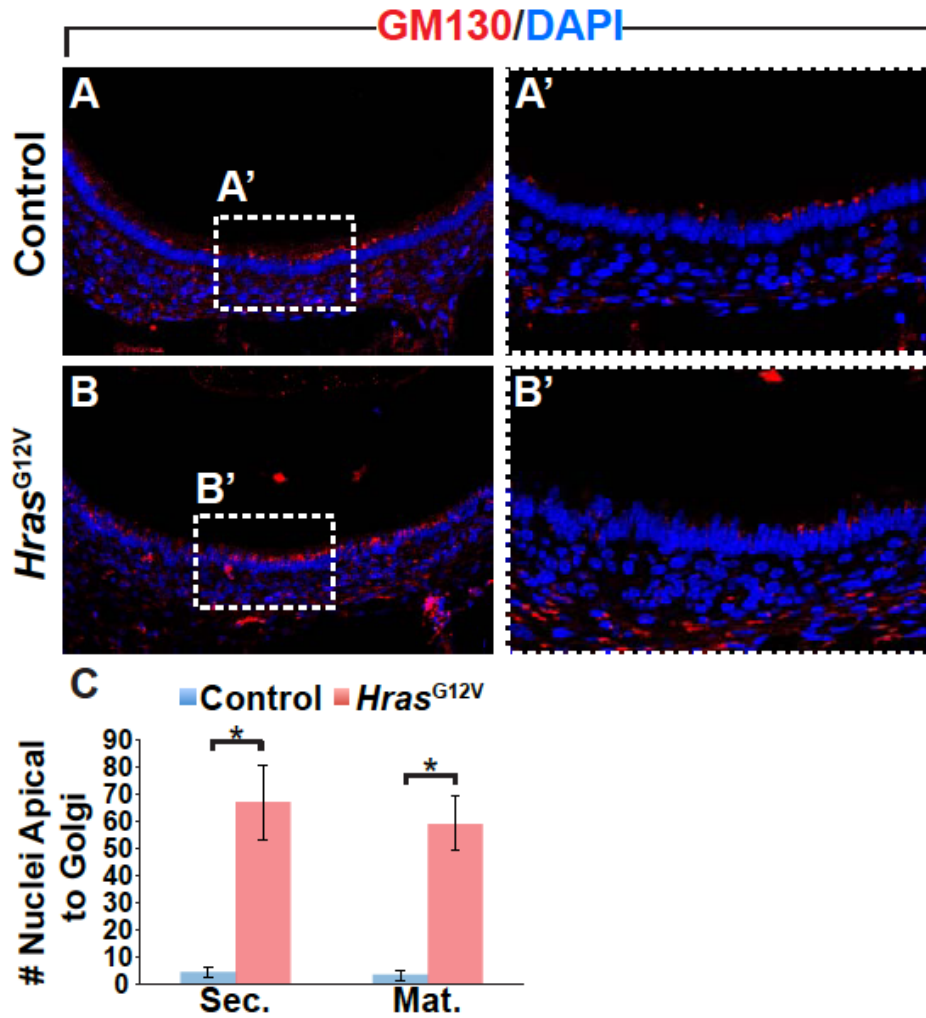
Supplemental Figure 2 CS (*Hras*[G12V]) ameloblasts have mis-oriented golgi relative to nuclei. Coronal sections of incisor in the plane of the 1st molar stained with anti-GM130 antibody and counterstained with DAPI showed that golgi is oriented apically relative to nuclei in the control (A,A') as expected in polarized epithelial cells. Golgi were mis-oriented basally relative to nuclei in CS (*Hras*[G12V]) incisors (B,B'). (C) Number of nuclei positioned apically with respect to the golgi is quantified (*p<0.0004).
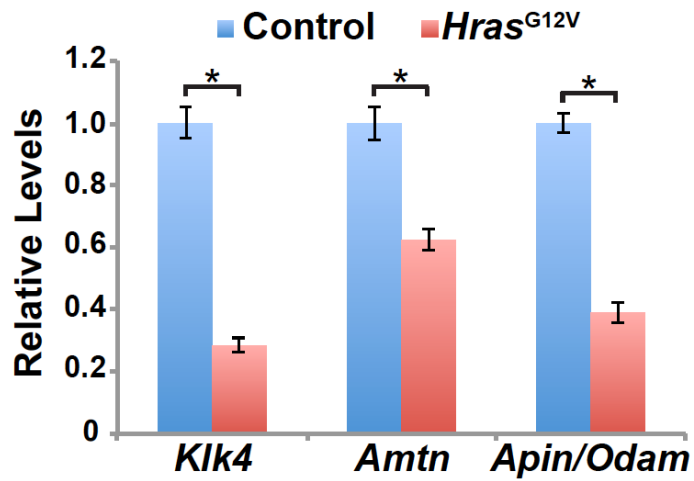
Supplemental Figure 3 CS (*Hras*[G12V]) maturation ameloblasts express decreased levels of enamel proteins. qPCR performed on RNA extracted from P11 molars in the maturation stage showed that CS (*Hras*[G12V]) ameloblasts expressed decreased levels of *Klk4*, *Amtn*, and *Apin/ODAM*, which encode maturation stage enamel proteins, relative to L19, compared to control (*$p < 0.01$).
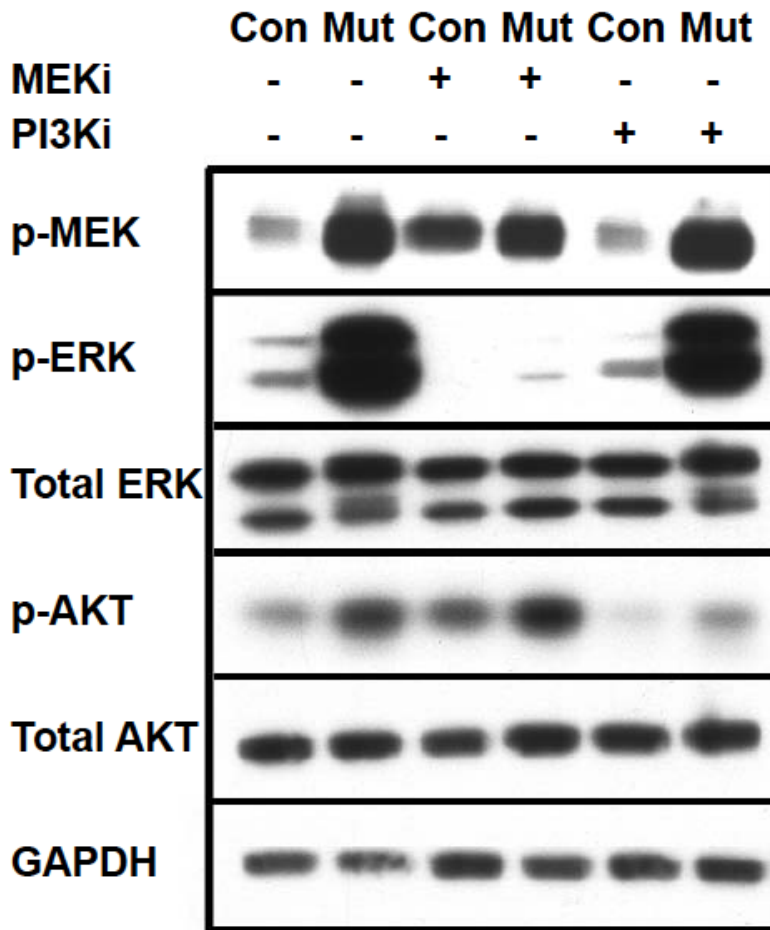
Supplemental Figure 4 Inhibitors specifically target particular effector pathways. To ascertain systemic inhibition, Ras/MAPK and PI3'K pathway signaling was examined in liver from control (Con) and CS (Mut) mice treated with or without MEK (MEKi) and PI3'K (PI3Ki) inhibitors. Ras/MAPK pathway activity was assessed by measuring the level of p-MEK1/2 and p-ERK. PI3'K pathway activity was assessed by the level of phosphorylated AKT (p-AKT). The activation of the Ras/MAPK pathway was confirmed as indicated by a marked increase in the levels of p-MEK and p-ERK in CS mice compared to control. There was also a marked increase in the levels of p-AKT in CS compared to control mice. Therefore, both Ras/MAPK and PI3'K pathways are activated in the liver of CS mice. Administration of the MEK specific inhibitor abrogated Ras/MAPK signaling without affecting PI3'K signaling; likewise, the PI3'K inhibitor markedly reduced PI3'K activity as indicated by the levels of p-AKT, without reducing Ras/MAPK signaling.
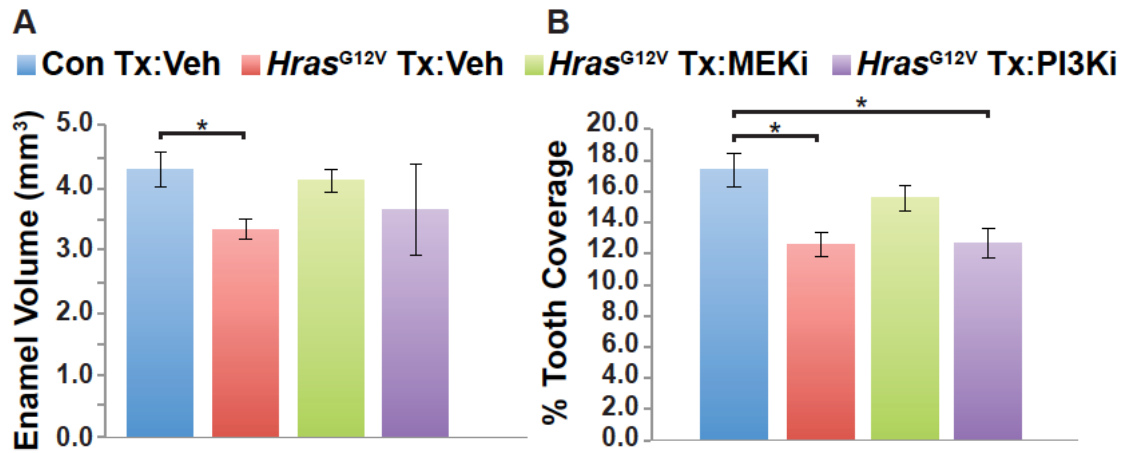
Supplemental Figure 5 Treatment of CS mice with MEKi rescues the enamel volume and distribution phenotype. Quantification of the enamel volume (A) and percent area of the tooth covered by enamel (B) based on microCT (µCT) data for control and CS (*Hras*[G12V]) mice treated with MEKi or PI3Ki (*p<0.01).

REFERENCES

Abou-Alfa, G.K. 2009. Commentary: Sorafenib -- the end of a long journey in search of systemic therapy for hepatocellular carcinoma, or the beginning? *Oncologist*. 14:92–94.

Aguirre, A.J., N. Bardeesy, M. Sinha, L. Lopez, D.A. Tuveson, J. Horner, M.S. Redston, et al. 2003. Activated Kras and Ink4a/Arf deficiency cooperate to produce metastatic pancreatic ductal adenocarcinoma. *Genes Dev*. 17:3112–3126.

Ahearn, I.M., K. Haigis, D. Bar-Sagi and M.R. Philips. 2011. Regulating the regulator: post-translational modification of RAS. *Nat Rev Mol Cell Biol.* 13:39-51.

Aiba, Y., M. Oh-hora, S. Kiyonaka, Y. Kimura, A. Hijikata, Y. Mori, et al. 2004. Activation of RasGRP3 by phosphorylation of Thr-133 is required for B cell receptor-mediated Ras activation. *Proc Natl Acad Sci.* 101:16612–16617.

Anastasaki, C., K.A. Rauen, and E.E. Patton. 2012. Continual low-level MEK inhibition ameliorates cardio-facio-cutaneous phenotypes in zebrafish. *Dis Model Mech.* 5:546–552.

Andl, T., S.T. Reddy, T. Gaddapara, and S.E. Millar. 2002. WNT signals are required for the initiation of hair follicle development. *Dev Cell*. 2:643–653.

Andreadi, C., L.-K. Cheung, S. Giblett, B. Patel, H. Jin, K. Mercer, et al. 2012. The intermediate-activity (L597V)BRAF mutant acts as an epistatic modifier of oncogenic RAS by enhancing signaling through the RAF/MEK/ERK pathway. *Genes Dev*. 26:1945–1958.

Aoki, Y., T. Niihori, H. Kawame, K. Kurosawa, H. Ohashi, Y. Tanaka, M. et al. 2005. Germline mutations in HRAS proto-oncogene cause Costello syndrome. *Nat Genet*. 37:1038–1040.

Aoki, Y., T. Niihori, Y. Narumi, S. Kure, and Y. Matsubara. 2008. The RAS/MAPK syndromes: novel roles of the RAS pathway in human genetic disorders. *Hum Mutat.* 29:992–1006.

Armour, C.M., and J.E. Allanson. 2008. Further delineation of cardio-facio-cutaneous syndrome: clinical features of 38 individuals with proven mutations. *J Med Genet*. 45:249–254.

Barbie, D.A., P. Tamayo, J.S. Boehm, S.Y. Kim, S.E. Moody, I.F. Dunn, et al. 2009. Systematic RNA interference reveals that oncogenic KRAS-driven cancers require TBK1. *Nature*. 462:108–112.

Bartlett, J.D., Z. Skobe, A. Nanci, and C.E. Smith. 2011. Matrix

metalloproteinase 20 promotes a smooth enamel surface, a strong dentino-enamel junction, and a decussating enamel rod pattern. *Eur J Oral Sci*. 119 Suppl 1:199–205.

Becktor, K.B., J.P. Becktor, P.S. Karnes, and E.E. Keller. 2002. Craniofacial and dental manifestations of Proteus syndrome: a case report. *Cleft Palate Craniofac J.* 39:233–245.

Bei, M., and R. Maas. 1998. FGFs and BMP4 induce both Msx1-independent and Msx1-dependent signaling pathways in early tooth development. *Development*. 125:4325–4333.

Biehs, B., J.K.-H. Hu, N.B. Strauli, E. Sangiorgi, H. Jung, R.-P. Herber, et al. Bmi1 represses Ink4a/Arf and Hox genes to regulate stem cells in the rodent incisor. *Nat Cell Biol*. In Press.

Bollag, G., and F. McCormick. 1991. Differential regulation of RasGAP and neurofibromatosis gene product activities. *Nature*. 351:576–579.

Bollag, G., P. Hirth, J. Tsai, J. Zhang, P.N. Ibrahim, H. Cho, et al. 2010. Clinical efficacy of a RAF inhibitor needs broad target blockade in BRAF-mutant melanoma. *Nature*. 467:596–599.

Boon, L.M., J.B. Mulliken, and M. Vikkula. 2005. RASA1: variable phenotype with capillary and arteriovenous malformations. *Curr Opin Genet Dev*. 15:265-269.

Boriack-Sjodin, P.A., S.M. Margarit, D. Bar-Sagi, and J. Kuriyan. 1998. The structural basis of the activation of Ras by Sos. *Nature*. 394:337–343.

Bos, J.L. 1989. Ras oncogenes in human cancer: a review. *Cancer Res*. 49:4682-4689.

Bos, J.L., H. Rehmann, and A. Wittinghofer. 2007. GEFs and GAPs: Critical Elements in the Control of Small G Proteins. *Cell*. 129:865–877.

Boyartchuk, V.L., M.N. Ashby, and J. Rine. 1997. Modulation of Ras and a-factor function by carboxyl-terminal proteolysis. *Science*. 275:1796-1800.

Brems, H., M. Chmara, M. Sahbatou, and E. Denayer. 2007. Germline loss-of-function mutations in SPRED1 cause a neurofibromatosis 1–like phenotype. *Nat Genet*. 39:1120-1126.

Brodie, C., R. Steinhart, G. Kazimirsky, H. Rubinfeld, T. Hyman, J.N. Ayres, et al. 2004. PKCδ associates with and is involved in the phosphorylation of RasGRP3 in response to phorbol esters. *Mol Pharmacol.* 66:76-84.

Cantwell-Dorris, E.R., J.J. O'Leary, and O.M. Sheils. 2011. BRAFV600E:

implications for carcinogenesis and molecular therapy. *Mol Cancer Ther.* 10:385–394.

Casey, P.J., P.A. Solski, C.J. Der, and J.E.Buss. 1989. p21ras is modified by a farnesyl isoprenoid. *Proc Natl Acad Sci.* 82:8323-8237.

Castellano, E., and J. Downward. 2011. RAS Interaction with PI3K: More Than Just Another Effector Pathway. *Genes Cancer*. 2:261–274.

Caterina, J.J., Z. Skobe, J. Shi, Y. Ding, J.P. Simmer, H. Birkedal-Hansen, et al. 2002. Enamelysin (matrix metalloproteinase 20)-deficient mice display an amelogenesis imperfecta phenotype. *J Biol Chem.* 277:49598–49604.

Cawthon, R.M., P. O'Connell, A.M. Buchberg, D. Viskochil, R.B. Weiss, M. Culver, et al. 1990. Identification and characterization of transcripts from the neurofibromatosis 1 region: the sequence and genomic structure of EVI2 and mapping of other transcripts. *Genomics*. 7:555–565.

Cen, H., A.G. Papageorge, W.C. Vass, K.E. Zhang, and D.R. Lowy. 1993. Regulated and constitutive activity by CDC25Mm (GRF), a Ras-specific exchange factor. *Mol Cell Biol*. 13:7718–7724.

Chambard, J.-C., R. Lefloch, J. Pouysségur, and P. Lenormand. 2007. ERK implication in cell cycle regulation. *Biochim Biophys Acta*. 1773:1299–1310.

Chandra, A., H.E. Grecco, V. Pisupati, D. Perera, L. Cassidy, F. Skoulidis, et al. 2011. The GDI-like solubilizing factor PDE [delta] sustains the spatial organization and signalling of Ras family proteins. *Nat Cell Biol.* 14:148-158.

Chang, E.H., M.A. Gonda, R.W. Ellis, E.M. Scolnick, and D.R. Lowy. 1982. Human genome contains four genes homologous to transforming genes of Harvey and Kirsten murine sarcoma viruses. *Proc Natl Acad Sci.* 79:4848–4852.

Chang, T., K. Krisman, E.H. Theobald, J. Xu, J. Akutagawa, J.O. Lauchle, et al. 2013. Sustained MEK inhibition abrogates myeloproliferative disease in Nf1 mutant mice. *J Clin Invest.* 123:335–339.

Charles, C., M. Hovorakova, Y. Ahn, D.B. Lyons, P. Marangoni, S. Churava, et al. 2011. Regulation of tooth number by fine-tuning levels of receptor-tyrosine kinase signaling. *Development*. 138:4063–4073.

Chavez, M.G., W. Yu, B. Biehs, H. Harada, M.L. Snead, J.S. Lee, et al. 2013. Characterization of dental epithelial stem cells from the mouse incisor with two-dimensional and three-dimensional platforms. *Tissue Eng Part C Methods*. 19:15–24.

Chen, D., S.B. Waters, K.H. Holt, and J.E. PESSIN. 1996. SOS

phosphorylation and disassociation of the Grb2-SOS complex by the ERK and JNK signaling pathways. *J Biol Chem*. 271:6328-6332.

Chen, L.S., R.I. Couwenhoven, D. Hsu, W. Luo, and M.L. Snead. 1992. Maintenance of amelogenin gene expression by transformed epithelial cells of mouse enamel organ. *Arch Oral Biol*. 37:771–778.

Chen, P.-C., H. Wakimoto, D. Conner, T. Araki, T. Yuan, A. Roberts, et al. 2010. Activation of multiple signaling pathways causes developmental defects in mice with a Noonan syndrome–associated Sos1 mutation. *J Clin Invest.* 120:4353–4365.

Chen, R.H., S. Corbalan-Garcia, and D. Bar-Sagi. 1997. The role of the PH domain in the signal-dependent membrane targeting of Sos. *EMBO J*. 16:1351–1359.

Chen, X., N. Mitsutake, K. LaPerle, N. Akeno, P. Zanzonico, V.A. Longo, et al. 2009. Endogenous expression of HrasG12V induces developmental defects and neoplasms with copy number imbalances of the oncogene. *Proc Natl Acad Sci*. 106:7979–7984.

Chiu, V.K., T. Bivona, A. Hach, J.B. Sajous, J. Silletti, H. Wiener, et al. 2002. Ras signalling on the endoplasmic reticulum and the Golgi. *Nat Cell Biol.* 4:343-350.

Cho, K.-W., J. Cai, H.-Y. Kim, A. Hosoya, H. Ohshima, K.-Y. Choi, et al. 2009. ERK activation is involved in tooth development via FGF10 signaling. *J Exp Zool.* 312B:901–911.

Choy, E., V.K. Chiu, J. Silletti, M. Feoktistov, T. Morimoto, D. Michaelson, et al. 1999. Endomembrane trafficking of ras: the CAAX motif targets proteins to the ER and Golgi. *Cell*. 98:69–80.

Coughlin, J.J., S.L. Stang, N.A. Dower, and J.C. Stone. 2005. RasGRP1 and RasGRP3 regulate B cell proliferation by facilitating B cell receptor-Ras signaling. *J Immunol.* 175:7179-7184.

Courtney, K.D., R.B. Corcoran, and J.A. Engelman. 2010. The PI3K pathway as drug target in human cancer. *J Clin Oncol*. 28:1075-1083.

Cox, A.D., and C.J. Der. 2010. Ras history: The saga continues. *Small GTPases*. 1:2–27.

Cuisinier, F.J., P. Steuer, B. Senger, J.C. Voegel, and R.M. Frank. 1992. Human amelogenesis. I: High resolution electron microscopy study of ribbon-like crystals. *Calcif Tissue Int.* 51:259–268.

Dai, Q., E. Choy, V. Chiu, J. Romano, S.R. Slivka, S.A. Steitz, et al. 1998.

Mammalian prenylcysteine carboxyl methyltransferase is in the endoplasmic reticulum. *J Biol Chem.* 273:15030–15034.

De Moerlooze, L., B. Spencer-Dene, J.M. Revest, M. Hajihosseini, I. Rosewell and C. Dickson. 2000. An important role for the IIIb isoform of fibroblast growth factor receptor 2 (FGFR2) in mesenchymal-epithelial signalling during mouse organogenesis. *Development*. 127:483-492.

Deakins, M., and J.F. Volker. 1941. Amount of organic matter in enamel from several types of human teeth. *J Dent Res*. 20:117.

DeFeo, D., M.A. Gonda, H.A. Young, E.H. Chang, D.R. Lowy, E.M. Scolnick, et al. 1981. Analysis of two divergent rat genomic clones homologous to the transforming gene of Harvey murine sarcoma virus. *Proc Natl Acad Sci.* 78:3328–3332.

Der, C.J., T. Finkel, and G.M. Cooper. 1986. Biological and biochemical properties of human rasH genes mutated at codon 61. *Cell*. 44:167–176.

Digilio, M.C., E. Conti, A. Sarkozy, R. Mingarelli, T. Dottorini, B. Marino, et al. 2002. Grouping of multiple-lentigines/LEOPARD and Noonan syndromes on the PTPN11 gene. *Am J Hum Genet*. 71:389-394.

Dower, N.A., S.L. Stang, D.A. Bottorff, J.O. Ebinu, P. Dickie, H.L. Ostergaard, and J.C. Stone. 2000. RasGRP is essential for mouse thymocyte differentiation and TCR signaling. *Nat Immunol.* 1:317–321.

Downward, J. 2003. Targeting RAS signalling pathways in cancer therapy. *Nat Rev Cancer*. 3:11–22.

Ebinu, J.O., D.A. Bottorff, E. Chan, S.L. Stang, R.J. Dunn, and J.C. Stone. 1998. RasGRP, a Ras guanyl nucleotide-releasing protein with calcium-and diacylglycerol-binding motifs. *Science*. 280:1082-1086.

Ebinu, J.O., S.L. Stang, C. Teixeira, D.A. Bottorff, J. Hooton, P.M. Blumberg, et al. 2000. RasGRP links T-cell receptor signaling to Ras. *Blood*. 95:3199–3203.

Eerola, I., L.M. Boon, J.B. Mulliken, P.E. Burrows, A. Dompmartin, S. Watanabe, et al. 2003. Capillary malformation-arteriovenous malformation, a new clinical and genetic disorder caused by RASA1 mutations. *Am J Hum Genet.* 73:1240–1249.

Ellis, R.W., D. DeFeo, M.E. Furth, and E.M. Scolnick. 1982. Mouse cells contain two distinct ras gene mRNA species that can be translated into a p21 onc protein. *Mol Cell Biol.* 2:1339–1345.

Esteban, L.M., and C. Vicario-Abejón. 2001. Targeted genomic disruption of

H-ras and N-ras, individually or in combination, reveals the dispensability of both loci for mouse growth and development. *Mol Cell Biol*. 21:1444-1452.

Estep, A.L., W.E. Tidyman, M.A. Teitell, P.D. Cotter, and K.A. Rauen. 2006. HRAS mutations in Costello syndrome: detection of constitutional activating mutations in codon 12 and 13 and loss of wild-type allele in malignancy. *Am J Med Genet.* 140:8–16.

Feng, L., S. Yunoue, H. Tokuo, T. Ozawa, and D. Zhang. 2004. PKA phosphorylation and 14-3-3 interaction regulate the function of neurofibromatosis type I tumor suppressor, neurofibromin. *FEBS Lett*. 557:275-282.

Fernández-Medarde, A., and E. Santos. 2011. The RasGrf family of mammalian guanine nucleotide exchange factors. *Biochim Biophys Acta*. 1815:170–188.

Ferro, E., and L. Trabalzini. 2010. RalGDS family members couple Ras to Ral signalling and that's not all. *Cell Signal*. 22:1804–1810.

Fincham, A.G., J. Moradian-Oldak, T.G. Diekwisch, D.M. Lyaruu, J.T. Wright, P. Bringas, et al. 1995. Evidence for amelogenin "nanospheres" as functional components of secretory-stage enamel matrix. *J Struct Biol.* 115:50–59.

Fiordalisi, J.J., R.L. Johnson, C.A. Weinbaum, K. Sakabe, Z. Chen, P.J. Casey, et al. 2003. High affinity for farnesyltransferase and alternative prenylation contribute individually to K-Ras4B resistance to farnesyltransferase inhibitors. *J Biol Chem.* 278:41718–41727.

Folkes, A.J., K. Ahmadi, W.K. Alderton, S. Alix, S.J. Baker, G. Box, et al. 2008. The Identification of 2-(1 H-Indazol-4-yl)-6-(4-methanesulfonyl-piperazin-1-ylmethyl)-4-morpholin-4-yl-thieno [3, 2-d] pyrimidine (GDC-0941) as a potent, selective, orally bioavailable inhibitor of class I PI3 kinase for the treatment of cancer. *J Med Chem.* 51:5522-5532.

Fujita, J., O. Yoshida, Y. Yuasa, J.S. Rhim, M. Hatanaka, and S.A. Aaronson. 1984. Ha-ras oncogenes are activated by somatic alterations in human urinary tract tumours. *Nature*. 309:464–466.

Fukumoto, S. 2004. Ameloblastin is a cell adhesion molecule required for maintaining the differentiation state of ameloblasts. *J Cell Biol*. 167:973–983.

Fukumoto, S., A. Yamada, K. Nonaka, and Y. Yamada. 2006. Essential roles of ameloblastin in maintaining ameloblast differentiation and enamel formation. *Cells Tissues Organs*. 181:189-195.

Fürthauer, M., W. Lin, S.-L. Ang, B. Thisse, and C. Thisse. 2002. Sef is a feedback-induced antagonist of Ras/MAPK-mediated FGF signalling. *Nat Cell*

Biol. 4:170–174.

Gelb, B.D. 2006. Noonan syndrome and related disorders: dysregulated RAS-mitogen activated protein kinase signal transduction. *Hum Mol Genet*. 15:R220–R226.

Gibson, C.W., Z.A. Yuan, B. Hall, G. Longenecker, E. Chen, T. Thyagarajan, et al. 2001. Amelogenin-deficient mice display an amelogenesis imperfecta phenotype. *J Biol Chem.* 276:31871–31875.

Goodwin, A., S. Oberoi, M. Landan, C. Charles, J. Groth, A. Martinez, et al. 2012. Craniofacial and dental development in cardio-facio-cutaneous syndrome: the importance of Ras signaling homeostasis. *Clin Genet.* 83:539-544.

Goodwin, J.S., K.R. Drake, C. Rogers, L. Wright, J. Lippincott-Schwartz, M.R. Philips, et al. 2005. Depalmitoylated Ras traffics to and from the Golgi complex via a nonvesicular pathway. *J Cell Biol*. 170:261–272.

Gripp, K.W. 2005. Tumor predisposition in Costello syndrome. *Am J Med Genet.* 137C:72–77.

Gripp, K.W., A.E. Lin, D.L. Stabley, L. Nicholson, C.I. Scott, D. Doyle, et al. 2005. HRAS mutation analysis in Costello syndrome: Genotype and phenotype correlation. *Am J Med Genet.* 140A:1–7.

Gronthos, S., M. Mankani, J. Brahim, P.G. Robey, and S. Shi. 2000. Postnatal human dental pulp stem cells (DPSCs) in vitro and in vivo. *Proc Nat Acad Sci*. 97:13625-13630.

Gureasko, J., W.J. Galush, S. Boykevisch, H. Sondermann, D. Bar-Sagi, J.T. Groves, et al. 2008. Membrane-dependent signal integration by the Ras activator Son of sevenless. *Nat Struct Mol Biol.* 15:452–461.

Gysin, S., M. Salt, A. Young, and F. McCormick. 2011. Therapeutic strategies for targeting ras proteins. *Genes Cancer*. 2:359–372.

Habets, G., E. Scholtes, D. Zuydgeest, R.A. van der Kammen, J.C. Stam, A. Berns, et al. 1994. Identification of an invasion-inducing gene, Tiam-1, that encodes a protein with homology to GDP-GTP exchangers for Rho-like proteins. *Cell*. 77:537-549.

Haigis, K.M., K.R. Kendall, Y. Wang, A. Cheung, M.C. Haigis, J.N. Glickman, et al. 2008. Differential effects of oncogenic K-Ras and N-Ras on proliferation, differentiation and tumor progression in the colon. *Nat Genet*. 40:600–608.

Hall, A., C.J. Marshall, N.K. Spurr, and R.A. Weiss. 1983. Identification of transforming gene in two human sarcoma cell lines as a new member of the

ras gene family located on chromosome 1. *Nature*. 303:396–400.

Hanafusa, H., S. Torii, T. Yasunaga, and E. Nishida. 2002. Sprouty1 and Sprouty2 provide a control mechanism for the Ras/MAPK signalling pathway. *Nat Cell Biol*. 4:850–858.

Hancock, J.F., H. Paterson, and C.J. Marshall. 1990. A polybasic domain or palmitoylation is required in addition to the CAAX motif to localize p21 ras to the plasma membrane. *Cell*. 63:133-139.

Hanna, J.H., K. Saha, and R. Jaenisch. 2010. Pluripotency and cellular reprogramming: facts, hypotheses, unresolved issues. *Cell*. 143:508–525.

Hao, Y., R. Wong, and L.A. Feig. 2008. RalGDS Couples Growth Factor Signaling to Akt Activation. *Mol Cell Biol*. 28:2851–2859.

Harada, H., P. Kettunen, H.S. Jung, T. Mustonen, Y.A. Wang, and I. Thesleff. 1999. Localization of putative stem cells in dental epithelium and their association with Notch and FGF signaling. *J Cell Biol*. 147:105–120.

Hart, P.S., T.C. Hart, M.D. Michalec, O.H. Ryu, D. Simmons, S. Hong et al. 2004. Mutation in kallikrein 4 causes autosomal recessive hypomaturation amelogenesis imperfecta. *J Med Genet*. 41:545–549.

Hart, T.C., Y. Zhang, M.C. Gorry, P.S. Hart, M. Cooper, M.L. Marazita, et al. 2002. A mutation in the SOS1 gene causes hereditary gingival fibromatosis type 1. *Am J Hum Genet.* 70:943–954.

Hatzivassiliou, G., K. Song, I. Yen, B.J. Brandhuber, D.J. Anderson, R. Alvarado, et al. 2010. RAF inhibitors prime wild-type RAF to activate the MAPK pathway and enhance growth. *Nature*. 464:431-435.

Hingorani, S.R., L. Wang, A.S. Multani, C. Combs, T.B. Deramaudt, R.H. Hruban, et al. 2005. Trp53R172H and KrasG12D cooperate to promote chromosomal instability and widely metastatic pancreatic ductal adenocarcinoma in mice. *Cancer Cell*. 7:469-483.

Ho, S.P., S.J. Marshall, M.I. Ryder, and G.W. Marshall. 2007. The tooth attachment mechanism defined by structure, chemical composition and mechanical properties of collagen fibers in the periodontium. *Biomaterials*. 28:5238–5245.

Hong, D.S., D.W. Bowles, G.S. Falchook, W.A. Messersmith, G.C. George, C.L. O'Bryant, et al. 2012. A multicenter phase I trial of PX-866, an oral irreversible phosphatidylinositol 3-kinase inhibitor, in patients with advanced solid tumors. *Clin Cancer Res.* 18:4173–4182.

Hu, J., Y. Hu, C.E. Smith, M.D. McKee, J.T. Wright, Y. Yamakoshi, et al. 2008.

Enamel defects and ameloblast-specific expression in Enam knock-out/lacz knock-in mice. *J Biol Chem.* 283:10858-10871.

Hu, J.C.C., Y.-H.P. Chun, T. Al Hazzazzi, and J.P. Simmer. 2007. Enamel Formation and Amelogenesis Imperfecta. *Cells Tissues Organs.* 186:78–85.

Huang, Z., J. Kim, R.S. Lacruz, P. Bringas, M. Glogauer, T.G. Bromage, et al. 2011. Epithelial-specific knockout of the Rac1 gene leads to enamel defects. *Eur J Oral Sci.* 119 Suppl 1:168–176.

Iwasaki, K., E. Bajenova, E. Somogyi-Ganss, M. Miller, V. Nguyen, H. Nourkeyhani, et al. 2005. Amelotin--a novel secreted, ameloblast-specific protein. *J Dent Res.* 84:1127–1132.

Järvinen, E., M. Tummers, and I. Thesleff. 2009. The role of the dental lamina in mammalian tooth replacement. *J Exp Zool.* 312B:281–291.

Jernvall, J., and I. Thesleff. 2000. Reiterative signaling and patterning during mammalian tooth morphogenesis. *Mech Dev.* 92:19–29.

Jernvall, J., P. Kettunen, I. Karavanova, L.B. Martin, and I. Thesleff. 1994. Evidence for the role of the enamel knot as a control center in mammalian tooth cusp formation: non-dividing cells express growth stimulating Fgf-4 gene. *Int J Dev Biol.* 38:463–469.

Jernvall, J., T. Aberg, P. Kettunen, S. Keränen, and I. Thesleff. 1998. The life history of an embryonic signaling center: BMP-4 induces p21 and is associated with apoptosis in the mouse tooth enamel knot. *Development.* 125:161–169.

Jernvall, J., T. Aberg, P. Kettunen, S. Keränen, and I. Thesleff. 1998. The life history of an embryonic signaling center: BMP-4 induces p21 and is associated with apoptosis in the mouse tooth enamel knot. *Development.* 125:161–169.

Jessen, W.J., S.J. Miller, E. Jousma, J. Wu, T.A. Rizvi, M.E. Brundage, et al. 2013. MEK inhibition exhibits efficacy in human and mouse neurofibromatosis tumors. *J Clin Invest.* 123:340–347.

Jheon, A.H., K. Seidel, B. Biehs, and O.D. Klein. 2012. From molecules to mastication: the development and evolution of teeth. *Wiley Interdisc Rev Dev Biol.* 2:165–192.

Jheon, A.H., P. Mostowfi, M.L. Snead, R.A. Ihrie, E. Sone, T. Pramparo, et al. 2011. PERP regulates enamel formation via effects on cell-cell adhesion and gene expression. *J Cell Sci.* 124:745–754.

Johnson, L., D. Greenbaum, K. Cichowski, K. Mercer, E. Murphy, E. Schmitt,

et al. 1997. K-ras is an essential gene in the mouse with partial functional overlap with N-ras. *Genes Dev*. 11:2468-2481.

Juuri, E., K. Saito, L. Ahtiainen, K. Seidel, M. Tummers, K. Hochedlinger, et al. 2012. Sox2+ stem cells contribute to all epithelial lineages of the tooth via Sfrp5+ progenitors. *Dev Cell*. 23:317–328.

Karlsson, L. 2010. Caries detection methods based on changes in optical properties between healthy and carious tissue. *Int J Dent*. 2010:270729.

Karnoub, A.E., and R.A. Weinberg. 2008. Ras oncogenes: split personalities. *Nat Rev Mol Cell Biol*. 9:517–531.

Kato, R., A. Nonami, T. Taketomi, T. Wakioka, A. Kuroiwa, Y. Matsuda, et al. 2003. Molecular cloning of mammalian Spred-3 which suppresses tyrosine kinase-mediated Erk activation. *Biochem Biophys Res Commun*. 302:767–772.

Kawano, S., T. Morotomi, T. Toyono, N. Nakamura, T. Uchida, M. Ohishi, et al. 2002. Establishment of dental epithelial cell line (HAT-7) and the cell differentiation dependent on notch signaling pathway. *Connect Tissue Res*. 43:409–412.

Kerr, B., M.A. Delrue, S. Sigaudy, R. Perveen, M. Marche, I. Burgelin, et al. 2006. Genotype-phenotype correlation in Costello syndrome: HRAS mutation analysis in 43 cases. *J Med Genet*. 43:401–405.

Kettunen, P., I. Karavanova, and I. Thesleff. 1998. Responsiveness of developing dental tissues to fibroblast growth factors: expression of splicing alternatives of FGFR1, -2, -3, and of FGFR4; and stimulation of cell proliferation by FGF-2, -4, -8, and -9. *Dev Genet.* 22:374–385.

Kettunen, P., J. Laurikkala, P. Itäranta, S. Vainio, N. Itoh, and I. Thesleff. 2000. Associations of FGF-3 and FGF-10 with signaling networks regulating tooth morphogenesis. *Dev Dyn*. 219:322-332

Kim, H.J., and D. Bar-Sagi. 2004. Modulation of signalling by Sprouty: a developing story. *Nat Rev Mol Cell Biol*. 5:441–450.

Kim, J.-W., J.P. Simmer, T.C. Hart, P.S. Hart, M.D. Ramaswami, J.D. Bartlett, et al. 2005. MMP-20 mutation in autosomal recessive pigmented hypomaturation amelogenesis imperfecta. *J Medical Genet*. 42:271–275.

Kim, J.-W., S.-K. Lee, Z.H. Lee, J.-C. Park, K.-E. Lee, M.-H. Lee, et al. 2008. FAM83H mutations in families with autosomal-dominant hypocalcified amelogenesis imperfecta. *Am J Hum Genet.* 82:489–494.

Klein, O.D., D.B. Lyons, G. Balooch, G.W. Marshall, M.A. Basson, M. Peterka,

et al. 2007. An FGF signaling loop sustains the generation of differentiated progeny from stem cells in mouse incisors. *Development*. 135:377–385.

Klein, O.D., G. Minowada, R. Peterkova, A. Kangas, B.D. Yu, H. Lesot, et al. 2006. Sprouty genes control diastema tooth development via bidirectional antagonism of epithelial-mesenchymal FGF signaling. *Dev Cell*. 11:181–190.

Koera, K., K. Nakamura, K. Nakao, J. Miyoshi, K. Toyoshima, T. Hatta, et al. 1997. K-ras is essential for the development of the mouse embryo. *Oncogene*. 15:1151–1159.

Kohl, N.E., C.A. Omer, M.W. Conner, N.J. Anthony, J.P. Davide, S.J. deSolms, et al. 1995. Inhibition of farnesyltransferase induces regression of mammary and salivary carcinomas in ras transgenic mice. *Nat Med*. 1:792-797.

Kollar, E.J., and G.R. Baird. 1969. The influence of the dental papilla on the development of tooth shape in embryonic mouse tooth germs. *J Embryol Exp Morphol*. 21:131–148.

Kollar, E.J., and G.R. Baird. 1970. Tissue interactions in embryonic mouse tooth germs II. The inductive role of the dental papilla. *J Embryol Exp Morphol*. 24:173-186.

Kontaridis, M.I., K.D. Swanson, F.S. David, D. Barford, and B.G. Neel. 2006. PTPN11 (Shp2) mutations in LEOPARD syndrome have dominant negative, not activating, effects. *J Biol Chem*. 281:6785-6792.

Koshiba, S., T. Kigawa, J.H. Kim, M. Shirouzu, D. Bowtell, and S. Yokoyama. 1997. The solution structure of the pleckstrin homology domain of mouse Son-of-sevenless 1 (mSos1). *J Mol Biol.* 269:579–591.

Kubiseski, T.J., Y.M. Chook, W.E. Parris, M. Rozakis-Adcock, and T. Pawson. 1997. High affinity binding of the pleckstrin homology domain of mSos1 to phosphatidylinositol (4,5)-bisphosphate. *J Biol Chem.* 272:1799–1804.

Kweon, Y.-S., K.-E. Lee, J. Ko, J.C.C. Hu, J.P. Simmer, and J.-W. Kim. 2013. Effects of Fam83h overexpression on enamel and dentine formation. *Arch Oral Biol*. doi:10.1016/j.archoralbio.2013.03.001.

Lagerström, M., N. Dahl, L. Iselius, B. Bäckman, and U. Pettersson. 1990. Mapping of the gene for X-linked amelogenesis imperfecta by linkage analysis. *Am J Hum Genet.* 46:120–125.

Lee, H.-K., D.-S. Lee, H.-M. Ryoo, J.-T. Park, S.-J. Park, H.-S. Bae, et al. 2010. The odontogenic ameloblast-associated protein (ODAM) cooperates with RUNX2 and modulates enamel mineralization via regulation of MMP-20. *J Cell Biochem.* 111:755–767.

Legius, E., C. Schrander-Stumpel, E. Schollen, C. Pulles-Heintzberger, M. Gewillig, and J.P. Fryns. 2002. PTPN11 mutations in LEOPARD syndrome. *J Med Genet*. 39:571–574.

Li, C.-Y., W. Cha, H.-U. Luder, R.-P. Charles, M. McMahon, T.A. Mitsiadis, et al. 2012. E-cadherin regulates the behavior and fate of epithelial stem cells and their progeny in the mouse incisor. *Dev Biol*. 366:357–366.

Lin, A.E., P.D. Grossfeld, R.M. Hamilton, L. Smoot, K.W. Gripp, V. Proud, et al. 2002. Further delineation of cardiac abnormalities in Costello syndrome. *Am J Med Genet.* 111:115–129.

Liu, H. 2004. Polarity and proliferation are controlled by distinct signaling pathways downstream of PI3-kinase in breast epithelial tumor cells. *J Cell Biol*. 164:603–612.

Liu, W., J. Selever, M.-F. Lu, and J.F. Martin. 2003. Genetic dissection of Pitx2 in craniofacial development uncovers new functions in branchial arch morphogenesis, late aspects of tooth morphogenesis and cell migration. *Development*. 130:6375–6385.

Lobell, R.B., C.A. Omer, M.T. Abrams, H.G. Bhimnathwala, M.J. Brucker, C.A. Buseret al. 2001. Evaluation of farnesyl: protein transferase and geranylgeranyl: protein transferase inhibitor combinations in preclinical models. *Cancer Res*. 61:8758-8768.

Rodriguez-Lozano, F.J., C. Bueno, C.L Insausti, L. Meseguer, M.C. Ramirez, M. Blanquer. 2011. Mesenchymal stem cells derived from dental tissues. *Int Endod J.* 44:800-806.

Lumsden, A.G. 1988. Spatial organization of the epithelium and the role of neural crest cells in the initiation of the mammalian tooth germ. *Development*. 103 Suppl:155–169.

Luo, J., M.J. Emanuele, D. Li, C.J. Creighton, M.R. Schlabach, T.F. Westbrook, et al. 2009. A genome-wide RNAi screen identifies multiple synthetic lethal interactions with the Ras oncogene. *Cell*. 137:835–848.

Luo, T., K. Masson, J.D. Jaffe, W. Silkworth, N.T. Ross, C.A. Scherer, et al. 2012. STK33 kinase inhibitor BRD-8899 has no effect on KRAS-dependent cancer cell viability. *Proc Natl Acad Sci*. 109:2860–2865.

Macdonald, J.S., S. McCoy, R.P. Whitehead, S. Iqbal, J.L. Wade, J.K. Giguere, et al. 2005. A phase II study of farnesyl transferase inhibitor R115777 in pancreatic cancer: a Southwest oncology group (SWOG 9924) study. *Invest New Drugs*. 23:485–487.

Magudia, K., A. Lahoz, and A. Hall. 2012. K-Ras and B-Raf oncogenes inhibit

146

colon epithelial polarity establishment through up-regulation of c-myc. *J Cell Biol*. 198:185–194.

Malumbres, M., and M. Barbacid. 2003. RAS oncogenes: the first 30 years. *Nat Rev Cancer*. 3:459–465.

Margarit, S.M., H. Sondermann, B.E. Hall, B. Nagar, A. Hoelz, M. Pirruccello, et al. 2003. Structural evidence for feedback activation by Ras.GTP of the Ras-specific nucleotide exchange factor SOS. *Cell*. 112:685–695.

Meloche, S., and J. Pouysségur. 2007. The ERK1/2 mitogen-activated protein kinase pathway as a master regulator of the G1- to S-phase transition. *Oncogene*. 26:3227–3239.

Michiels, F., G. Habets, J.C. Stam, R.A. Vanderkammen, and J.G. Collard. 1995. A Role for Rac in Tiam1-Induced Membrane Ruffling and Invasion. *Nature*. 375:338–340.

Miller, C.S., and D.D. Damm. 1992. Incidence of verapamil-induced gingival hyperplasia in a dental population. *J Periodontol.* 63:453–456.

Mina, M., and E.J. Kollar. 1987. The induction of odontogenesis in non-dental mesenchyme combined with early murine mandibular arch epithelium. *Arch Oral Biol*. 32:123–127.

Moffatt, P., C.E. Smith, R. St-Arnaud, and A. Nanci. 2008. Characterization of Apin, a secreted protein highly expressed in tooth-associated epithelia. *J Cell Biochem.* 103:941–956.

Mor, A., and M.R. Philips. 2006. Compartmentalized Ras/MAPK signaling. *Annu Rev Immunol.* 24:771–800.

Pinkham, J., P. Casamassimo, H.W. Fields, D.J. McTigue, and A. Nowak. 2012. Pediatric Dentistry: Infancy through Adolescence. *WB Saunders*.

Mucchielli, M.L., T.A. Mitsiadis, S. Raffo, J.F. Brunet, J.P. Proust, and C. Goridis. 1997. Mouse Otlx2/RIEG expression in the odontogenic epithelium precedes tooth initiation and requires mesenchyme-derived signals for its maintenance. *Dev Biol*. 189:275–284.

Muda, M., U. Boschert, R. Dickinson, J.C. Martinou, I. Martinou, M. Camps, et al. 1996. MKP-3, a novel cytosolic protein-tyrosine phosphatase that exemplifies a new class of mitogen-activated protein kinase phosphatase. *J Biol Chem.* 271:4319-4326.

Nakamura, T., J. Gulick, R. Pratt, and J. Robbins. 2009. Noonan syndrome is associated with enhanced pERK activity, the repression of which can prevent craniofacial malformations. *Proc Natl Acad Sci*. 106:15436–15441.

Nakao, K., R. Morita, Y. Saji, K. Ishida, Y. Tomita, M. Ogawa, et al. 2007. The development of a bioengineered organ germ method. *Nat Methods*. 4:227–230.

Neubüser, A., H. Peters, R. Balling, and G.R. Martin. 1997. Antagonistic interactions between FGF and BMP signaling pathways: a mechanism for positioning the sites of tooth formation. *Cell*. 90:247-255.

Nie, X., K. Luukko, and P. Kettunen. 2006. FGF signalling in craniofacial development and developmental disorders. *Oral Diseases*. 12:102–111.

Niihori, T., Y. Aoki, Y. Narumi, G. Neri, H. Cavé, A. Verloes, et al. 2006. Germline KRAS and BRAF mutations in cardio-facio-cutaneous syndrome. *Nat Genet*. 38:294–296.

Nonami, A., T. Taketomi, A. Kimura, K. Saeki, H. Takaki, T. Sanada, et al. 2005. The Sprouty-related protein, Spred-1, localizes in a lipid raft/caveola and inhibits ERK activation in collaboration with caveolin-1. *Genes Cells*. 10:887–895.

Ohren, J.F., H. Chen, A. Pavlovsky, C. Whitehead, E. Zhang, P. Kuffa, et al. 2004. Structures of human MAP kinase kinase 1 (MEK1) and MEK2 describe novel noncompetitive kinase inhibition. *Nat Struct Mol Biol.* 11:1192–1197.

Oldak, J.M., J.P. Simmer, E.C. Lau, P.E. Sarte, H.C. Slavkin, and A.G. Fincham. 1994. Detection of monodisperse aggregates of a recombinant amelogenin by dynamic light scattering. *Biopolymers.* 34:1339-1347.

Oshima, M., M. Mizuno, A. Imamura, M. Ogawa, M. Yasukawa, H. Yamazaki, et al. 2011. Functional tooth regeneration using a bioengineered tooth unit as a mature organ replacement regenerative therapy. *PLoS ONE*. 6:e21531.

Pacold, M.E., S. Suire, O. Perisic, S. Lara-Gonzalez, C.T. Davis, E.H. Walker, et al. 2000. Crystal structure and functional analysis of Ras binding to its effector phosphoinositide 3-kinase gamma. *Cell*. 103:931–943.

Pandit, B., A. Sarkozy, L.A. Pennacchio, C. Carta, K. Oishi, S. Martinelli, et al. 2007. Gain-of-function RAF1 mutations cause Noonan and LEOPARD syndromes with hypertrophic cardiomyopathy. *Nat Genet*. 39:1007–1012.

Patil, S., and R.S. Chamberlain. 2012. Neoplasms associated with germline and somatic NF1 gene mutations. *Oncologist*. 17:101–116.

Peterkova, R., S. Churava, H. Lesot, M. Rothova, J. Prochazka, M. Peterka, et al. 2009. Revitalization of a diastemal tooth primordium in Spry2 null mice results from increased proliferation and decreased apoptosis. *J Exp Zool.* 312B:292–308.

Peters, H., A. Neubüser, K. Kratochwil, and R. Balling. 1998. Pax9-deficient mice lack pharyngeal pouch derivatives and teeth and exhibit craniofacial and limb abnormalities. *Genes Dev*. 12:2735–2747.

Pispa, J., and I. Thesleff. 2003. Mechanisms of ectodermal organogenesis. *Dev Biol*. 262:195–205.

Potenza, N., C. Vecchione, A. Notte, A. De Rienzo, et al. 2005. Replacement of K-Ras with H-Ras supports normal embryonic development despite inducing cardiovascular pathology in adult mice. *EMBO Rep*. 6:432-437.

Poulikakos, P.I., C. Zhang, G. Bollag, K.M. Shokat, and N. Rosen. 2010. RAF inhibitors transactivate RAF dimers and ERK signalling in cells with wild-type BRAF. *Nature*. 464:427-430.

Premkumar, S., S. Avathvadi Venkatesan, and S. Rangachari. 2011. Altered oral sensory perception in tongue thrusters with an anterior open bite. *Eur J Orthod*. 33:139–142.

Proffit, W.R., H.W. Fields Jr, and D.M. Sarver. 2006. Contemporary orthodontics. *Mosby Elsevier*.

Rajpar, M.H., K. Harley, C. Laing, R.M. Davies, and M.J. Dixon. 2001. Mutation of the gene encoding the enamel-specific protein, enamelin, causes autosomal-dominant amelogenesis imperfecta. *Hum Mol Genet*. 10:1673–1677.

Rasband, W.S. ImageJ, U.S. National Institutes of Health, Bethesda, MD, USA. *http://imagej.nih.hob/ij/*.

Rauen, K.A. 2007. HRAS and the Costello syndrome. *Clin Genet.* 71:101–108.

Rauen, K.A., A. Banerjee, W.R. Bishop, J.O. Lauchle, F. McCormick, M. McMahon, et al. 2011. Costello and cardio-facio-cutaneous syndromes: Moving toward clinical trials in RASopathies. *Am J Med Genet.* 157:136–146.

Rauen, K.A., L. Schoyer, F. McCormick, A.E. Lin, J.E. Allanson, D.A. Stevenson, et al. 2010. Proceedings from the 2009 genetic syndromes of the Ras/MAPK pathway: From bedside to bench and back. *Am J Med Genet.* 152A:4-24.

Razzaque, M.A., T. Nishizawa, Y. Komoike, H. Yagi, M. Furutani, R. Amo, et al. 2007. Germline gain-of-function mutations in RAF1 cause Noonan syndrome. *Nat Genet*. 39:1013–1017.

Reiss, Y., J.L. Goldstein, M.C. Seabra, P.J. Casey, and M.S. Brown. 1990. Inhibition of purified p21ras farnesyl:protein transferase by Cys-AAX

149

tetrapeptides. *Cell*. 62:81–88.

Resende, R.G., J.A.R. Brito, L.N. Souza, R.S. Gomez, and R.A. Mesquita. 2011. Peripheral calcifying odontogenic cyst: a case report and review of the literature. *Head and Neck Pathol*. 5:76–80.

Rinehart, J., A.A. Adjei, P.M. Lorusso, D. Waterhouse, J.R. Hecht, R.B. Natale, et al. 2004. Multicenter phase II study of the oral MEK inhibitor, CI-1040, in patients with advanced non-small-cell lung, breast, colon, and pancreatic cancer. *J Clin Oncol*. 22:4456–4462.

Riolo, M.L. 2002. Essentials for Orthodontic Practice. 1st ed. EFOP Press.

Roberts, A., J. Allanson, S.K. Jadico, M.I. Kavamura, J. Noonan, J.M. Opitz, et al. 2006. The cardiofaciocutaneous syndrome. *J Med Genet*. 43:833–842.

Roberts, A.E., J.E. Allanson, M. Tartaglia, and B.D. Gelb. 2013. Noonan syndrome. *Lancet*. 381:333–342.

Roberts, A.E., T. Araki, K.D. Swanson, K.T. Montgomery, T.A. Schiripo, V.A. Joshi, et al. 2006. Germline gain-of-function mutations in SOS1 cause Noonan syndrome. *Nat Genet*. 39:70-74.

Roberts, P.J., and C.J. Der. 2007. Targeting the Raf-MEK-ERK mitogen-activated protein kinase cascade for the treatment of cancer. *Oncogene*. 26:3291–3310.

Rocks, O., A. Peyker, M. Kahms, P.J. Verveer, C. Koerner, M. Lumbierres, et al. 2005. An acylation cycle regulates localization and activity of palmitoylated Ras isoforms. *Science*. 307:1746–1752.

Rodriguez-Viciana, P., O. Tetsu, W.E. Tidyman, A.L. Estep, B.A. Conger, M.S. Cruz, et al. 2006. Germline mutations in genes within the MAPK pathway cause Cardio-facio-cutaneous syndrome. *Science*. 311:1287–1290.

Rodriguez-Viciana, P., P.H. Warne, R. Dhand, B. Vanhaesebroeck, I. Gout, M.J. Fry. 1994. Phosphatidylinositol-3-OH kinase direct target of Ras. *Nature*. 370:527-532.

Roose, J.P., M. Mollenauer, M. Ho, T. Kurosaki, and A. Weiss. 2007. Unusual interplay of two types of Ras activators, RasGRP and SOS, establishes sensitive and robust Ras activation in lymphocytes. *Mol Cell Biol*. 27:2732–2745.

Roose, J.P., M. Mollenauer, V.A. Gupta, J. Stone, and A. Weiss. 2005. A diacylglycerol-protein kinase C-RasGRP1 pathway directs Ras activation upon antigen receptor stimulation of T cells. *Mol Cell Biol*. 25:4426–4441.

Ruggieri, M., and R.J. Packer. 2001. Why do benign astrocytomas become malignant in NF1? *Neurology*. 56:827–829.

Sakamoto, Y., H. Nakajima, K. Kishi, R. Shimizu, and T. Nakajima. 2010. Management of craniofacial hyperostosis in Proteus syndrome. *J Craniofac Surg*. 21:414–418.

Santoriello, C., G. Deflorian, F. Pezzimenti, K. Kawakami, L. Lanfrancone, F. d'Adda di Fagagna, et al. 2009. Expression of H-RASV12 in a zebrafish model of Costello syndrome causes cellular senescence in adult proliferating cells. *Dis Model Mech. 2:56-67.*

Santos, E., D. Martin-Zanca, E.P. Reddy, M.A. Pierotti, G. Della Porta, and M. Barbacid. 1984. Malignant activation of a K-ras oncogene in lung carcinoma but not in normal tissue of the same patient. *Science*. 223:661-664.

Sarkozy, A., M.C. Digilio, and B. Dallapiccola. 2008. Leopard syndrome. *Orphanet J Rare Dis*. 3:13.

Sasaki, A.T. 2004. Localized Ras signaling at the leading edge regulates PI3K, cell polarity, and directional cell movement. *J Cell Biol*. 167:505–518.

Scheffzek, K., M.R. Ahmadian, W. Kabsch, L. Wiesmüller, A. Lautwein, F. Schmitz, and A. Wittinghofer. 1997. The Ras-RasGAP complex: structural basis for GTPase activation and its loss in oncogenic Ras mutants. *Science*. 277:333–338.

Scholl, C., S. Fröhling, I.F. Dunn, A.C. Schinzel, D.A. Barbie, S.Y. Kim, et al. 2009. Synthetic Lethal Interaction between Oncogenic KRAS Dependency and STK33 Suppression in Human Cancer Cells. *Cell*. 137:821-834.

Schubbert, S., G. Bollag, and K. Shannon. 2007. Deregulated Ras signaling in developmental disorders: new tricks for an old dog. *Curr Opin Genet Dev*. 17:15–22.

Schubbert, S., K. Shannon, and G. Bollag. 2007b. Hyperactive Ras in developmental disorders and cancer. *Nat Rev Cancer*. 7:295–308.

Schubbert, S., M. Zenker, S.L. Rowe, S. Böll, C. Klein, G. Bollag, et al. 2006. Germline KRAS mutations cause Noonan syndrome. *Nat Genet*. 38:331–336.

Schuhmacher, A.J., C. Guerra, V. Sauzeau, M. Cañamero, X.R. Bustelo, and M. Barbacid. 2008. A mouse model for Costello syndrome reveals an Ang II–mediated hypertensive condition. *J Clin Invest*. 118:2169-2179.

Scolnick, E.M., and W.P. Parks. 1974. Harvey sarcoma virus: a second murine type C sarcoma virus with rat genetic information. *J Virol*. 13:1211–1219.

Scolnick, E.M., E. Rands, D. Williams, and W.P. Parks. 1973. Studies on the nucleic acid sequences of Kirsten sarcoma virus: a model for formation of a mammalian RNA-containing sarcoma virus. *J Virol.* 12:458–463.

Sebolt-Leopold, J.S. 2008. Advances in the development of cancer therapeutics directed against the RAS-mitogen-activated protein kinase pathway. *Clin Cancer Res*. 14:3651-3656.

Sebolt-Leopold, J.S., D.T. Dudley, R. Herrera, K. Van Becelaere, A. Wiland, et al. 1999. Blockade of the MAP kinase pathway suppresses growth of colon tumors in vivo. *Nat Med*. 5:810-816.

Seidel, K., C.P. Ahn, D. Lyons, A. Nee, K. Ting, I. Brownell, et al. 2010. Hedgehog signaling regulates the generation of ameloblast progenitors in the continuously growing mouse incisor. *Development*. 137:3753–3761.

Seo, B.-M., M. Miura, S. Gronthos, P.M. Bartold, S. Batouli, J. Brahim, et al. 2004. Investigation of multipotent postnatal stem cells from human periodontal ligament. *Lancet*. 364:149–155.

Serth, J., A. Lautwein, M. Frech, A. Wittinghofer A. Pingoud. 1991. The Inhibition of the GTPase activating protein-Ha-ras interaction by acidic lipids is due to physical association of the C-terminal domain of the GTPase activating protein with micellar structures. *EMBO J.* 10:1325-1330.

Shinmura, Y., S. Tsuchiya, K. Hata, and M.J. Honda. 2008. Quiescent epithelial cell rests of Malassez can differentiate into ameloblast-like cells. *J Cell Physiol.* 217:728-738.

Siegel, D.H., J.A. Mann, A.L. Krol, and K.A. Rauen. 2012. Dermatological phenotype in Costello syndrome: consequences of Ras dysregulation in development. *Br J Dermatol.* 166:601–607.

Simmer, J.P., C.C. Hu, E.C. Lau, P. Sarte, H.C. Slavkin, and A.G. Fincham. 1994. Alternative splicing of the mouse amelogenin primary RNA transcript. *Calcif Tissue Int.* 55:302–310.

Simmer, J.P., Y. Hu, R. Lertlam, Y. Yamakoshi, and J.C.C. Hu. 2009. Hypomaturation enamel defects in Klk4 knockout/LacZ knockin mice. *J Biol Chem.* 284:19110–19121.

Sinn, E., W. Muller, P. Pattengale, I. Tepler, R. Wallace, and P. Leder. 1987. Coexpression of MMTV/v-Ha-ras and MMTV/c-myc genes in transgenic mice: synergistic action of oncogenes in vivo. *Cell*. 49:465–475.

Smith, C.E., A.S. Richardson, Y. Hu, J.D. Bartlett, J.C.C. Hu, and J.P. Simmer. 2011. Effect of kallikrein 4 loss on enamel mineralization: comparison with mice lacking matrix metalloproteinase 20. *J Biol Chem*.

286:18149–18160.

Smith, C.E., and H. Warshawsky. 1975. Cellular renewal in the enamel organ and the odontoblast layer of the rat incisor as followed by radioautography using 3H-thymidine. *Anat Rec*. 183:523–561.

Smith, C.E., and H. Warshawsky. 1977. Quantitative analysis of cell turnover in the enamel organ of the rat incisor. Evidence for ameloblast death immediately after enamel matrix secretion. *Anat Rec*. 187:63–98.

Somogyi-Ganss, E., Y. Nakayama, K. Iwasaki, Y. Nakano, D. Stolf, M.D. McKee, et al. 2012. Comparative temporospatial expression profiling of murine amelotin protein during amelogenesis. *Cells Tissues Organs*. 195:535–549.

Sondermann, H., S.M. Soisson, S. Boykevisch, S.-S. Yang, D. Bar-Sagi, and J. Kuriyan. 2004. Structural analysis of autoinhibition in the Ras activator Son of sevenless. *Cell*. 119:393–405.

Sparling, J.D., C.-H. Hong, J.S. Brahim, J. Moss, and T.N. Darling. 2007. Oral findings in 58 adults with tuberous sclerosis complex. *J Am Acad Dermatol*. 56:786–790.

St Amand, T.R., Y. Zhang, E.V. Semina, X. Zhao, Y. Hu, L. Nguyen, et al. 2000. Antagonistic signals between BMP4 and FGF8 define the expression of Pitx1 and Pitx2 in mouse tooth-forming anlage. *Dev Biol*. 217:323–332.

Steelman, L.S., S.C. Pohnert, J.G. Shelton, R.A. Franklin, F.E. Bertrand, and J.A. McCubrey. 2004. JAK/STAT, Raf/MEK/ERK, PI3K/Akt and BCR-ABL in cell cycle progression and leukemogenesis. *Leukemia*. 18:189–218.

Stevenson, D.A., E.L. Schwarz, J.C. Carey, D.H. Viskochil, H. Hanson, S. Bauer, et al. 2011. Bone resorption in syndromes of the Ras/MAPK pathway. *Clin Genet.* 80:566–573.

Stevenson, D.A., S. Allen, W.E. Tidyman, J.C. Carey, D.H. Viskochil, A. Stevens, et al. 2012. Peripheral muscle weakness in RASopathies. *Muscle Nerve*. 46:394–399.

Stowe, I.B., E.L. Mercado, T.R. Stowe, E.L. Bell, J.A. Oses-Prieto, H. Hernández, et al. 2012. A shared molecular mechanism underlies the human rasopathies Legius syndrome and Neurofibromatosis-1. *Genes Dev*. 26:1421–1426.

Sun, H., C.H. Charles, L.F. Lau, and N.K. Tonks. 1993. MKP-1 (3CH134), an immediate early gene product, is a dual specificity phosphatase that dephosphorylates MAP kinase in vivo. *Cell*. 75:487–493.

Takahashi, M., and H. Ohashi. 2012. Craniofacial and dental malformations in Costello syndrome: a detailed evaluation by using multi-detector row computed tomography. *Congen Anomal*. doi:10.1111/cga.12004.

Takamori, K., R. Hosokawa, X. Xu, X. Deng, P. Bringas, and Y. Chai. 2008. Epithelial fibroblast growth factor receptor 1 regulates enamel formation. *J Dent Res*. 87:238–243.

Tang, N., W.F. Marshall, M. McMahon, R.J. Metzger, and G.R. Martin. 2011. Control of mitotic spindle angle by the RAS-regulated ERK1/2 pathway determines lung tube shape. *Science*. 333:342-345.

Taparowsky, E., K. Shimizu, M. Goldfarb, and M. Wigler. 1983. Structure and activation of the human N- ras gene. *Cell*. 34:581-586.

Tartaglia, M., E.L. Mehler, R. Goldberg, G. Zampino, H.G. Brunner, H. Kremer,et al. 2001. Mutations in PTPN11, encoding the protein tyrosine phosphatase SHP-2, cause Noonan syndrome. *Nat Genet*. 29:465–468.

Tartaglia, M., L.A. Pennacchio, C. Zhao, K.K. Yadav, V. Fodale, A. Sarkozy, et al. 2007. Gain-of-function SOS1 mutations cause a distinctive form of Noonan syndrome. *Nat Genet*. 39:75–79.

Tartaglia, M., S. Martinelli, L. Stella, G. Bocchinfuso, E. Flex, V. Cordeddu et al. 2006. Diversity and Functional Consequences of Germline and Somatic PTPN11 Mutations in Human Disease. *Am J Hum Genet*. 78:279-290.

Thesleff, I., and K. Hurmerinta. 1981. Tissue interactions in tooth development. *Differentiation*. 18:75-88.

Thomas, B.L., A.S. Tucker, M. Qui, C.A. Ferguson, Z. Hardcastle, J.L. Rubenstein, et al. 1997. Role of Dlx-1 and Dlx-2 genes in patterning of the murine dentition. *Development.* 124:4811-4818.

Tidyman, W.E., and K.A. Rauen. 2009. The RASopathies: developmental syndromes of Ras/MAPK pathway dysregulation. *Curr Opin Genet Dev*. 19:230–236.

Tidyman, W.E., H.S. Lee, and K.A. Rauen. 2011. Skeletal muscle pathology in Costello and cardio-facio-cutaneous syndromes: developmental consequences of germline Ras/MAPK activation on myogenesis. *Am J Med Genet C Semin Med Genet*. 157:104–114.

To, M.D., C.E. Wong, A.N. Karnezis, R. Del Rosario, R. Di Lauro, and A. Balmain. 2008. Kras regulatory elements and exon 4A determine mutation specificity in lung cancer. *Nat Genet*. 40:1240–1244.

Trumpp, A., M.J. Depew, J.L. Rubenstein, J.M. Bishop, and G.R. Martin. 1999.

154

Cre-mediated gene inactivation demonstrates that FGF8 is required for cell survival and patterning of the first branchial arch. *Genes Dev*. 13:3136–3148.

Tsai, M.H., C.L. Yu, F.S. Wei, and D.W. Stacey. 1989. The effect of GTPase activating protein upon ras is inhibited by mitogenically responsive lipids. *Science*. 243:522–526.

Tsang, M. 2004. Promotion and attenuation of FGF signaling through the Ras-MAPK pathway. *Science's STKE*. 2004:pe17–pe17.

Tsuboi, T., S. Mizutani, M. Nakano, K. Hirukawa, and A. Togari. 2003. Fgf-2 regulates enamel and dentine formation in mouse tooth germ. *Calcif Tissue Int.* 73:496–501.

Tucker, A., and P. Sharpe. 2004. The cutting-edge of mammalian development; how the embryo makes teeth. *Nat Rev Genet*. 5:499–508.

Tucker, A.S. 1998. Transformation of tooth type induced by inhibition of BMP signaling. *Science*. 282:1136–1138.

Umanoff, H., W. Edelmann, A. Pellicer, and R. Kucherlapati. 1995. The murine N-ras gene is not essential for growth and development. *Proc Natl Acad Sci.* 92:1709-1713.

Urosevic, J., V. Sauzeau, M.L. Soto-Montenegro, S. Reig, M. Desco, E.M.B. Wright, et al. 2011. Constitutive activation of B-Raf in the mouse germ line provides a model for human cardio-facio-cutaneous syndrome. *Proc Natl Acad Sci.* 108:5015–5020.

Vetter, I.R. 2001. The guanine nucleotide-binding switch in three dimensions. *Science*. 294:1299–1304.

Viskochil, D., A.M. Buchberg, G. Xu, R.M. Cawthon, J. Stevens, R.K. Wolff, et al. 1990. Deletions and a translocation interrupt a cloned gene at the neurofibromatosis type 1 locus. *Cell*. 62:187–192.

Wakioka, T., A. Sasaki, R. Kato, T. Shouda, A. Matsumoto, K. Miyoshi, et al. 2001. Spred is a Sprouty-related suppressor of Ras signalling. *Nature*. 412:647-651.

Wallace, M.R., D.A. Marchuk, L.B. Andersen, R. Letcher, et al. 1990. Type 1 neurofibromatosis gene: identification of a large transcript disrupted in three NF1 patients. *Science*. 249:181-186.

Wang, X.-P., M. Suomalainen, S. Felszeghy, L.C. Zelarayan, M.T. Alonso, M.V. Plikus, R.L. Maas, C.-M. Chuong, T. Schimmang, and I. Thesleff. 2007. An Integrated Gene Regulatory Network Controls Stem Cell Proliferation in Teeth. *Plos Biol*. 5:e159. doi:10.1371/journal.pbio.0050159.sg003.

Wang, X.P., D.J. O'Connell, J.J. Lund, I. Saadi, M. Kuraguchi, A. Turbe-Doan, et al. 2009. Apc inhibition of Wnt signaling regulates supernumerary tooth formation during embryogenesis and throughout adulthood. *Development*. 136:1939–1949.

Wang, Y., E. Kim, X. Wang, B.G. Novitch, K. Yoshikawa, L.-S. Chang, et al. 2012. ERK inhibition rescues defects in fate specification of Nf1-deficient neural progenitors and brain abnormalities. *Cell*. 150:816–830.

Welch, H.C.E., W.J. Coadwell, L.R. Stephens, and P.T. Hawkins. 2003. Phosphoinositide 3-kinase-dependent activation of Rac. *FEBS Letters*. 546:93–97.

Whyte, D.B., P. Kirschmeier, T.N. Hockenberry, I. Nunez-Oliva, L. James, J.J. Catino, et al. 1997. K-and N-Ras are geranylgeranylated in cells treated with farnesyl protein transferase inhibitors. *J Biol Chem.* 272:14459-14464.

Wilhelm, S.M., C. Carter, L.Y. Tang, D. Wilkie, A. McNabola, H. Rong, et al. 2004. BAY 43-9006 exhibits broad spectrum oral antitumor activity and targets the RAF/MEK/ERK pathway and receptor tyrosine kinases involved in tumor progression and angiogenesis. *Cancer Res*. 64:7099-77109.

Williams, V.C., J. Lucas, M.A. Babcock, D.H. Gutmann, B. Korf, and B.L. Maria. 2009. Neurofibromatosis type 1 revisited. *Pediatrics*. 123:124–133.

Wise, G.E. 2009. Cellular and molecular basis of tooth eruption. *Orthod Craniofac Res*. 12:67–73.

Wodarz, A. 2002. Establishing cell polarity in development. *Nat Cell Biol*. 4:E39-44.

Worman, H.J., L.G. Fong, A. Muchir, and S.G. Young. 2009. Laminopathies and the long strange trip from basic cell biology to therapy. *J Clin Invest.* 119:1825–1836.

Abou-Alfa, G.K. 2009. Commentary: Sorafenib -- the end of a long journey in search of systemic therapy for hepatocellular carcinoma, or the beginning? *Oncologist*. 14:92–94.

Anastasaki, C., K.A. Rauen, and E.E. Patton. 2012. Continual low-level MEK inhibition ameliorates cardio-facio-cutaneous phenotypes in zebrafish. *Dis Model Mech.* 5:546–552.

Andl, T., S.T. Reddy, T. Gaddapara, and S.E. Millar. 2002. WNT signals are required for the initiation of hair follicle development. *Dev Cell*. 2:643–653.

Andreadi, C., L.-K. Cheung, S. Giblett, B. Patel, H. Jin, K. Mercer, et al. 2012. The intermediate-activity (L597V)BRAF mutant acts as an epistatic modifier of

oncogenic RAS by enhancing signaling through the RAF/MEK/ERK pathway. *Genes Dev*. 26:1945–1958.

Aoki, Y., T. Niihori, H. Kawame, K. Kurosawa, H. Ohashi, Y. Tanaka, M. et al. 2005. Germline mutations in HRAS proto-oncogene cause Costello syndrome. *Nat Genet*. 37:1038–1040.

Aoki, Y., T. Niihori, Y. Narumi, S. Kure, and Y. Matsubara. 2008. The RAS/MAPK syndromes: novel roles of the RAS pathway in human genetic disorders. *Hum Mutat.* 29:992–1006.

Armour, C.M., and J.E. Allanson. 2008. Further delineation of cardio-facio-cutaneous syndrome: clinical features of 38 individuals with proven mutations. *J Med Genet*. 45:249–254.

Ashar, H.R., L. James, K. Gray, D. Carr, M. McGuirk, E. Maxwell, et al. 2001. The farnesyl transferase inhibitor SCH 66336 induces a G(2) --> M or G(1) pause in sensitive human tumor cell lines. *Exp Cell Res*. 262:17–27.

Bartlett, J.D., Z. Skobe, A. Nanci, and C.E. Smith. 2011. Matrix metalloproteinase 20 promotes a smooth enamel surface, a strong dentino-enamel junction, and a decussating enamel rod pattern. *Eur J Oral Sci*. 119 Suppl 1:199–205.

Becktor, K.B., J.P. Becktor, P.S. Karnes, and E.E. Keller. 2002. Craniofacial and dental manifestations of Proteus syndrome: a case report. *Cleft Palate Craniofac J.* 39:233–245.

Bei, M., and R. Maas. 1998. FGFs and BMP4 induce both Msx1-independent and Msx1-dependent signaling pathways in early tooth development. *Development*. 125:4325–4333.

Biehs, B., J.K.-H. Hu, N.B. Strauli, E. Sangiorgi, H. Jung, R.-P. Herber, et al. Bmi1 represses Ink4a/Arf and Hox genes to regulate stem cells in the rodent incisor. *Nat Cell Biol*. In Press.

Bollag, G., P. Hirth, J. Tsai, J. Zhang, P.N. Ibrahim, H. Cho, et al. 2010. Clinical efficacy of a RAF inhibitor needs broad target blockade in BRAF-mutant melanoma. *Nature*. 467:596–599.

Boon, L.M., J.B. Mulliken, and M. Vikkula. 2005. RASA1: variable phenotype with capillary and arteriovenous malformations. *Curr Opin Genet Dev*. 15:265-269.

Bos, J.L. 1989. Ras oncogenes in human cancer: a review. *Cancer Res*. 49:4682-4689.

Bos, J.L., H. Rehmann, and A. Wittinghofer. 2007. GEFs and GAPs: Critical

157

Elements in the Control of Small G Proteins. *Cell*. 129:865–877.

Brems, H., M. Chmara, M. Sahbatou, and E. Denayer. 2007. Germline loss-of-function mutations in SPRED1 cause a neurofibromatosis 1–like phenotype. *Nat Genet*. 39:1120-1126.

Cantwell-Dorris, E.R., J.J. O'Leary, and O.M. Sheils. 2011. BRAFV600E: implications for carcinogenesis and molecular therapy. *Mol Cancer Ther.* 10:385–394.

Caterina, J.J., Z. Skobe, J. Shi, Y. Ding, J.P. Simmer, H. Birkedal-Hansen, et al. 2002. Enamelysin (matrix metalloproteinase 20)-deficient mice display an amelogenesis imperfecta phenotype. *J Biol Chem.* 277:49598–49604.

Cawthon, R.M., P. O'Connell, A.M. Buchberg, D. Viskochil, R.B. Weiss, M. Culver, et al. 1990. Identification and characterization of transcripts from the neurofibromatosis 1 region: the sequence and genomic structure of EVI2 and mapping of other transcripts. *Genomics*. 7:555–565.

Chang, E.H., M.A. Gonda, R.W. Ellis, E.M. Scolnick, and D.R. Lowy. 1982. Human genome contains four genes homologous to transforming genes of Harvey and Kirsten murine sarcoma viruses. *Proc Natl Acad Sci.* 79:4848–4852.

Chang, T., K. Krisman, E.H. Theobald, J. Xu, J. Akutagawa, J.O. Lauchle, et al. 2013. Sustained MEK inhibition abrogates myeloproliferative disease in Nf1 mutant mice. *J Clin Invest.* 123:335–339.

Charles, C., M. Hovorakova, Y. Ahn, D.B. Lyons, P. Marangoni, S. Churava, et al. 2011. Regulation of tooth number by fine-tuning levels of receptor-tyrosine kinase signaling. *Development*. 138:4063–4073.

Chen, P.-C., H. Wakimoto, D. Conner, T. Araki, T. Yuan, A. Roberts, et al. 2010. Activation of multiple signaling pathways causes developmental defects in mice with a Noonan syndrome–associated Sos1 mutation. *J Clin Invest.* 120:4353–4365.

Chen, X., N. Mitsutake, K. LaPerle, N. Akeno, P. Zanzonico, V.A. Longo, et al. 2009. Endogenous expression of HrasG12V induces developmental defects and neoplasms with copy number imbalances of the oncogene. *Proc Natl Acad Sci*. 106:7979–7984.

Cho, K.-W., J. Cai, H.-Y. Kim, A. Hosoya, H. Ohshima, K.-Y. Choi, et al. 2009. ERK activation is involved in tooth development via FGF10 signaling. *J Exp Zool.* 312B:901–911.

Courtney, K.D., R.B. Corcoran, and J.A. Engelman. 2010. The PI3K pathway as drug target in human cancer. *J Clin Oncol*. 28:1075-1083.

Cuisinier, F.J., P. Steuer, B. Senger, J.C. Voegel, and R.M. Frank. 1992. Human amelogenesis. I: High resolution electron microscopy study of ribbon-like crystals. *Calcif Tissue Int.* 51:259–268.

De Moerlooze, L., B. Spencer-Dene, J.M. Revest, M. Hajihosseini, I. Rosewell and C. Dickson. 2000. An important role for the IIIb isoform of fibroblast growth factor receptor 2 (FGFR2) in mesenchymal-epithelial signalling during mouse organogenesis. *Development.* 127:483-492.

Deakins, M., and J.F. Volker. 1941. Amount of organic matter in enamel from several types of human teeth. *J Dent Res.* 20:117.

DeFeo, D., M.A. Gonda, H.A. Young, E.H. Chang, D.R. Lowy, E.M. Scolnick, et al. 1981. Analysis of two divergent rat genomic clones homologous to the transforming gene of Harvey murine sarcoma virus. *Proc Natl Acad Sci.* 78:3328–3332.

Digilio, M.C., E. Conti, A. Sarkozy, R. Mingarelli, T. Dottorini, B. Marino, et al. 2002. Grouping of multiple-lentigines/LEOPARD and Noonan syndromes on the PTPN11 gene. *Am J Hum Genet.* 71:389-394.

Downward, J. 2003. Targeting RAS signalling pathways in cancer therapy. *Nat Rev Cancer.* 3:11–22.

Eerola, I., L.M. Boon, J.B. Mulliken, P.E. Burrows, A. Dompmartin, S. Watanabe, et al. 2003. Capillary malformation-arteriovenous malformation, a new clinical and genetic disorder caused by RASA1 mutations. *Am J Hum Genet.* 73:1240–1249.

Ellis, R.W., D. DeFeo, M.E. Furth, and E.M. Scolnick. 1982. Mouse cells contain two distinct ras gene mRNA species that can be translated into a p21 onc protein. *Mol Cell Biol.* 2:1339–1345.

Esteban, L.M., and C. Vicario-Abejón. 2001. Targeted genomic disruption of H-ras and N-ras, individually or in combination, reveals the dispensability of both loci for mouse growth and development. *Mol Cell Biol.* 21:1444-1452.

Estep, A.L., W.E. Tidyman, M.A. Teitell, P.D. Cotter, and K.A. Rauen. 2006. HRAS mutations in Costello syndrome: detection of constitutional activating mutations in codon 12 and 13 and loss of wild-type allele in malignancy. *Am J Med Genet.* 140:8–16.

Fincham, A.G., J. Moradian-Oldak, T.G. Diekwisch, D.M. Lyaruu, J.T. Wright, P. Bringas, et al. 1995. Evidence for amelogenin "nanospheres" as functional components of secretory-stage enamel matrix. *J Struct Biol.* 115:50–59.

Fiordalisi, J.J., R.L. Johnson, C.A. Weinbaum, K. Sakabe, Z. Chen, P.J. Casey, et al. 2003. High affinity for farnesyltransferase and alternative

159

prenylation contribute individually to K-Ras4B resistance to farnesyltransferase inhibitors. *J Biol Chem.* 278:41718–41727.

Folkes, A.J., K. Ahmadi, W.K. Alderton, S. Alix, S.J. Baker, G. Box, et al. 2008. The Identification of 2-(1 H-Indazol-4-yl)-6-(4-methanesulfonyl-piperazin-1-ylmethyl)-4-morpholin-4-yl-thieno [3, 2-d] pyrimidine (GDC-0941) as a potent, selective, orally bioavailable inhibitor of class I PI3 kinase for the treatment of cancer. *J Med Chem.* 51:5522-5532.

Fujita, J., O. Yoshida, Y. Yuasa, J.S. Rhim, M. Hatanaka, and S.A. Aaronson. 1984. Ha-ras oncogenes are activated by somatic alterations in human urinary tract tumours. *Nature*. 309:464–466.

Fukumoto, S. 2004. Ameloblastin is a cell adhesion molecule required for maintaining the differentiation state of ameloblasts. *J Cell Biol*. 167:973–983.

Fukumoto, S., A. Yamada, K. Nonaka, and Y. Yamada. 2006. Essential roles of ameloblastin in maintaining ameloblast differentiation and enamel formation. *Cells Tissues Organs*. 181:189-195.

Gelb, B.D. 2006. Noonan syndrome and related disorders: dysregulated RAS-mitogen activated protein kinase signal transduction. *Hum Mol Genet*. 15:R220–R226.

Gibson, C.W., Z.A. Yuan, B. Hall, G. Longenecker, E. Chen, T. Thyagarajan, et al. 2001. Amelogenin-deficient mice display an amelogenesis imperfecta phenotype. *J Biol Chem.* 276:31871–31875.

Goodwin, A., S. Oberoi, M. Landan, C. Charles, J. Groth, A. Martinez, et al. 2012. Craniofacial and dental development in cardio-facio-cutaneous syndrome: the importance of Ras signaling homeostasis. *Clin Genet.* 83:539-544.

Gripp, K.W. 2005. Tumor predisposition in Costello syndrome. *Am J Med Genet.* 137C:72–77.

Gripp, K.W., A.E. Lin, D.L. Stabley, L. Nicholson, C.I. Scott, D. Doyle, et al. 2005. HRAS mutation analysis in Costello syndrome: Genotype and phenotype correlation. *Am J Med Genet.* 140A:1–7.

Gronthos, S., M. Mankani, J. Brahim, P.G. Robey, and S. Shi. 2000. Postnatal human dental pulp stem cells (DPSCs) in vitro and in vivo. *Proc Nat Acad Sci*. 97:13625-13630.

Gysin, S., M. Salt, A. Young, and F. McCormick. 2011. Therapeutic strategies for targeting ras proteins. *Genes Cancer*. 2:359–372.

Haigis, K.M., K.R. Kendall, Y. Wang, A. Cheung, M.C. Haigis, J.N. Glickman,

et al. 2008. Differential effects of oncogenic K-Ras and N-Ras on proliferation, differentiation and tumor progression in the colon. *Nat Genet*. 40:600–608.

Hall, A., C.J. Marshall, N.K. Spurr, and R.A. Weiss. 1983. Identification of transforming gene in two human sarcoma cell lines as a new member of the ras gene family located on chromosome 1. *Nature*. 303:396–400.

Hanna, J.H., K. Saha, and R. Jaenisch. 2010. Pluripotency and cellular reprogramming: facts, hypotheses, unresolved issues. *Cell*. 143:508–525.

Hao, Y., R. Wong, and L.A. Feig. 2008. RalGDS Couples Growth Factor Signaling to Akt Activation. *Mol Cell Biol*. 28:2851–2859.

Harada, H., P. Kettunen, H.S. Jung, T. Mustonen, Y.A. Wang, and I. Thesleff. 1999. Localization of putative stem cells in dental epithelium and their association with Notch and FGF signaling. *J Cell Biol*. 147:105–120.

Hart, P.S., T.C. Hart, M.D. Michalec, O.H. Ryu, D. Simmons, S. Hong et al. 2004. Mutation in kallikrein 4 causes autosomal recessive hypomaturation amelogenesis imperfecta. *J Med Genet*. 41:545–549.

Hart, T.C., Y. Zhang, M.C. Gorry, P.S. Hart, M. Cooper, M.L. Marazita, et al. 2002. A mutation in the SOS1 gene causes hereditary gingival fibromatosis type 1. *Am J Hum Genet.* 70:943–954.

Ho, S.P., S.J. Marshall, M.I. Ryder, and G.W. Marshall. 2007. The tooth attachment mechanism defined by structure, chemical composition and mechanical properties of collagen fibers in the periodontium. *Biomaterials*. 28:5238–5245.

Hong, D.S., D.W. Bowles, G.S. Falchook, W.A. Messersmith, G.C. George, C.L. O'Bryant, et al. 2012. A multicenter phase I trial of PX-866, an oral irreversible phosphatidylinositol 3-kinase inhibitor, in patients with advanced solid tumors. *Clin Cancer Res.* 18:4173–4182.

Hu, J., Y. Hu, C.E. Smith, M.D. McKee, J.T. Wright, Y. Yamakoshi, et al. 2008. Enamel defects and ameloblast-specific expression in Enam knock-out/lacz knock-in mice. *J Biol Chem.* 283:10858-10871.

Hu, J.C.C., Y.-H.P. Chun, T. Al Hazzazzi, and J.P. Simmer. 2007. Enamel Formation and Amelogenesis Imperfecta. *Cells Tissues Organs*. 186:78–85.

Huang, Z., J. Kim, R.S. Lacruz, P. Bringas, M. Glogauer, T.G. Bromage, et al. 2011. Epithelial-specific knockout of the Rac1 gene leads to enamel defects. *Eur J Oral Sci*. 119 Suppl 1:168–176.

Iwasaki, K., E. Bajenova, E. Somogyi-Ganss, M. Miller, V. Nguyen, H. Nourkeyhani, et al. 2005. Amelotin--a novel secreted, ameloblast-specific

161

protein. *J Dent Res*. 84:1127–1132.

Järvinen, E., M. Tummers, and I. Thesleff. 2009. The role of the dental lamina in mammalian tooth replacement. *J Exp Zool.* 312B:281–291.

Jernvall, J., and I. Thesleff. 2000. Reiterative signaling and patterning during mammalian tooth morphogenesis. *Mech Dev.* 92:19–29.

Jernvall, J., P. Kettunen, I. Karavanova, L.B. Martin, and I. Thesleff. 1994. Evidence for the role of the enamel knot as a control center in mammalian tooth cusp formation: non-dividing cells express growth stimulating Fgf-4 gene. *Int J Dev Biol.* 38:463–469.

Jernvall, J., T. Aberg, P. Kettunen, S. Keränen, and I. Thesleff. 1998. The life history of an embryonic signaling center: BMP-4 induces p21 and is associated with apoptosis in the mouse tooth enamel knot. *Development*. 125:161–169.

Jessen, W.J., S.J. Miller, E. Jousma, J. Wu, T.A. Rizvi, M.E. Brundage, et al. 2013. MEK inhibition exhibits efficacy in human and mouse neurofibromatosis tumors. *J Clin Invest.* 123:340–347.

Jheon, A.H., K. Seidel, B. Biehs, and O.D. Klein. 2012. From molecules to mastication: the development and evolution of teeth. *Wiley Interdisc Rev Dev Biol*. 2:165–192.

Jheon, A.H., P. Mostowfi, M.L. Snead, R.A. Ihrie, E. Sone, T. Pramparo, et al. 2011. PERP regulates enamel formation via effects on cell-cell adhesion and gene expression. *J Cell Sci.* 124:745–754.

Johnson, L., D. Greenbaum, K. Cichowski, K. Mercer, E. Murphy, E. Schmitt, et al. 1997. K-ras is an essential gene in the mouse with partial functional overlap with N-ras. *Genes Dev*. 11:2468-2481.

Juuri, E., K. Saito, L. Ahtiainen, K. Seidel, M. Tummers, K. Hochedlinger, et al. 2012. Sox2+ stem cells contribute to all epithelial lineages of the tooth via Sfrp5+ progenitors. *Dev Cell*. 23:317–328.

Karlsson, L. 2010. Caries detection methods based on changes in optical properties between healthy and carious tissue. *Int J Dent*. 2010:270729.

Karnoub, A.E., and R.A. Weinberg. 2008. Ras oncogenes: split personalities. *Nat Rev Mol Cell Biol*. 9:517–531.

Kerr, B., M.A. Delrue, S. Sigaudy, R. Perveen, M. Marche, I. Burgelin, et al. 2006. Genotype-phenotype correlation in Costello syndrome: HRAS mutation analysis in 43 cases. *J Med Genet*. 43:401–405.

Kettunen, P., I. Karavanova, and I. Thesleff. 1998. Responsiveness of developing dental tissues to fibroblast growth factors: expression of splicing alternatives of FGFR1, -2, -3, and of FGFR4; and stimulation of cell proliferation by FGF-2, -4, -8, and -9. *Dev Genet.* 22:374–385.

Kettunen, P., J. Laurikkala, P. Itäranta, S. Vainio, N. Itoh, and I. Thesleff. 2000. Associations of FGF-3 and FGF-10 with signaling networks regulating tooth morphogenesis. *Dev Dyn.* 219:322-332

Kim, H.J., and D. Bar-Sagi. 2004. Modulation of signalling by Sprouty: a developing story. *Nat Rev Mol Cell Biol.* 5:441–450.

Kim, J.-W., J.P. Simmer, T.C. Hart, P.S. Hart, M.D. Ramaswami, J.D. Bartlett, et al. 2005. MMP-20 mutation in autosomal recessive pigmented hypomaturation amelogenesis imperfecta. *J Medical Genet.* 42:271–275.

Kim, J.-W., S.-K. Lee, Z.H. Lee, J.-C. Park, K.-E. Lee, M.-H. Lee, et al. 2008. FAM83H mutations in families with autosomal-dominant hypocalcified amelogenesis imperfecta. *Am J Hum Genet.* 82:489–494.

Klein, O.D., D.B. Lyons, G. Balooch, G.W. Marshall, M.A. Basson, M. Peterka, et al. 2007. An FGF signaling loop sustains the generation of differentiated progeny from stem cells in mouse incisors. *Development.* 135:377–385.

Klein, O.D., G. Minowada, R. Peterkova, A. Kangas, B.D. Yu, H. Lesot, et al. 2006. Sprouty genes control diastema tooth development via bidirectional antagonism of epithelial-mesenchymal FGF signaling. *Dev Cell.* 11:181–190.

Koera, K., K. Nakamura, K. Nakao, J. Miyoshi, K. Toyoshima, T. Hatta, et al. 1997. K-ras is essential for the development of the mouse embryo. *Oncogene.* 15:1151–1159.

Kollar, E.J., and G.R. Baird. 1969. The influence of the dental papilla on the development of tooth shape in embryonic mouse tooth germs. *J Embryol Exp Morphol.* 21:131–148.

Kollar, E.J., and G.R. Baird. 1970. Tissue interactions in embryonic mouse tooth germs II. The inductive role of the dental papilla. *J Embryol Exp Morphol.* 24:173-186.

Kontaridis, M.I., K.D. Swanson, F.S. David, D. Barford, and B.G. Neel. 2006. PTPN11 (Shp2) mutations in LEOPARD syndrome have dominant negative, not activating, effects. *J Biol Chem.* 281:6785-6792.

Kweon, Y.-S., K.-E. Lee, J. Ko, J.C.C. Hu, J.P. Simmer, and J.-W. Kim. 2013. Effects of Fam83h overexpression on enamel and dentine formation. *Arch Oral Biol.* doi:10.1016/j.archoralbio.2013.03.001.

Lagerström, M., N. Dahl, L. Iselius, B. Bäckman, and U. Pettersson. 1990. Mapping of the gene for X-linked amelogenesis imperfecta by linkage analysis. *Am J Hum Genet.* 46:120–125.

Lee, H.-K., D.-S. Lee, H.-M. Ryoo, J.-T. Park, S.-J. Park, H.-S. Bae, et al. 2010. The odontogenic ameloblast-associated protein (ODAM) cooperates with RUNX2 and modulates enamel mineralization via regulation of MMP-20. *J Cell Biochem.* 111:755–767.

Legius, E., C. Schrander-Stumpel, E. Schollen, C. Pulles-Heintzberger, M. Gewillig, and J.P. Fryns. 2002. PTPN11 mutations in LEOPARD syndrome. *J Med Genet*. 39:571–574.

Li, C.-Y., W. Cha, H.-U. Luder, R.-P. Charles, M. McMahon, T.A. Mitsiadis, et al. 2012. E-cadherin regulates the behavior and fate of epithelial stem cells and their progeny in the mouse incisor. *Dev Biol*. 366:357–366.

Lin, A.E., P.D. Grossfeld, R.M. Hamilton, L. Smoot, K.W. Gripp, V. Proud, et al. 2002. Further delineation of cardiac abnormalities in Costello syndrome. *Am J Med Genet.* 111:115–129.

Liu, H. 2004. Polarity and proliferation are controlled by distinct signaling pathways downstream of PI3-kinase in breast epithelial tumor cells. *J Cell Biol*. 164:603–612.

Liu, W., J. Selever, M.-F. Lu, and J.F. Martin. 2003. Genetic dissection of Pitx2 in craniofacial development uncovers new functions in branchial arch morphogenesis, late aspects of tooth morphogenesis and cell migration. *Development*. 130:6375–6385.

Lobell, R.B., C.A. Omer, M.T. Abrams, H.G. Bhimnathwala, M.J. Brucker, C.A. Buseret al. 2001. Evaluation of farnesyl: protein transferase and geranylgeranyl: protein transferase inhibitor combinations in preclinical models. *Cancer Res*. 61:8758-8768.

Rodriguez-Lozano, F.J., C. Bueno, C.L Insausti, L. Meseguer, M.C. Ramirez, M. Blanquer. 2011. Mesenchymal stem cells derived from dental tissues. *Int Endod J.* 44:800-806.

Lumsden, A.G. 1988. Spatial organization of the epithelium and the role of neural crest cells in the initiation of the mammalian tooth germ. *Development*. 103 Suppl:155–169.

Magudia, K., A. Lahoz, and A. Hall. 2012. K-Ras and B-Raf oncogenes inhibit colon epithelial polarity establishment through up-regulation of c-myc. *J Cell Biol*. 198:185–194.

Malumbres, M., and M. Barbacid. 2003. RAS oncogenes: the first 30 years.

164

Nat Rev Cancer. 3:459–465.

Meloche, S., and J. Pouysségur. 2007. The ERK1/2 mitogen-activated protein kinase pathway as a master regulator of the G1- to S-phase transition. *Oncogene*. 26:3227–3239.

Miller, C.S., and D.D. Damm. 1992. Incidence of verapamil-induced gingival hyperplasia in a dental population. *J Periodontol.* 63:453–456.

Mina, M., and E.J. Kollar. 1987. The induction of odontogenesis in non-dental mesenchyme combined with early murine mandibular arch epithelium. *Arch Oral Biol*. 32:123–127.

Moffatt, P., C.E. Smith, R. St-Arnaud, and A. Nanci. 2008. Characterization of Apin, a secreted protein highly expressed in tooth-associated epithelia. *J Cell Biochem.* 103:941–956.

Mor, A., and M.R. Philips. 2006. Compartmentalized Ras/MAPK signaling. *Annu Rev Immunol.* 24:771–800.

Pinkham, J., P. Casamassimo, H.W. Fields, D.J. McTigue, and A. Nowak. 2012. Pediatric Dentistry: Infancy through Adolescence. *WB Saunders*.

Mucchielli, M.L., T.A. Mitsiadis, S. Raffo, J.F. Brunet, J.P. Proust, and C. Goridis. 1997. Mouse Otlx2/RIEG expression in the odontogenic epithelium precedes tooth initiation and requires mesenchyme-derived signals for its maintenance. *Dev Biol*. 189:275–284.

Nakamura, T., J. Gulick, R. Pratt, and J. Robbins. 2009. Noonan syndrome is associated with enhanced pERK activity, the repression of which can prevent craniofacial malformations. *Proc Natl Acad Sci*. 106:15436–15441.

Nakao, K., R. Morita, Y. Saji, K. Ishida, Y. Tomita, M. Ogawa, et al. 2007. The development of a bioengineered organ germ method. *Nat Methods*. 4:227–230.

Neubüser, A., H. Peters, R. Balling, and G.R. Martin. 1997. Antagonistic interactions between FGF and BMP signaling pathways: a mechanism for positioning the sites of tooth formation. *Cell*. 90:247-255.

Nie, X., K. Luukko, and P. Kettunen. 2006. FGF signalling in craniofacial development and developmental disorders. *Oral Diseases*. 12:102–111.

Niihori, T., Y. Aoki, Y. Narumi, G. Neri, H. Cavé, A. Verloes, et al. 2006. Germline KRAS and BRAF mutations in cardio-facio-cutaneous syndrome. *Nat Genet*. 38:294–296.

Ohren, J.F., H. Chen, A. Pavlovsky, C. Whitehead, E. Zhang, P. Kuffa, et al.

2004. Structures of human MAP kinase kinase 1 (MEK1) and MEK2 describe novel noncompetitive kinase inhibition. *Nat Struct Mol Biol.* 11:1192–1197.

Oldak, J.M., J.P. Simmer, E.C. Lau, P.E. Sarte, H.C. Slavkin, and A.G. Fincham. 1994. Detection of monodisperse aggregates of a recombinant amelogenin by dynamic light scattering. *Biopolymers.* 34:1339-1347.

Oshima, M., M. Mizuno, A. Imamura, M. Ogawa, M. Yasukawa, H. Yamazaki, et al. 2011. Functional tooth regeneration using a bioengineered tooth unit as a mature organ replacement regenerative therapy. *PLoS ONE.* 6:e21531.

Pandit, B., A. Sarkozy, L.A. Pennacchio, C. Carta, K. Oishi, S. Martinelli, et al. 2007. Gain-of-function RAF1 mutations cause Noonan and LEOPARD syndromes with hypertrophic cardiomyopathy. *Nat Genet.* 39:1007–1012.

Patil, S., and R.S. Chamberlain. 2012. Neoplasms associated with germline and somatic NF1 gene mutations. *Oncologist.* 17:101–116.

Peterkova, R., S. Churava, H. Lesot, M. Rothova, J. Prochazka, M. Peterka, et al. 2009. Revitalization of a diastemal tooth primordium in Spry2 null mice results from increased proliferation and decreased apoptosis. *J Exp Zool.* 312B:292–308.

Peters, H., A. Neubüser, K. Kratochwil, and R. Balling. 1998. Pax9-deficient mice lack pharyngeal pouch derivatives and teeth and exhibit craniofacial and limb abnormalities. *Genes Dev.* 12:2735–2747.

Pispa, J., and I. Thesleff. 2003. Mechanisms of ectodermal organogenesis. *Dev Biol.* 262:195–205.

Potenza, N., C. Vecchione, A. Notte, A. De Rienzo, et al. 2005. Replacement of K-Ras with H-Ras supports normal embryonic development despite inducing cardiovascular pathology in adult mice. *EMBO Rep.* 6:432-437.

Premkumar, S., S. Avathvadi Venkatesan, and S. Rangachari. 2011. Altered oral sensory perception in tongue thrusters with an anterior open bite. *Eur J Orthod.* 33:139–142.

Proffit, W.R., H.W. Fields Jr, and D.M. Sarver. 2006. Contemporary orthodontics. *Mosby Elsevier.*

Rajpar, M.H., K. Harley, C. Laing, R.M. Davies, and M.J. Dixon. 2001. Mutation of the gene encoding the enamel-specific protein, enamelin, causes autosomal-dominant amelogenesis imperfecta. *Hum Mol Genet.* 10:1673–1677.

Rasband, W.S. ImageJ, U.S. National Institutes of Health, Bethesda, MD, USA. *http://imagej.nih.hob/ij/.*

Rauen, K.A. 2007. HRAS and the Costello syndrome. *Clin Genet.* 71:101–108.

Rauen, K.A., A. Banerjee, W.R. Bishop, J.O. Lauchle, F. McCormick, M. McMahon, et al. 2011. Costello and cardio-facio-cutaneous syndromes: Moving toward clinical trials in RASopathies. *Am J Med Genet.* 157:136–146.

Rauen, K.A., L. Schoyer, F. McCormick, A.E. Lin, J.E. Allanson, D.A. Stevenson, et al. 2010. Proceedings from the 2009 genetic syndromes of the Ras/MAPK pathway: From bedside to bench and back. *Am J Med Genet.* 152A:4-24.

Razzaque, M.A., T. Nishizawa, Y. Komoike, H. Yagi, M. Furutani, R. Amo, et al. 2007. Germline gain-of-function mutations in RAF1 cause Noonan syndrome. *Nat Genet*. 39:1013–1017.

Resende, R.G., J.A.R. Brito, L.N. Souza, R.S. Gomez, and R.A. Mesquita. 2011. Peripheral calcifying odontogenic cyst: a case report and review of the literature. *Head and Neck Pathol*. 5:76–80.

Riolo, M.L. 2002. Essentials for Orthodontic Practice. 1st ed. EFOP Press.

Roberts, A., J. Allanson, S.K. Jadico, M.I. Kavamura, J. Noonan, J.M. Opitz, et al. 2006. The cardiofaciocutaneous syndrome. *J Med Genet*. 43:833–842.

Roberts, A.E., J.E. Allanson, M. Tartaglia, and B.D. Gelb. 2013. Noonan syndrome. *Lancet*. 381:333–342.

Roberts, A.E., T. Araki, K.D. Swanson, K.T. Montgomery, T.A. Schiripo, V.A. Joshi, et al. 2006. Germline gain-of-function mutations in SOS1 cause Noonan syndrome. *Nat Genet.* 39:70-74.

Rodriguez-Viciana, P., O. Tetsu, W.E. Tidyman, A.L. Estep, B.A. Conger, M.S. Cruz, et al. 2006. Germline mutations in genes within the MAPK pathway cause Cardio-facio-cutaneous syndrome. *Science*. 311:1287–1290.

Ruggieri, M., and R.J. Packer. 2001. Why do benign astrocytomas become malignant in NF1? *Neurology*. 56:827–829.

Sakamoto, Y., H. Nakajima, K. Kishi, R. Shimizu, and T. Nakajima. 2010. Management of craniofacial hyperostosis in Proteus syndrome. *J Craniofac Surg*. 21:414–418.

Santos, E., D. Martin-Zanca, E.P. Reddy, M.A. Pierotti, G. Della Porta, and M. Barbacid. 1984. Malignant activation of a K-ras oncogene in lung carcinoma but not in normal tissue of the same patient. *Science*. 223:661-664.

Sarkozy, A., M.C. Digilio, and B. Dallapiccola. 2008. Leopard syndrome.

Orphanet J Rare Dis. 3:13.

Sasaki, A.T. 2004. Localized Ras signaling at the leading edge regulates PI3K, cell polarity, and directional cell movement. *J Cell Biol*. 167:505–518.

Schubbert, S., G. Bollag, and K. Shannon. 2007. Deregulated Ras signaling in developmental disorders: new tricks for an old dog. *Curr Opin Genet Dev*. 17:15–22.

Schubbert, S., M. Zenker, S.L. Rowe, S. Böll, C. Klein, G. Bollag, et al. 2006. Germline KRAS mutations cause Noonan syndrome. *Nat Genet*. 38:331–336.

Schuhmacher, A.J., C. Guerra, V. Sauzeau, M. Cañamero, X.R. Bustelo, and M. Barbacid. 2008. A mouse model for Costello syndrome reveals an Ang II–mediated hypertensive condition. *J Clin Invest*. 118:2169-2179.

Sebolt-Leopold, J.S. 2008. Advances in the development of cancer therapeutics directed against the RAS-mitogen-activated protein kinase pathway. *Clin Cancer Res*. 14:3651-3656.

Sebolt-Leopold, J.S., D.T. Dudley, R. Herrera, K. Van Becelaere, A. Wiland, et al. 1999. Blockade of the MAP kinase pathway suppresses growth of colon tumors in vivo. *Nat Med*. 5:810-816.

Seidel, K., C.P. Ahn, D. Lyons, A. Nee, K. Ting, I. Brownell, et al. 2010. Hedgehog signaling regulates the generation of ameloblast progenitors in the continuously growing mouse incisor. *Development*. 137:3753–3761.

Seo, B.-M., M. Miura, S. Gronthos, P.M. Bartold, S. Batouli, J. Brahim, et al. 2004. Investigation of multipotent postnatal stem cells from human periodontal ligament. *Lancet*. 364:149–155.

Shinmura, Y., S. Tsuchiya, K. Hata, and M.J. Honda. 2008. Quiescent epithelial cell rests of Malassez can differentiate into ameloblast-like cells. *J Cell Physiol.* 217:728-738.

Siegel, D.H., J.A. Mann, A.L. Krol, and K.A. Rauen. 2012. Dermatological phenotype in Costello syndrome: consequences of Ras dysregulation in development. *Br J Dermatol.* 166:601–607.

Simmer, J.P., C.C. Hu, E.C. Lau, P. Sarte, H.C. Slavkin, and A.G. Fincham. 1994. Alternative splicing of the mouse amelogenin primary RNA transcript. *Calcif Tissue Int.* 55:302–310.

Simmer, J.P., Y. Hu, R. Lertlam, Y. Yamakoshi, and J.C.C. Hu. 2009. Hypomaturation enamel defects in Klk4 knockout/LacZ knockin mice. *J Biol Chem.* 284:19110–19121.

Smith, C.E., A.S. Richardson, Y. Hu, J.D. Bartlett, J.C.C. Hu, and J.P. Simmer. 2011. Effect of kallikrein 4 loss on enamel mineralization: comparison with mice lacking matrix metalloproteinase 20. *J Biol Chem*. 286:18149–18160.

Smith, C.E., and H. Warshawsky. 1975. Cellular renewal in the enamel organ and the odontoblast layer of the rat incisor as followed by radioautography using 3H-thymidine. *Anat Rec*. 183:523–561.

Smith, C.E., and H. Warshawsky. 1977. Quantitative analysis of cell turnover in the enamel organ of the rat incisor. Evidence for ameloblast death immediately after enamel matrix secretion. *Anat Rec*. 187:63–98.

Somogyi-Ganss, E., Y. Nakayama, K. Iwasaki, Y. Nakano, D. Stolf, M.D. McKee, et al. 2012. Comparative temporospatial expression profiling of murine amelotin protein during amelogenesis. *Cells Tissues Organs*. 195:535–549.

Sparling, J.D., C.-H. Hong, J.S. Brahim, J. Moss, and T.N. Darling. 2007. Oral findings in 58 adults with tuberous sclerosis complex. *J Am Acad Dermatol.* 56:786–790.

St Amand, T.R., Y. Zhang, E.V. Semina, X. Zhao, Y. Hu, L. Nguyen, et al. 2000. Antagonistic signals between BMP4 and FGF8 define the expression of Pitx1 and Pitx2 in mouse tooth-forming anlage. *Dev Biol*. 217:323–332.

Steelman, L.S., S.C. Pohnert, J.G. Shelton, R.A. Franklin, F.E. Bertrand, and J.A. McCubrey. 2004. JAK/STAT, Raf/MEK/ERK, PI3K/Akt and BCR-ABL in cell cycle progression and leukemogenesis. *Leukemia*. 18:189–218.

Stevenson, D.A., E.L. Schwarz, J.C. Carey, D.H. Viskochil, H. Hanson, S. Bauer, et al. 2011. Bone resorption in syndromes of the Ras/MAPK pathway. *Clin Genet.* 80:566–573.

Stevenson, D.A., S. Allen, W.E. Tidyman, J.C. Carey, D.H. Viskochil, A. Stevens, et al. 2012. Peripheral muscle weakness in RASopathies. *Muscle Nerve*. 46:394–399.

Takahashi, M., and H. Ohashi. 2012. Craniofacial and dental malformations in Costello syndrome: a detailed evaluation by using multi-detector row computed tomography. *Congen Anomal*. doi:10.1111/cga.12004.

Takamori, K., R. Hosokawa, X. Xu, X. Deng, P. Bringas, and Y. Chai. 2008. Epithelial fibroblast growth factor receptor 1 regulates enamel formation. *J Dent Res*. 87:238–243.

Tang, N., W.F. Marshall, M. McMahon, R.J. Metzger, and G.R. Martin. 2011. Control of mitotic spindle angle by the RAS-regulated ERK1/2 pathway

determines lung tube shape. *Science*. 333:342-345.

Taparowsky, E., K. Shimizu, M. Goldfarb, and M. Wigler. 1983. Structure and activation of the human N- ras gene. *Cell*. 34:581-586.

Tartaglia, M., E.L. Mehler, R. Goldberg, G. Zampino, H.G. Brunner, H. Kremer,et al. 2001. Mutations in PTPN11, encoding the protein tyrosine phosphatase SHP-2, cause Noonan syndrome. *Nat Genet*. 29:465–468.

Tartaglia, M., L.A. Pennacchio, C. Zhao, K.K. Yadav, V. Fodale, A. Sarkozy, et al. 2007. Gain-of-function SOS1 mutations cause a distinctive form of Noonan syndrome. *Nat Genet*. 39:75–79.

Tartaglia, M., S. Martinelli, L. Stella, G. Bocchinfuso, E. Flex, V. Cordeddu et al. 2006. Diversity and Functional Consequences of Germline and Somatic PTPN11 Mutations in Human Disease. *Am J Hum Genet*. 78:279-290.

Thesleff, I., and K. Hurmerinta. 1981. Tissue interactions in tooth development. *Differentiation*. 18:75-88.

Thomas, B.L., A.S. Tucker, M. Qui, C.A. Ferguson, Z. Hardcastle, J.L. Rubenstein, et al. 1997. Role of Dlx-1 and Dlx-2 genes in patterning of the murine dentition. *Development.* 124:4811-4818.

Tidyman, W.E., and K.A. Rauen. 2009. The RASopathies: developmental syndromes of Ras/MAPK pathway dysregulation. *Curr Opin Genet Dev*. 19:230–236.

Tidyman, W.E., H.S. Lee, and K.A. Rauen. 2011. Skeletal muscle pathology in Costello and cardio-facio-cutaneous syndromes: developmental consequences of germline Ras/MAPK activation on myogenesis. *Am J Med Genet C Semin Med Genet*. 157:104–114.

To, M.D., C.E. Wong, A.N. Karnezis, R. Del Rosario, R. Di Lauro, and A. Balmain. 2008. Kras regulatory elements and exon 4A determine mutation specificity in lung cancer. *Nat Genet*. 40:1240–1244.

Trumpp, A., M.J. Depew, J.L. Rubenstein, J.M. Bishop, and G.R. Martin. 1999. Cre-mediated gene inactivation demonstrates that FGF8 is required for cell survival and patterning of the first branchial arch. *Genes Dev*. 13:3136–3148.

Tsang, M. 2004. Promotion and attenuation of FGF signaling through the Ras-MAPK pathway. *Science's STKE*. 2004:pe17–pe17.

Tsuboi, T., S. Mizutani, M. Nakano, K. Hirukawa, and A. Togari. 2003. Fgf-2 regulates enamel and dentine formation in mouse tooth germ. *Calcif Tissue Int.* 73:496–501.

Tucker, A., and P. Sharpe. 2004. The cutting-edge of mammalian development; how the embryo makes teeth. *Nat Rev Genet*. 5:499–508.

Tucker, A.S. 1998. Transformation of tooth type induced by inhibition of BMP signaling. *Science*. 282:1136–1138.

Umanoff, H., W. Edelmann, A. Pellicer, and R. Kucherlapati. 1995. The murine N-ras gene is not essential for growth and development. *Proc Natl Acad Sci*. 92:1709-1713.

Urosevic, J., V. Sauzeau, M.L. Soto-Montenegro, S. Reig, M. Desco, E.M.B. Wright, et al. 2011. Constitutive activation of B-Raf in the mouse germ line provides a model for human cardio-facio-cutaneous syndrome. *Proc Natl Acad Sci*. 108:5015–5020.

Viskochil, D., A.M. Buchberg, G. Xu, R.M. Cawthon, J. Stevens, R.K. Wolff, et al. 1990. Deletions and a translocation interrupt a cloned gene at the neurofibromatosis type 1 locus. *Cell*. 62:187–192.

Wallace, M.R., D.A. Marchuk, L.B. Andersen, R. Letcher, et al. 1990. Type 1 neurofibromatosis gene: identification of a large transcript disrupted in three NF1 patients. *Science*. 249:181-186.

Wang, X.-P., M. Suomalainen, S. Felszeghy, L.C. Zelarayan, M.T. Alonso, M.V. Plikus, R.L. Maas, C.-M. Chuong, T. Schimmang, and I. Thesleff. 2007. An Integrated Gene Regulatory Network Controls Stem Cell Proliferation in Teeth. *Plos Biol*. 5:e159. doi:10.1371/journal.pbio.0050159.sg003.

Wang, X.P., D.J. O'Connell, J.J. Lund, I. Saadi, M. Kuraguchi, A. Turbe-Doan, et al. 2009. Apc inhibition of Wnt signaling regulates supernumerary tooth formation during embryogenesis and throughout adulthood. *Development*. 136:1939–1949.

Wang, Y., E. Kim, X. Wang, B.G. Novitch, K. Yoshikawa, L.-S. Chang, et al. 2012. ERK inhibition rescues defects in fate specification of Nf1-deficient neural progenitors and brain abnormalities. *Cell*. 150:816–830.

Welch, H.C.E., W.J. Coadwell, L.R. Stephens, and P.T. Hawkins. 2003. Phosphoinositide 3-kinase-dependent activation of Rac. *FEBS Letters*. 546:93–97.

Williams, V.C., J. Lucas, M.A. Babcock, D.H. Gutmann, B. Korf, and B.L. Maria. 2009. Neurofibromatosis type 1 revisited. *Pediatrics*. 123:124–133.

Wise, G.E. 2009. Cellular and molecular basis of tooth eruption. *Orthod Craniofac Res*. 12:67–73.

Wodarz, A. 2002. Establishing cell polarity in development. *Nat Cell Biol*.

4:E39-44.

Wright, J.T., P.S. Hart, M.J. Aldred, and K. Seow. 2003. Relationship of phenotype and genotype in X-linked amelogenesis imperfecta. *Connect Tissue Res*. 44 Suppl 1:72-78.

Yap, T.A., L. Yan, A. Patnaik, I. Fearen, D. Olmos, K. Papadopoulos, et al. 2011. First-in-man clinical trial of the oral pan-AKT inhibitor MK-2206 in patients with advanced solid tumors. *J Clin Oncol.* 29:4688–4695.

Yoon, G., J. Rosenberg, S. Blaser, and K.A. Rauen. 2007. Neurological complications of cardio-facio-cutaneous syndrome. *Dev Med Child Neurol*. 49:894–899.

Yoshimura, T., N. Arimura, Y. Kawano, S. Kawabata, S. Wang, and K. Kaibuchi. 2006. Ras regulates neuronal polarity via the PI3-kinase/Akt/GSK-3β/CRMP-2 pathway. *Biochem Biophys Res Commun*. 340:62–68.

Zampino, G., F. Pantaleoni, C. Carta, G. Cobellis, I. Vasta, C. Neri, et al. 2007. Diversity, parental germline origin, and phenotypic spectrum of de novo HRAS missense changes in Costello syndrome. *Hum Mutat.* 28:265–272.

Zhang, H., X. Liu, K. Zhang, C.K. Chen, J.M. Frederick, G.D. Prestwich, et al. 2004. Photoreceptor cGMP phosphodiesterase δ subunit (PDEδ) functions as a prenyl-binding protein. *J Biol Chem.* 279:407-413.
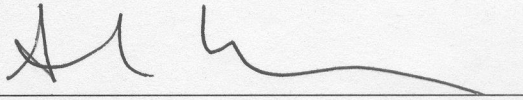
Zimmermann, G., B. Papke, S. Ismail, N. Vartak, A. Chandra, M. Hoffmann, et al. 2013. Small molecule inhibition of the KRAS-PDE [delta] interaction impairs oncogenic KRAS signalling. *Nature*. 497:638-642.

Publishing Agreement

It is the policy of the University to encourage the distribution of all theses, dissertations, and manuscripts. Copies of all UCSF theses, dissertations, and manuscripts will be routed to the library via the Graduate Division. The library will make all theses, dissertations, and manuscripts accessible to the public and will preserve these to the best of their abilities, in perpetuity.

Please sign the following statement:

I hereby grant permission to the Graduate Division of the University of California, San Francisco to release copies of my thesis, dissertation, or manuscript to the Campus Library to provide access and preservation, in whole or in part, in perpetuity.

_____   6/12/13
Author Signature   Date